รายงานวิจัยฉบับสมบูรณ์

โครงการ Bipyridyl Ligand Modification for
Supramolecular of Ruthenium-Cucurbiturils Complexes
as Dye-Sensitized Solar Cells

โดย ผู้ช่วยศาสตราจารย์ ดร. ธิตินันท์ กาพย์เกิด

กันยายน 2556

รายงานวิจัยฉบับสมบูรณ์

โครงการ Bipyridyl Ligand Modification for
Supramolecular of Ruthenium-Cucurbiturils Complexes
as Dye-Sensitized Solar Cells

ผู้ช่วยศาสตราจารย์ ดร. ธิตินันท์ กาพย์เกิด
ภาควิชาเคมี คณะวิทยาศาสตร์ มหาวิทยาลัยเกษตรศาสตร์

รูปแบบ **Abstract** (บทคัดย่อ)

Project Title : Bipyridyl Ligand Modification for Supramolecular of Ruthenium

Cucurbiturils Complexes as Dye-Sensitized Solar Cells

Investigator : Assist. Prof. Thitinun Karpkird, Ph.D

Department of Chemistry, Faculty of Science, Kasetsart University

Prof. Supa Hannongbua, Ph.D.   Mentor

Department of Chemistry, Faculty of Science, Kasetsart University

Prof. Licheng Sun, Ph.D.   Mentor

School of Chemical Science and Engineering, Department of Chemistry,

Organic Chemistry, Royal Institute of Technology (KTH)

E-mail Address : fscitnm@ku.ac.th

บทคัดย่อ

งานวิจัยนี้เป็นการสังเคราะห์สารประกอบเชิงซ้อนรูทีเนียม ออสเมียม ไบไพริดิล ที่มีโครงสร้าง
แบบไม่สามาตร 4 ชนิด ประกอบด้วย $Os(bpy)_3$-viologen-$Ru(bpy)_3$ (**1**; bpy = 2,2'-bipyridyl)
$Ru(bpy)_3$-viologen-$Ru(dcbpy)_3$ (**2**; dcbpy = 4,4'-dicarboxyl-2,2-bipyridyl) and $Os(bpy)_3$-
viologen-$Ru(dcbpy)_3$ (**3**) และ rotaxane **1**⊂CB[7] (CB[7]=cucurbit[7]uril) วิเคราะห์โครงสร้าง
ด้วยเทคนิค NMR การศึกษาคุณสมบัติเคมีไฟฟ้า และเคมีเชิงแสงในตัวทำละลายอินทรีย์ พบว่า
ในอะซิโตไนไทรล์ CB[7] อยู่ในตำแหน่งสายโซ่บิวทิวด้านที่ใกล้กับออสเมียม ซึ่งทำให้ค่าความ
ต่างศักย์ในการเกิดออกซิเดชันของออสเมียมต่ำลง   แต่ขณะที่ความต่างศักย์ของรูทีเนียมไม่
เปลี่ยนแปลง นอกจากนี้พบว่าค่าความต่างศักย์ในการเกิดออกซิเดชันซองสารประกอบ 2 และ 3
ของรูทีเนียม   สูงขึ้นเนื่องมาจากความสามารถในการดึงอิเล็กตรอนของหมู่คาร์บอกซิล
การศึกษาการเกิดอนุมูลอิสระของไวโอโลเจนด้วยเทคนิคยูวีวิสิเบิ้ลพบว่า   อนุมูลอิสระของไว
โอโลเจนสามารถเกิดขึ้นได้ในตัวทำละลายอินทรีย์

Abstract

Four unsymmetric dinuclear ruthenium and osmium complexes, Os(bpy)$_3$-viologen-Ru(bpy)$_3$ (**1**; bpy = 2,2'-bipyridyl), Ru(bpy)$_3$-viologen-Ru(dcbpy)$_3$ (**2**; dcbpy = 4,4'-dicarboxyl-2,2-bipyridyl) and Os(bpy)$_3$-viologen-Ru(dcbpy)$_3$ (**3**) and rotaxane **1**⊂CB[7] (CB[7]=cucurbit[7]uril), have been successfully synthesized. The NMR, electrochemistry and photochemistry studies of these complexes were performed in non-aqueous solutions. The results show that CB[7] host mainly locates at the butyl linker part of the osmium side in acetonitrile solution. This binding lowers the oxidation potential of the osmium whereas the oxidation potential of ruthenium does not change. The oxidation potential of ruthenium in complexes **2** and **3** is higher due to the electron withdrawing property of carboxylic anchor groups. Analysis with UV-Vis spectra shows the viologen radical formation and reversed process of these complexes in non-aqueous solution.

Objectives

1) To synthesize asymmetric homo and heterogenous metal bipyridine complexes.
2) To study the photophysical, photochemical and electrochemical properties of the synthesized complexes.

Materials and Methods

Instruments

HRMS: High-resolution mass spectrometry was carried out using a QTof micromass spectrometer (Micromass, Inc., Manchester, England).

UV/Vis absorption spectroscopy: UV/Vis absorption spectra were measured using a Jasco V-670 spectrophotometer (JASCO International.Co., Ltd., Tokyo).

Infrared spectroscopy: IR spectra were measured using a system 2000 FT-IR (Perkin Elmer, Beaconsfield bucks.).

*Nuclear Magnetic Resonance*: ^{1}H-NMR spectra were measured using a VARIAN INOVA NMR Spectrometer 400 MHz.

Methods

Photochemistry: Samples were prepared using 0.08 mM of the analyte dissolved in acetonitrile. Epson LCD projector Model: EMP-821 (SEIKO EPSON CORP., Beijing) was used as a light source.

Materials 4-(4-Bromobutyl)-4'-methyl-2,2'-bipyridine was synthesized according to literature procedures.[1] For the synthesis of ligand **L1** was synthesized followed to litereature.[2] Os(bpy)$_2$Cl$_2$ was synthesized according to Kober et.al.[3] Ru(dcbpy)$_2$Cl$_2$ was

synthesized according to literature procedures.[4] Other materials and solvents employed were commercially available and used as supplied without further purification.

Complexes **1-3** and **1⊂CB[7]** were synthesized follow the scheme 1.
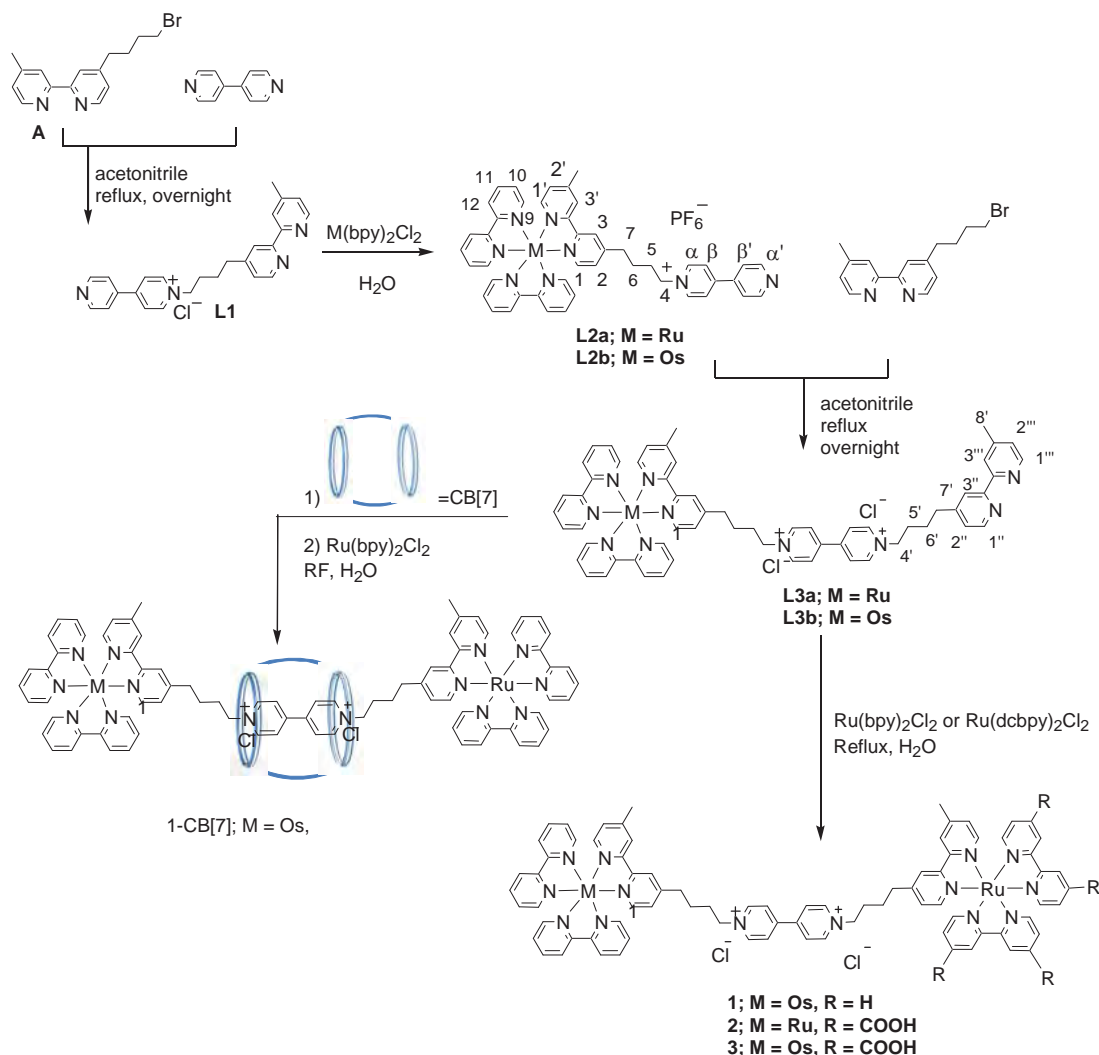
**Scheme 1**. Synthesis pathway of complex **1-3** and **3⊂CB[7]**

(1) Synthesis of compound A: compound **A** was synthesized follow the litereature [1] obtained pale yellow solid, 57% yield, confirmed by ^{1}H-NMR shown in Figure 1. ^{1}H-NMR (400 MHz, CDCl$_3$) δ ppm 8.55 (dd, 2H, J = 5.0Hz, J = 11.6Hz), 8.26 (s, 2H), 7.15 (d, 2H, J = 5.0Hz), 3.42 (t, 2H, J = 6.4Hz), 2.73 (t, 2H, J = 7.3Hz), 2.44 (s, 3H), 1.89 (m, 4H).

(2) Synthesis of compound L1; Compound L1 was synthesized follow the literature [2] obtained pink solid, 55% yield, confirmed by ^{1}H-NMR shown in Figure 2. ^{1}H-NMR (400 MHz, CD$_3$CN) δ ppm 8.84 (dd, 2H, J = 1.7Hz, J = 4.4Hz), 8.73 (d, 2H, J = 7.0Hz), 8.54

(d, 1H, J = 5.0Hz), 8.47 (d, 1H, J = 5.0Hz), 8.27 (d, 2H, J = 6.9Hz), 8.24 (s, 2H), 7.76 (dd, 2H, J = 1.7Hz, J = 4.5Hz), 7.22 (dt, 2H, J = 1.4Hz, J = 5.4Hz), 4.57 (t, 2H, J = 7.4Hz), 2.79 (t, 2H, J = 7.6Hz), 2.43 (s, 3H), 2.05 (m, 2H), 1.77 (m, 2H).
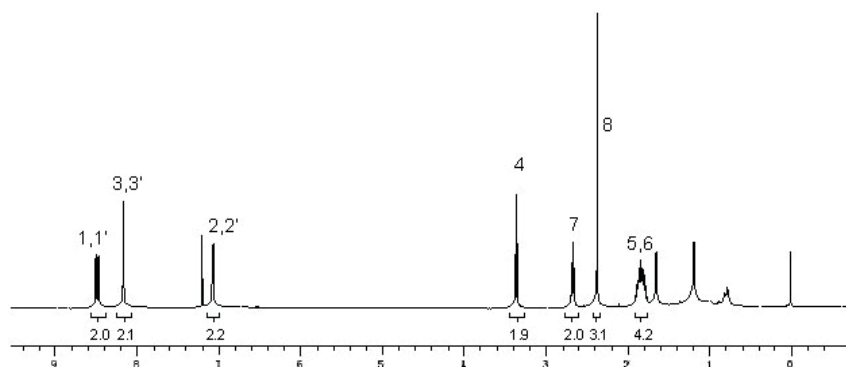

Figure 1 ^{1}H-NMR spectrum of compound A (400 MHz, CDCl$_3$).
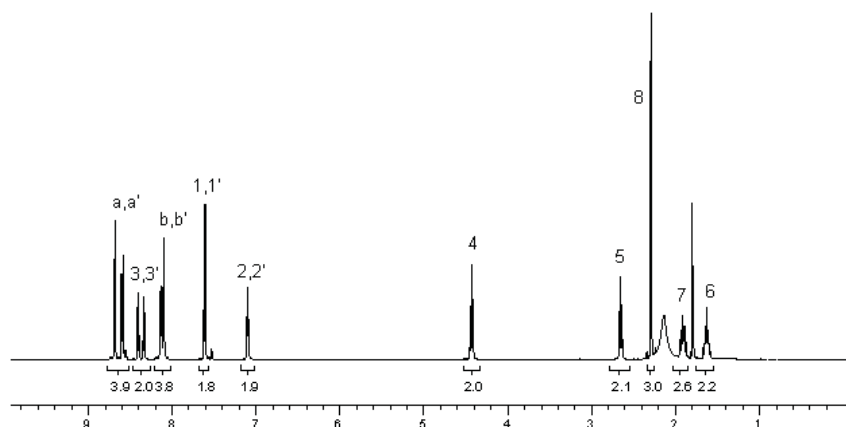
**Figure 2** ^{1}H-NMR spectrum of compound **L1** (400 MHz, CD$_3$CN).

(3) Synthesis of M(bpy)$_2$Cl$_2$;(M= Ru (II), Os (II) and Co(II); bpy = 2,2'-bipyridyl)

      (3.1) Ru(dcbpy)$_2$Cl$_2$ (dcbpy = 4,4'-dicarboxyl-2,2'-bipyridine) was synthesized according to literature procedures [4] yielding 79% yield red-purple solid. The chemical structure was confirmed by ^{1}H-NMR and ESI-MS as shown in Figure 3 and 4. ^{1}H-NMR (400 MHz, DMSO-d_6) δ ppm 10.03 (s, 2H), 9.12 (s, 2H), 8.97 (s, 2H), 8.23 (s, 2H), 7.66 (s, 2H), 7.53 (s, 2H), 4.52 (m, 4H), 4.37 (m, 4H), 1.45 (t, 6H, J = 6.7Hz), 1.31 (t, 6H, J = 6.6Hz). ESI-MS found [M+Na$^+$/1, 794.8796] and [2M+Na$^+$/1, 1568.8032].
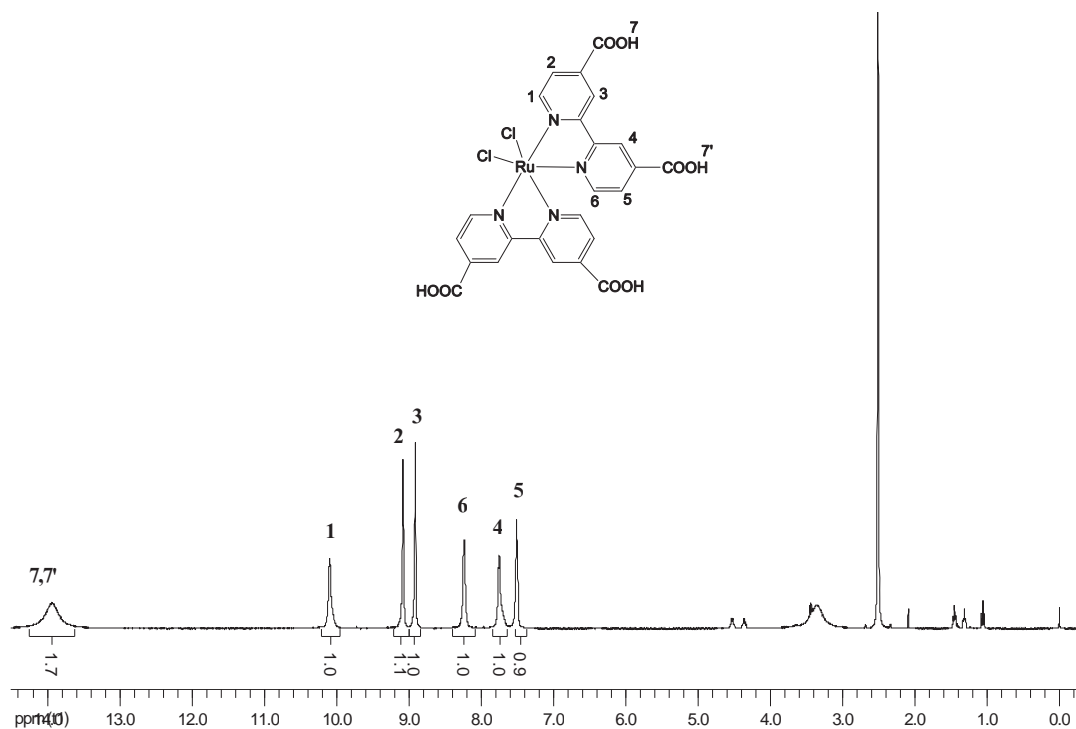
Figure 3. ^{1}H-NMR spectrum of Ru(dcbpy)$_2$Cl$_2$ in DMSO-d$_6$ (400MHz).
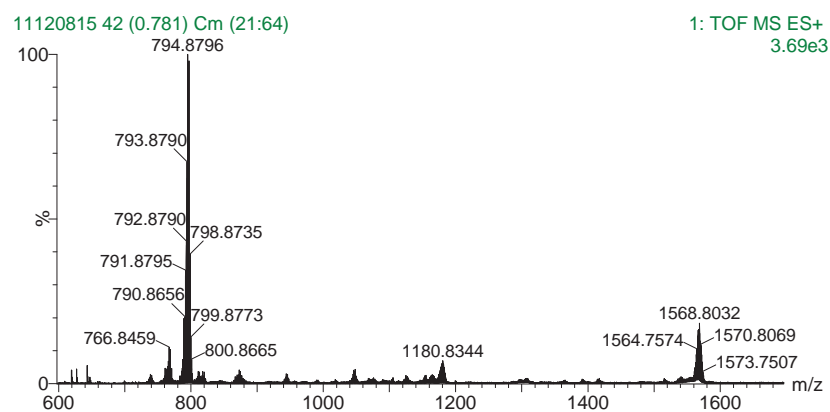
Figure 4 ESI- MS spectrum of Ru(dcbpy)$_2$Cl$_2$ in Methanol.

(3.2) Ru(bpy)$_2$Cl$_2$; yielding 65% of purple product. The chemical structure was confirmed by ^{1}H-NMR and MS shown in Figure 5 and 6.
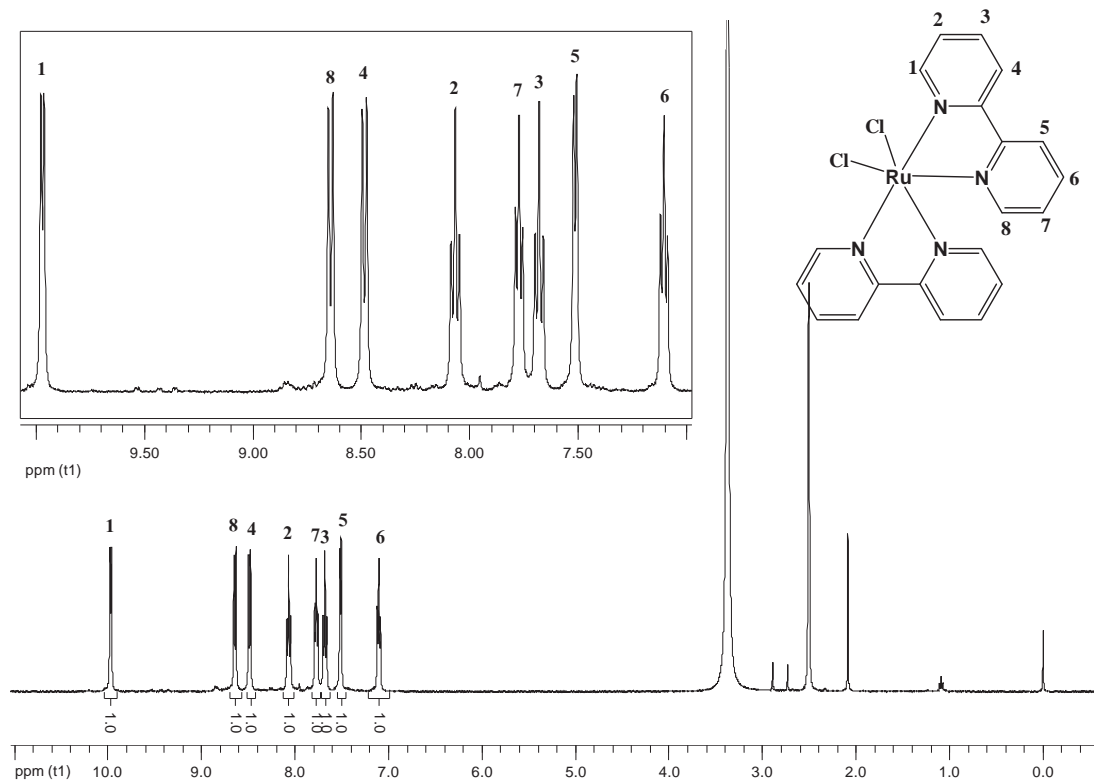
Figure 5 ^{1}H-NMR spectrum of Ru(bpy)$_2$Cl$_2$ in DMSO-d$_6$ (400MHz).
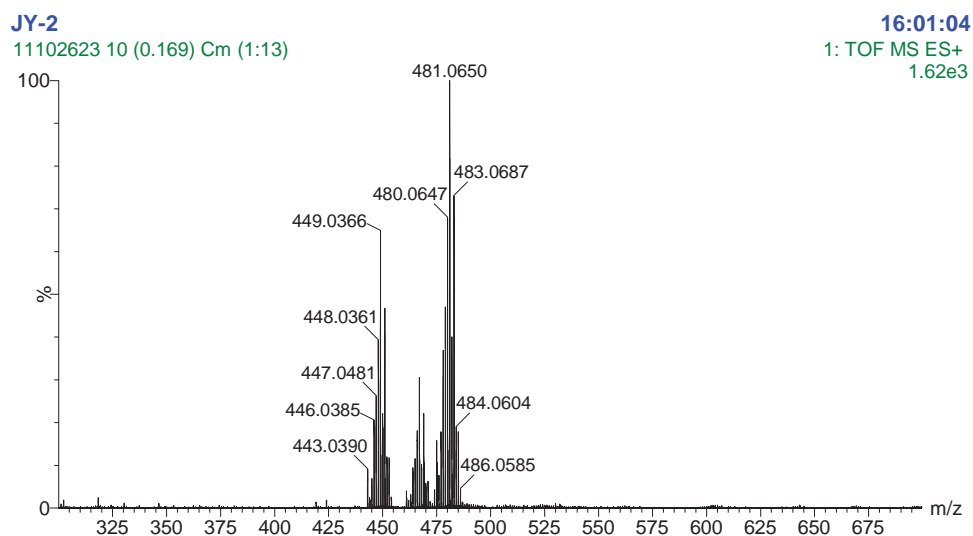
Figure 6 ESI-MS spectrum of Ru(bpy)$_2$Cl$_2$ in methanol.

The calculated molecular weight of Ru(bpy)$_2$Cl$_2$ (M) is m/z 483.98. MS spectra show [Ru(bpy)$_2$Cl-MeOH] m/z 481.0650 [calculated M-Cl+CH$_3$OH is m/z 481.0650] and [M-Cl] showed a signal at m/z 449.0366 [calculated M-Cl, 449.0366].

(3.3) Co(bpy)$_2$Cl$_2$ was synthesized followed literature[5] yielding 73% of pink solid. The chemical structure was confirmed by ^{1}H-NMR and MS shown in Figure 7.
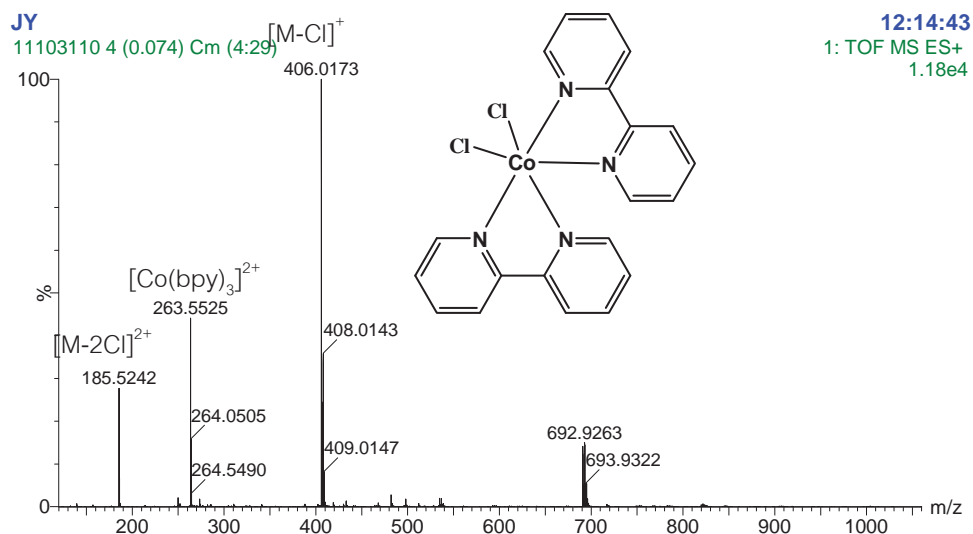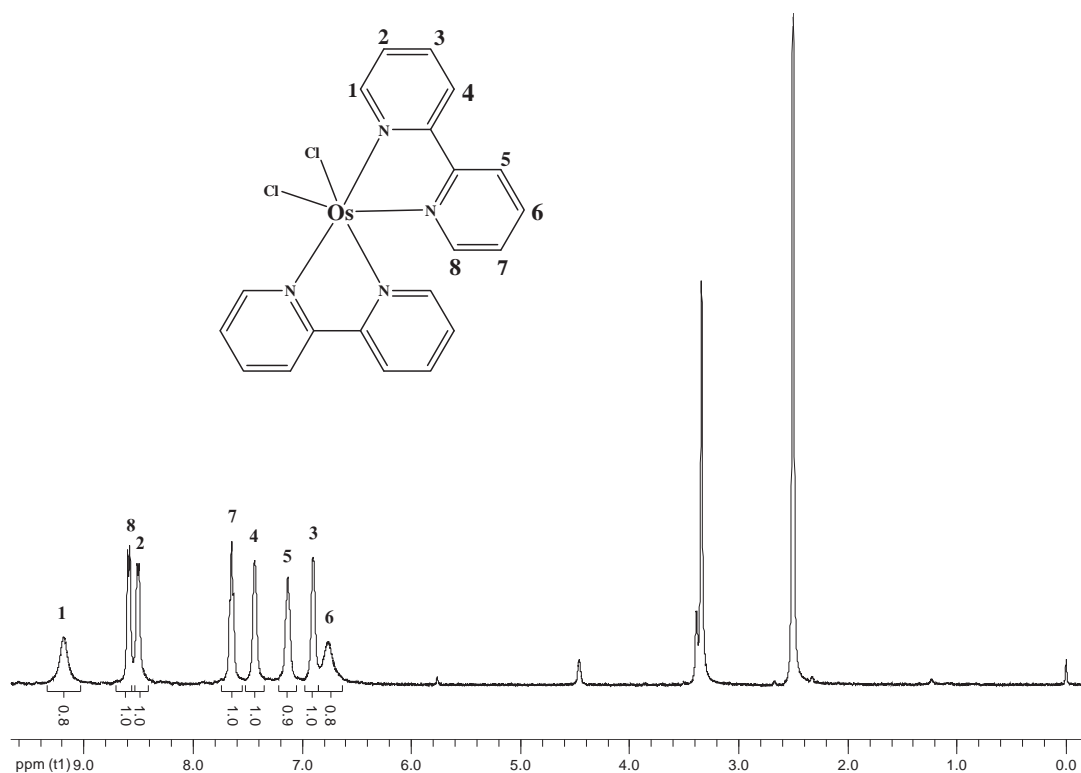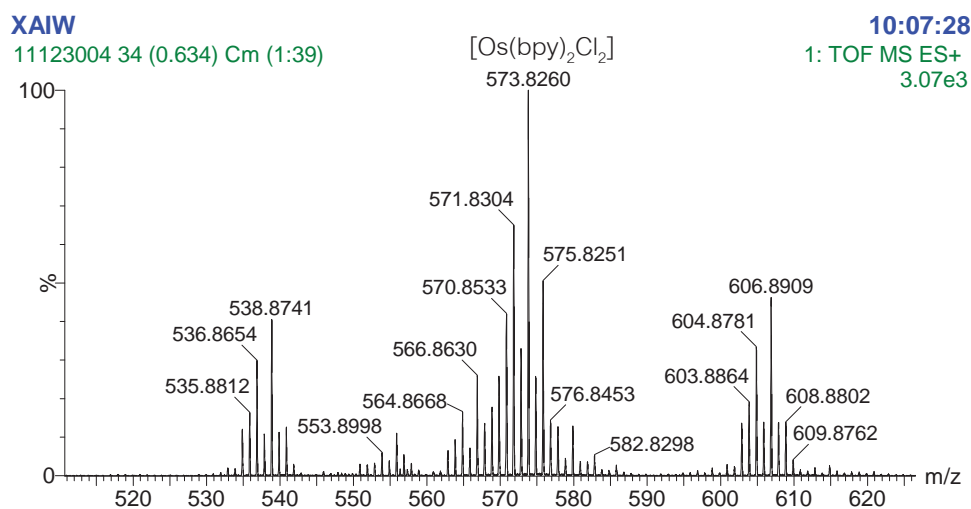
Figure 7 ESI-MS spectrum of Co(bpy)$_2$Cl$_2$ in H$_2$O.

Mass spectrum show a singlet peak at m/z 406.0173 corresponding to Co(bpy)$_2$Cl$_2$ (M) which loss one Cl atom [M-Cl/1+, 406.0173] and doublet signal at m/z 185.5242 corresponding to Co(bpy)$_2$Cl$_2$ which loss 2 Cl atoms [calculated M-2Cl/2+ is 185.5242]. Moreover, by product Co(bpy)$_3$$^{2+}$ could be detected at m/z 263.5525 but no effect to the next steps. ^{1}H-NMR could not be used to confirm this compound due to the paramagnetic property.

(3.4) Os(bpy)$_2$Cl$_2$ was synthesized according to Kober et.al.[3] yielding 61% of black purple solid. The chemical structure was confirmed by ^{1}H-NMR and MS shown in Figure 8. The signal of Os(III)(bpy)$_2$Cl$_2$ has been shown in the spectrum at m/z 573.8260.

Figure 8 ^{1}H-NMR spectrum of Os(bpy)$_2$Cl$_2$ in DMSO-d$_6$ (400MHz).

Figure 9. ESI-MS spectrum of Os(bpy)$_2$Cl$_2$ in methanol.

(4) Synthesis of Ru(bpy)$_3$-Viologen (L2a)

Ru(bpy)$_3$-viologen (**L2a· 3PF$_6^-$**): Compound **L1** 1.25 g (2.30 mmol) and Ru(bpy)$_2$Cl$_2$ 1.20 g (2.30 mmol) were refluxed in 20 ml of water under N$_2$ atmosphere at 90°C for 3 hours. After that, saturated aqueous solution of NH$_4$PF$_6$ was added in the cooled reaction mixture and isolated by filtration. The crude product was purified by column chromatography using silica gel and a mixture of CH$_3$CN/sat.KNO$_3$/H$_2$O as an eluent. The red solid was obtained (yield 30%). ^{1}H-NMR (400 MHz, CD$_3$CN) δ ppm 8.85 (dd,

2H, J=1.7Hz, J=4.5Hz) ppm 8.78 (d, 2H, J=7.0Hz) ppm 8.49 (d, 4H, J=8.2Hz) ppm 8.35 (dd, 4H, J=8.6Hz, J=15.9Hz) ppm 8.04 (m, 4H) ppm 7.83 (dd, 2H, J=1.7Hz, J=4.5Hz) ppm 7.71 (t, 4H, J=5.8Hz) ppm 7.54 (dd, 2H, J=5.8Hz, J=13.5Hz) ppm 7.39 (m, 4H) ppm 7.23 (d, 2H, J=5.9Hz) ppm 4.60 (m, 2H) ppm 2.86 (m, 2H) ppm 2.52 (s, 3H) ppm 2.07 (m, 2H) ppm 1.78 (m, 2H) ; ESI-MS: m/z found : [M^{3+}/3, 265.0995], [$M^{3+}+PF_6^-$/2, 470.1072] and [$M^{3+}+2PF_6^-$/1, 1085.1273]. (Figure 10 and 11)
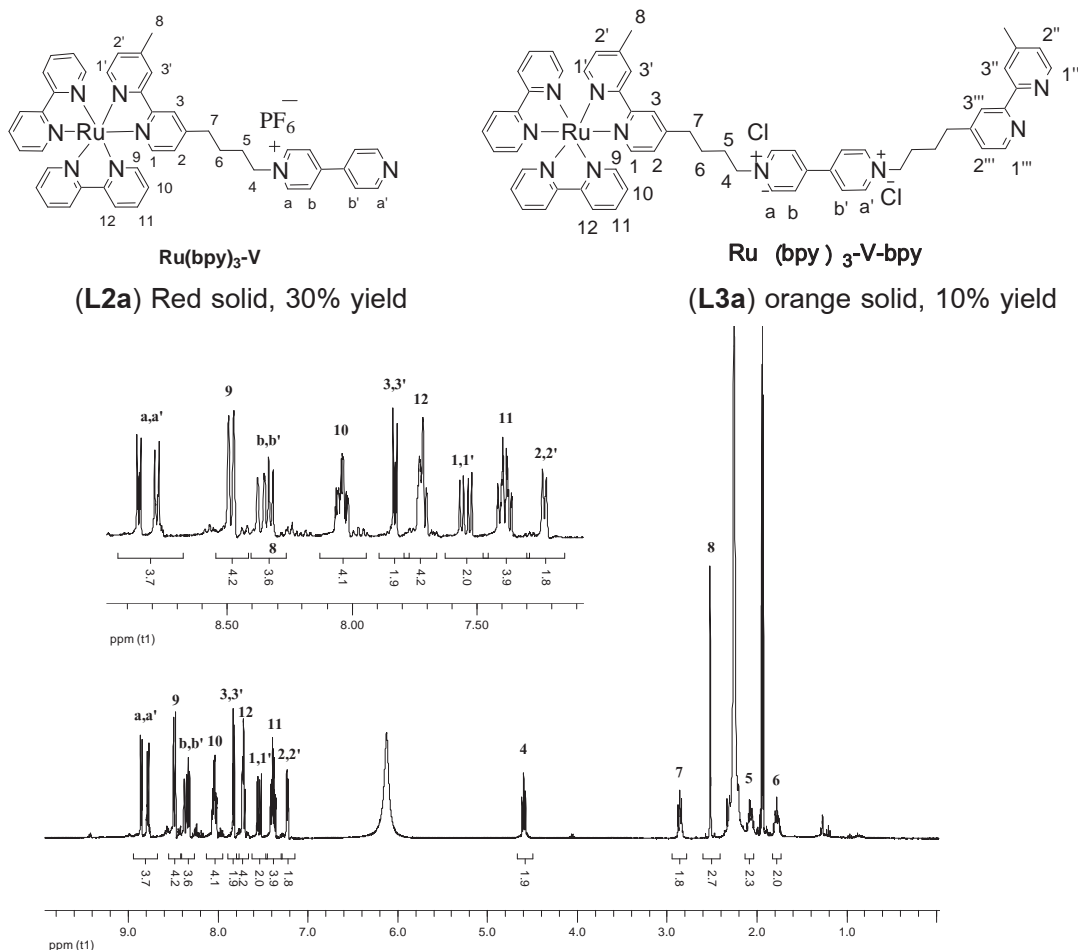

(**L2a**) Red solid, 30% yield   (**L3a**) orange solid, 10% yield

Figure 10 ^{1}H-NMR spectrum of **L2a** in CD$_3$CN (400MHz).
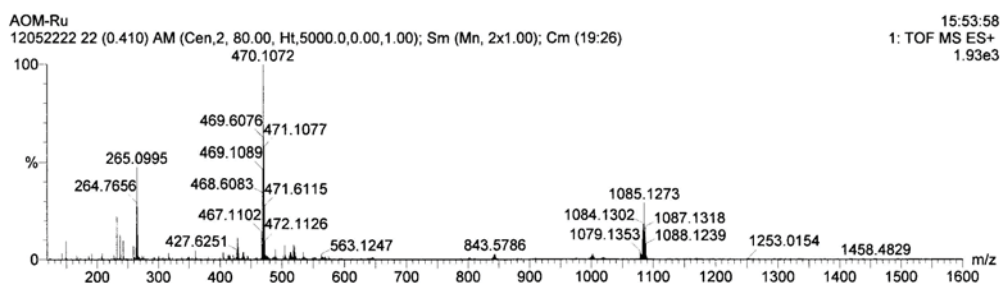
Figure 11 ESI-MS spectrum of **L2a**.

(5) Ru(bpy)₃-Viologen-bpy (L3a)

Ru(bpy)₃-viologen-bpy (**L3a· 4PF₆⁻**):Compound **L2a· 3PF₆⁻** 100.80 mg (0.11mmol) and A 130.00 mg (0.43 mmol) were refluxed in acetonitrile under N_2 atmosphere at 90°C for 5-6 days. After that, the most of acetonitrile was removed by a rotary evaporator. Then acetone was added to the reaction mixture for precipitation. The orange solid was filtered and washed by small amount of acetone. The orange solid was obtained (yield 90%). ^{1}H-NMR (400 MHz, CD₃CN) δ ppm 8.90 (d, 4H, J=6.3Hz) ppm 8.62 (d, 2H, J=5.1Hz) ppm 8.57 (s, 1H) ppm 8.56 (s, 1H) ppm 8.49 (d, 4H, J=8.1Hz) ppm 8.38 (d, 4H, J=9.0Hz) ppm 8.30 (s, 1H) ppm 8.27 (s, 1H) ppm 8.04 (t, 4H, J=7.9Hz) ppm 7.73 (d, 4H, J=5.8Hz) ppm 7.57 (d, 1H, J=5.8Hz) ppm 7.53 (d, 1H, J=5.8Hz) ppm 7.48 (t, 2H, J=4.4Hz) ppm 7.39 (m, 4H) ppm 7.24 (t, 2H, J=6.0Hz) ppm 4.66 (dt, 4H, J=3.0Hz, J=7.8Hz) ppm 2.90 (d, 2H, J=7.1Hz) ppm 2.86 (d, 2H, J=7.2Hz) ppm 2.54 (s, 3H) ppm 2.52 (s, 3H) ppm 2.11 (m, 4H) ppm 1.83 (m, 4H) ; ESI-MS: m/z found : [M^{4+}/4, 255.0758], [M^{4+}+PF₆⁻/3, 388.4272] and [M^{4+}+2PF₆⁻/2, 655.1365]. (Figure 12 and 13).
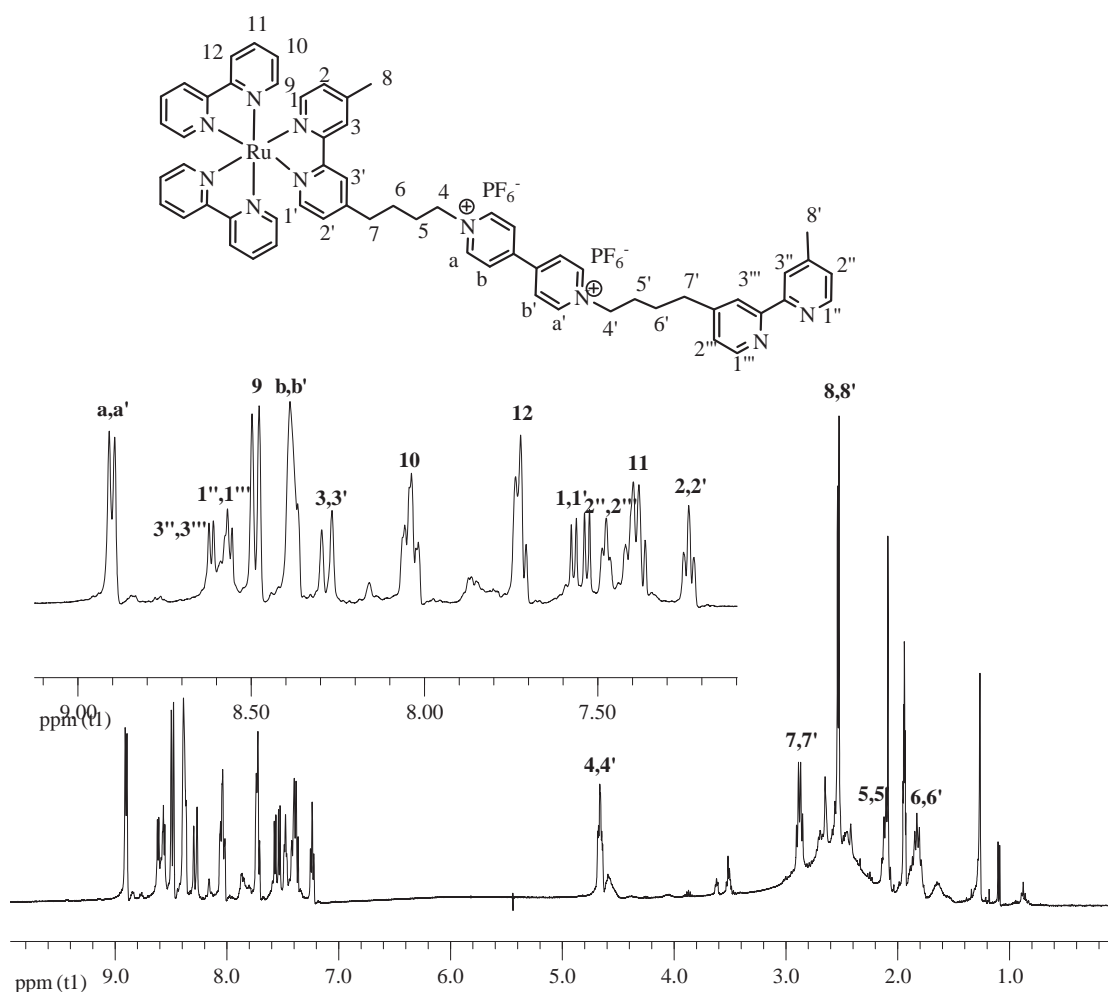
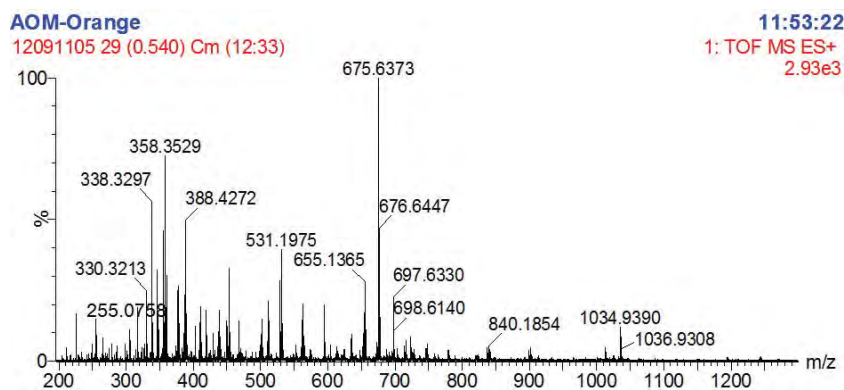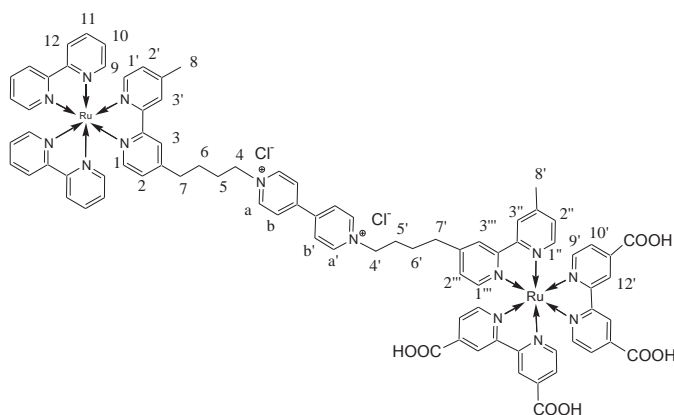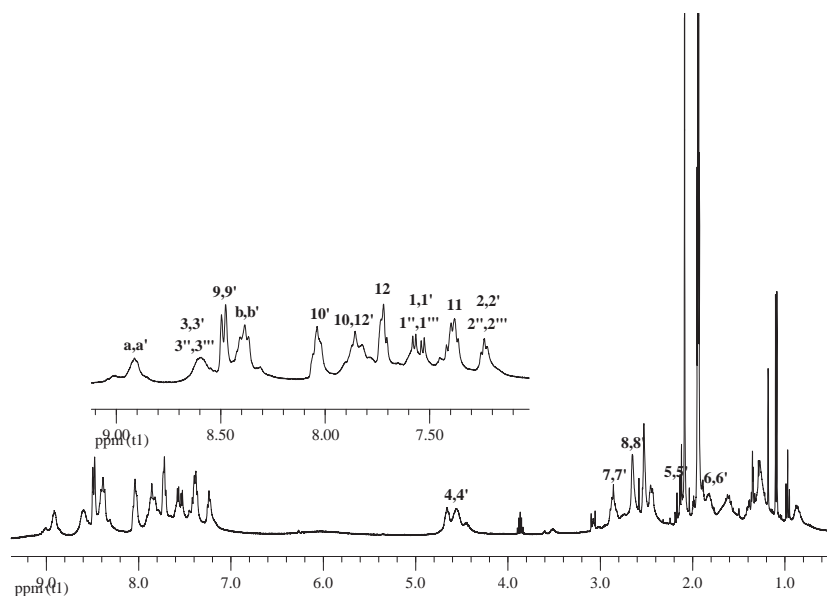**Figure 12** ^{1}H-NMR spectrum of **L3a** in CD₃CN (400MHz).
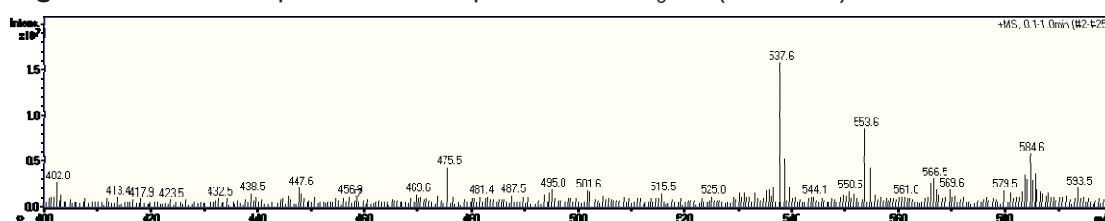
Figure 13 ESI-MS spectrum of **L3a**.

(6) Synthesis of Ru(bpy)₃-viologen-Ru(dcbpy)₂bpy (2)

Ru(bpy)₃-viologen-Ru(dcbpy)₂(bpy) (**2· 6PF₆⁻**): Ru(dcbpy)₂Cl₂ 17.00 mg (0.03 mmol) and compound **L3c· 4PF₆⁻** 22.00 mg (0.02 mmol), which was changed to **L3c· 4Cl⁻** by using tetrabutyl ammoniumchloride (Bu₄NCl⁻), were dissolved in 10 ml of water. Then the mixture was heated at 90°C under N₂ atmosphere for 2 days. The product was changed to PF₆⁻ and recrystallized by using acetone and dichloromethane. The red solid was isolated from solution by centrifugation. The red solid was obtained (yield 57%). ^{1}H-NMR (400 MHz, CD₃CN) δ ppm 8.91 (s, 4H) ppm 8.60 (s, 4H) ppm 8.49 (d, 4H, J=8.1Hz) ppm 8.39 (m, 8H) ppm 8.04 (t, 4H, J=7.5Hz) ppm 7.85 (m, 8H) ppm 7.72 (m, 4H) ppm 7.57 (d, 2H, J=5.8Hz) ppm 7.53 (d, 2H, J=5.8Hz) ppm 7.40 (m, 4H) ppm 7.24 (m, 4H) ppm 4.61 (m, 4H) ppm 2.87 (m, 4H) ppm 2.65 (s, 3H) ppm 2.53 (s, 3H) ppm 2.12 (m, 4H) ppm 1.81 (m, 4H); FT-IR: cm^{-1} found : [O-H stretch, 3475], [C=O, 1735], [C-O, 1217], [C=C, 1603], [C=N, 1637 and 1654], [C-N, 1354] and [C-H bend of aromatic, 841] (Figure 14 and 15).
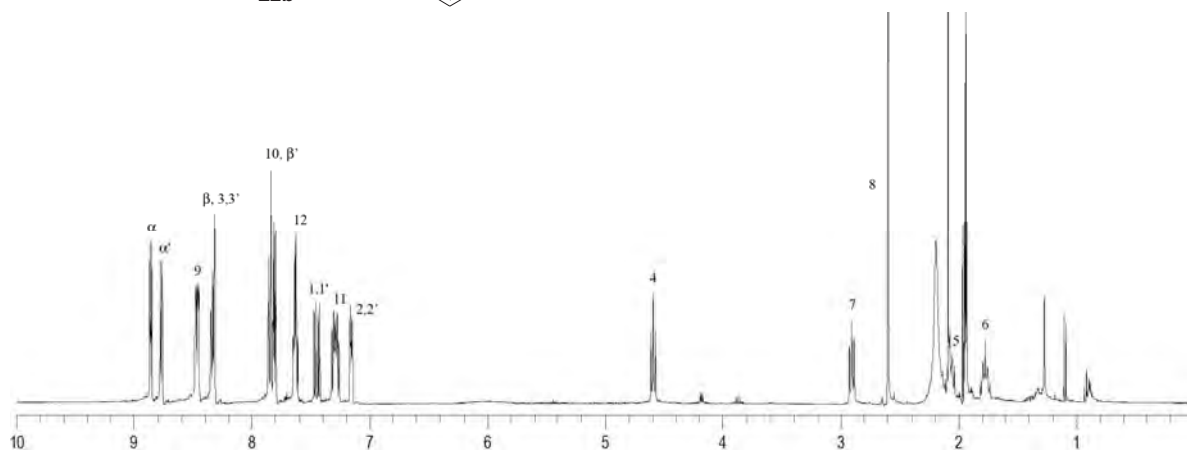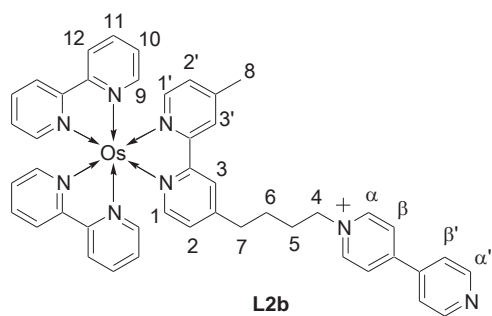
Figure 14. ^{1}H-NMR spectrum of compound **2** in CD$_3$CN (400 MHz).

Figure 15. ESI-MS spectrum of **2**.

(6) Synthesis of Os(bpy)$_3$-Viologen (L2b $\cdot$ 3PF$_6^-$)

Os(bpy)$_3$-viologen (**L2b** $\cdot$ **3PF$_6^-$**) was synthesized by using compound **L1** 0.50 g (0.95 mmol) and Os(bpy)$_2$Cl$_2$ 0.46g (0.79 mmol) were refluxed in 30 ml of (1:1, v/v) ethanol/water under N$_2$ atmosphere at 110°C for 24 hours. After that saturated aqueous solution of ammonium hexafluorophosphate (NH$_4$PF$_6$) was added in the cooled reaction mixture and isolated by filtration. The crude product was purified by column chromatography using silica gel and a mixture of CH$_3$CN/sat.KNO$_3$/H$_2$O as an eluent. The dark green solid was obtained (yield 63%). ^{1}H-NMR (400 MHz, CD$_3$CN) δ ppm 8.86 (dd, 2H, J=4.5Hz, J=1.7Hz) ppm 8.77 (d, 2H, J = 6.7Hz) ppm 8.46 (dd, 4H, J= 7.9Hz, J=2.9Hz) ppm 8.35 (s, 1H) ppm 8.33 (s, 1H) ppm 8.32 (s, 2H) ppm 7.84 (t, 4H, J=7.9Hz, J=7.9 Hz) ppm 7.80 (dd, 2H, J=4.5Hz, J=1.7Hz) ppm 7.67 (m, 4H) ppm 7.45 (dd, 2H, J=13.1Hz, J=5.9Hz) ppm 7.34 (m, 4H) ppm 7.16 (d, 2H, J=5.9Hz) ppm 4.59 (t, 2H, J=7.5Hz, J=7.5Hz) ppm 2.93 (m, 2H) ppm 2.60 (s, 3H) ppm 2.08-2.02 (m, 2H) ppm 1.83-1.73 (m, 2H) ; ESI-MS: m/z found : [M^{3+}/3, 295.1180], [M^{3+}+PF$_6^-$/2, 515.1345] and [M^{3+}+2PF$_6^-$/1, 1175.1862] (Figure 16 and 17).

Figure 16 ^{1}H-NMR spectrum of compound **L2b** in CD$_3$CN (400 MHz).
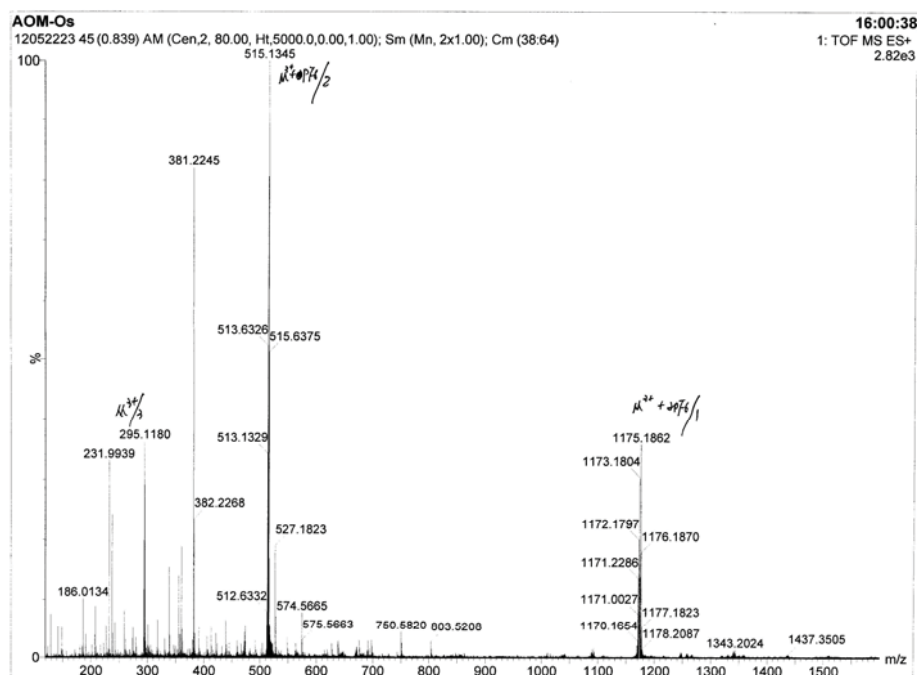
Figure 17. ESI-MS spectrum of compound **L2b** in acetonitrile.

(7) Os(bpy)$_3$-viologen-bpy (L3b $\cdot$ 4PF$_6^-$)

Os(bpy)$_3$-viologen-bpy (**L3b** $\cdot$ **4PF$_6^-$**): Compound **L2b** $\cdot$ **3PF$_6^-$** 142.00 mg (0.11 mmol) and compound **a** 130.00 mg (0.43 mmol) were refluxed in acetonitrile under N$_2$

atmosphere at 90°C for 5-6 days. The crude product was changed to PF_6^- and then purified by column chromatography using Sephadex LH20 and acetonitrile as an eluent. The dark green solid was obtained (yield 83%). ^{1}H-NMR (400 MHz, CD$_3$CN) δ ppm 8.90 (dd, 4H, J=2.0Hz, J=7.0Hz) ppm 8.66 (d, 1H, J=5.4Hz) ppm 8.61 (d, 1H, J=5.4Hz) ppm 8.46 (dd, 4H, J=3.4Hz, J=8.3Hz) ppm 8.39 (d, 4H, J=6.5Hz) ppm 8.35 (s, 2H) ppm 8.33 (s, 1H) ppm 8.29 (s, 1H) ppm 7.83 (t, 4H, J=7.9Hz) ppm 7.63 (m, 6H) ppm 7.47 (d, 1H, J=6.0Hz) ppm 7.43 (d, 1H, J=5.9Hz) ppm 7.29 (m, 4H) ppm 7.16 (t, 2H, J=4.2Hz) ppm 4.65 (m, 4H) ppm 2.92 (m, 4H) ppm 2.61 (s, 3H) ppm 2.60 (s, 3H) ppm 2.12 (m, 4H) ppm 1.82 (m, 4H); ESI-MS: m/z found: $[M^{4+}+PF_6^-/3, 418.4577]$ and $[M^{4+}+2PF_6^-/2, 697.6472]$ (Figure 18 and 19).
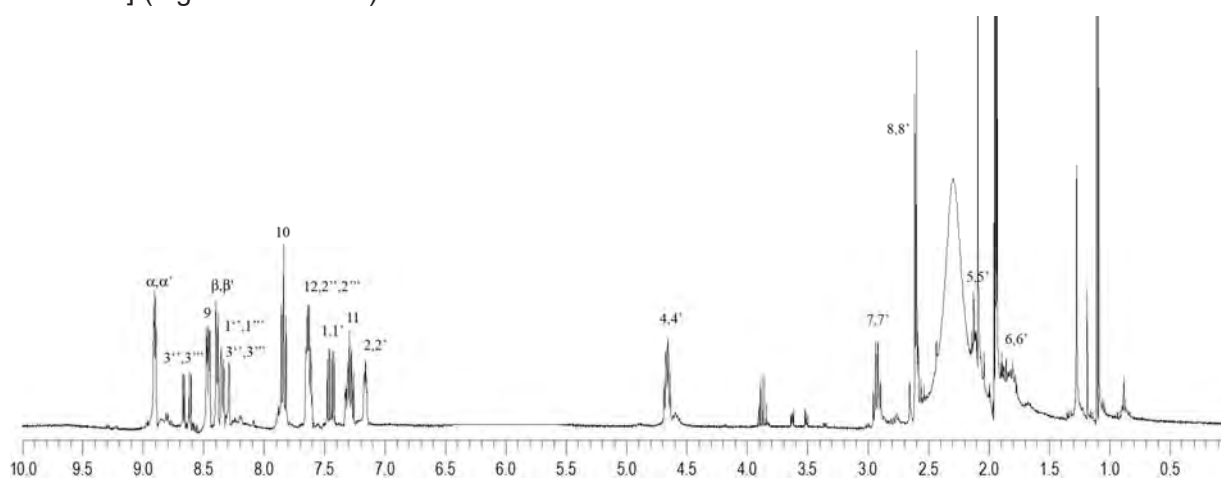
Figure 18. ^{1}H-NMR spectrum of compound **L3b** in CD$_3$CN (400 MHz).
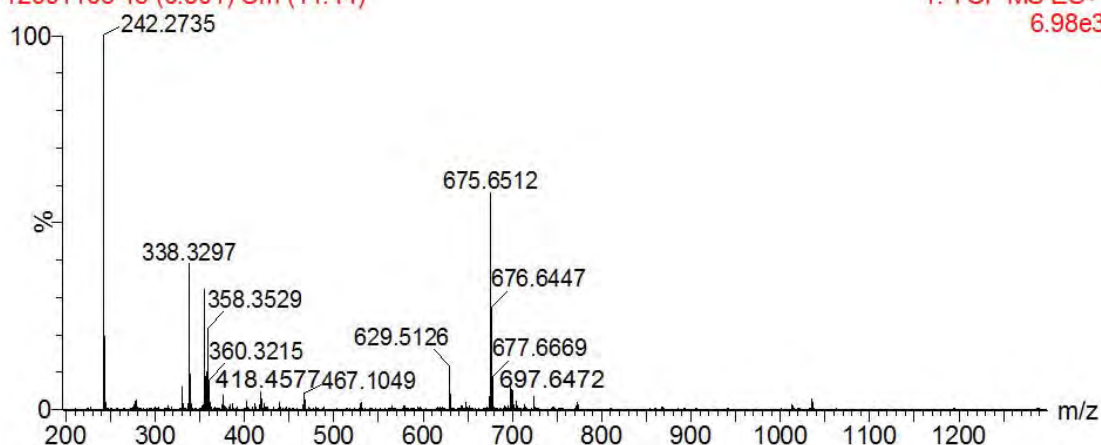
Figure 19. ESI-MS spectrum of compound **L3b** in acetonitrile.

(8) Synthesis of Os(bpy)$_3$-viologen-Ru(bpy)$_3$ (1$\cdot$ 6PF$_6^-$)

Os(bpy)$_3$-viologen-Ru(bpy)$_3$ **(1$\cdot$ 6PF$_6^-$)**: Compound **L3b**$\cdot$ 4PF$_6^-$ 75.20 mg (0.06 mmol) changed to **L3b**$\cdot$ 4Cl$^-$ by using Bu$_4$NCl, and Ru(bpy)$_2$Cl$_2$ 30.00 mg (0.06 mmol) was heated at 90°C in water under N$_2$ atmosphere for 3 h. The reaction mixture was

converted to PF_6^- counter ion and isolated by filtration. The crude product was purified by column chromatography using silica gel and a mixture of $CH_3CN/sat.KNO_3/H_2O$ as an eluent. The product was obtained as dark green solid (35%). ^{1}H-NMR (400 MHz, CD_3CN) δ ppm 8.94 (d, 4H, J = 6.7Hz), 8.51 (d, 4H, J = 7.9Hz), 8.48 (d, 4H, J = 3.1Hz), 8.42 (d, 4H, J = 6.6Hz), 8.39 (s, 2H), 8.37 (s, 2H), 8.06 (m, 4H), 7.86 (t, 4H, J = 7.9Hz), 7.74 (t, 4H, J = 6.4Hz), 7.65 (m, 4H), 7.59 (d, 1H, J = 5.8Hz), 7.55 (d, 1H, J = 5.8Hz), 7.49 (d, 1H, J = 5.8Hz), 7.45 (d, 1H, J = 6.0Hz), 7.40 (m, 4H), 7.33 (m, 4H), 7.26 (m, 2H), 7.18 (t, 2H, J = 4.5Hz), 4.68 (t, 4H, J = 7.5Hz), 2.95 (m, 4H), 2.62 (s, 3H), 2.54 (s, 3H), 2.13 (m, 4H), 1.83 (m, 4H). HR-MS was found at m/z 1051.1 for $[M^{6+}+4PF_6^-/2,]$ (Figure 20a and 21).
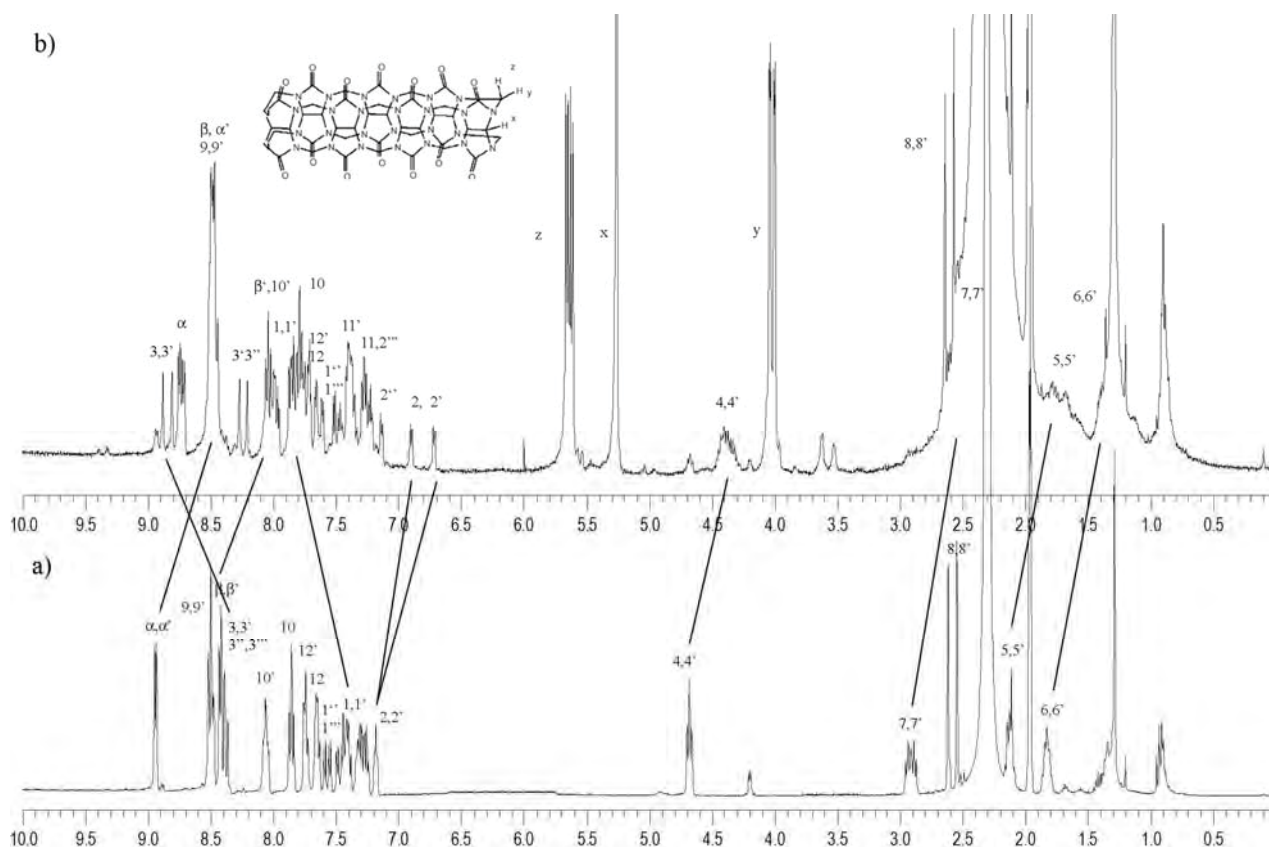
Figure 20. ^{1}H-NMR spectrum of (a) **1** and (b) **1**⊂CB[7] in CD_3CN (400 MHz).
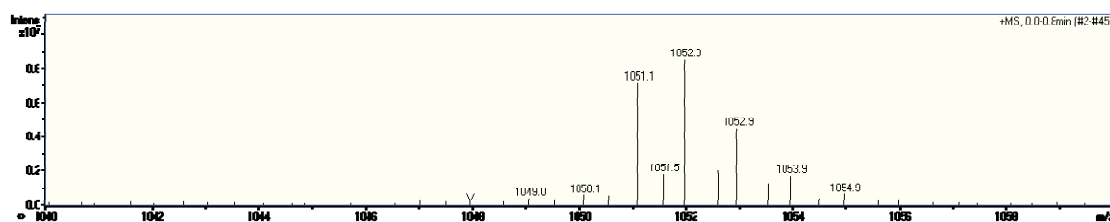
Figure 21. ESI-MS spectrum of compound **1** in acetonitrile.

(9) Synthesis of Os(bpy)₃-viologen-Ru(bpy)₃⊂CB[7] (1⊂CB[7] · 6PF₆⁻)

Os(bpy)₃-viologen-Ru(bpy)₃⊂CB[7] (1⊂CB[7] · 6PF₆⁻): Compound **L3b·** 4PF₆⁻ 20.00 mg (0.02 mmol) was changed to **L3b·** 4Cl⁻ by using Bu₄NCl and then dissolved in water. CB[7] 22.00 mg (0.02 mmol) was added in the solution. Ru(bpy)₂Cl₂ 10.00 mg (0.02 mmol) was also added to the solution mixture and then heated at 90°C under N₂ atmosphere for 3 h. The counter ion was changed to PF₆⁻. The crude product was purified by dissolving in small amount of acetone then added into dichloromethane to precipitate. The red product was isolated from solution by centrifugation and washed with dichloromethane. The product was obtained as dark green solid (55%). ¹H-NMR (400 MHz, CD₃CN) δ ppm 8.88 (s, 1H), 8.81 (s, 1H), 8.73 (dd, 4H, *J* = 6.5Hz, *J* = 12.8Hz), 8.49 (m, 12H), 8.27 (s, 1H), 8.21 (s, 1H), 8.01 (m, 4H), 7.86 (dd, 2H, *J* = 6.1Hz, *J* = 9.4Hz), 7.78 (m, 4H), 7.72 (m, 4H), 7.64 (dd, 4H, *J* = 5.4Hz, *J* = 21.3Hz), 7.52 (d, 1H, *J* = 5.7Hz), 7.48 (d, 1H, *J* = 6.4Hz), 7.39 (m, 4H), 7.27 (m, 4H), 7.22 (d, 1H, *J* = 5.1Hz), 7.14 (d, 1H, *J* = 5.8Hz), 6.90 (d, 1H, *J* = 5.6Hz), 6.72 (d, 1H, *J* = 6.0Hz), 5.64 (dd, 14H, *J* = 7.5Hz, *J* = 15.0Hz), 5.26 (s, 14H), 4.36 (m, 4H), 4.02 (dd, 14H, *J* = 3.1Hz, *J* = 14.9Hz), 2.64 (s, 3H), 2.61 (m, 4H), 2.57 (s, 3H), 1.71 (m, 4H), 1.39 (m, 4H). ESI-MS was found at *m/z* 447.6 for [M⁶⁺/6] (Figure 20b and 22).
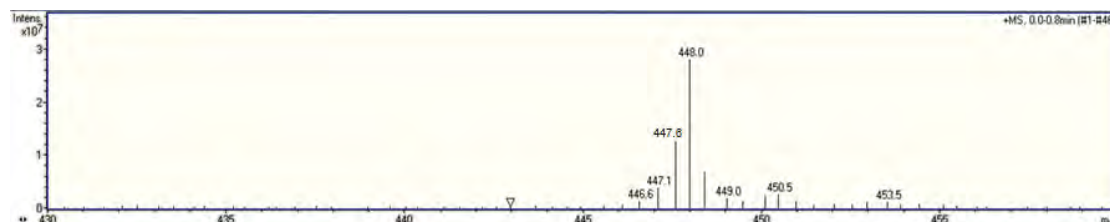
Figure 22. ESI-MS spectrum of compound **1**⊂CB[7] in acetonitrile.

(10) Synthesis of Ru(bpy)₃-viologen-Ru(dcbpy)₂(bpy) (2· 6PF₆⁻)

Ru(bpy)₃-viologen-Ru(dcbpy)₂(bpy) (2· 6PF₆⁻): Ru(dcbpy)₂Cl₂ 17.00 mg (0.03 mmol) and compound **L1c·** 4PF₆⁻ 22.00 mg (0.02 mmol), which was changed to **L1c·** 4Cl⁻ by using tetrabutyl ammoniumchloride (Bu₄NCl⁻), were dissolved in 10 ml of water. Then the mixture was heated at 90°C under N₂ atmosphere for 2 days. The product was changed to PF₆⁻ and recrystallized by using acetone and dichloromethane. The red solid (complex 1) was isolated from solution by centrifugation. The red solid was obtained (yield 57%). ¹H-NMR (400 MHz, CD₃CN) δ ppm 8.91 (s, 4H) ppm 8.60 (s, 4H) ppm 8.49 (d, 4H, J=8.1Hz) ppm 8.39 (m, 8H) ppm 8.04 (t, 4H, J=7.5Hz) ppm 7.85 (m, 8H) ppm 7.72 (m, 4H) ppm 7.57 (d, 2H, J=5.8Hz) ppm 7.53 (d, 2H, J=5.8Hz) ppm

7.40 (m, 4H) ppm 7.24 (m, 4H) ppm 4.61 (m, 4H) ppm 2.87 (m, 4H) ppm 2.65 (s, 3H) ppm 2.53 (s, 3H) ppm 2.12 (m, 4H) ppm 1.81 (m, 4H); FT-IR: cm^{-1} found : [O-H stretch, 3475], [C=O, 1735], [C-O, 1217], [C=C, 1603], [C=N, 1637 and 1654], [C-N, 1354] and [C-H bend of aromatic, 841] (Figure 23 and 24).
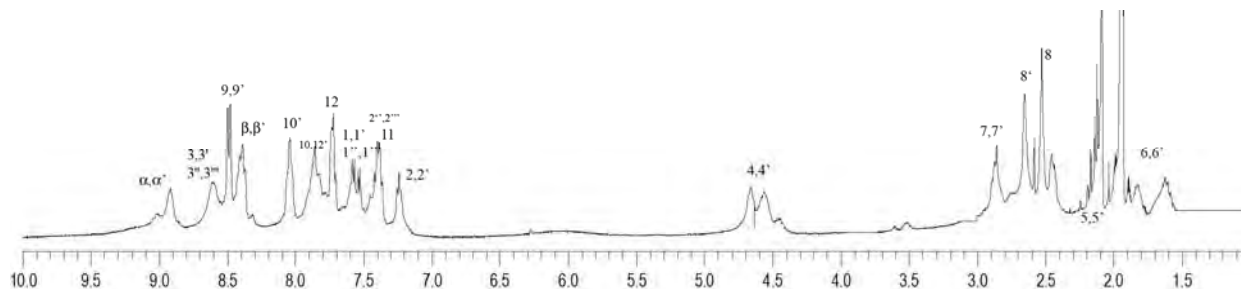
Figure 23. ^{1}H-NMR spectrum of compound **2** in CD$_3$CN (400 MHz).
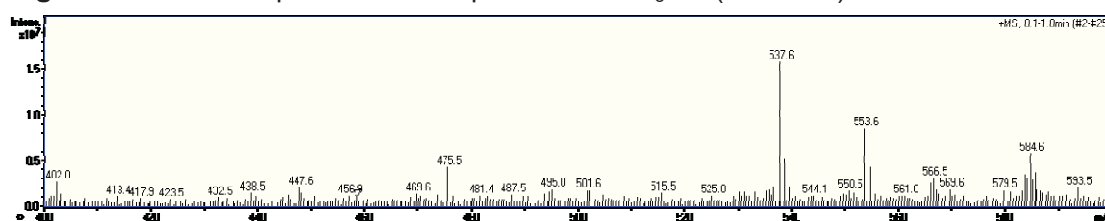
Figure 24. ESI-MS spectrum of compound **2** in acetonitrile.

(11) Synthesis of Os(bpy)$_3$-viologen-Ru(dcbpy)$_2$(bpy) (3· 6PF$_6^-$)

*Os(bpy)$_3$-viologen-Ru(dcbpy)$_2$(bpy) (**3**· **6PF$_6^-$**):* This complex was synthesized from Ru(dcbpy)$_2$Cl$_2$ 10.00 mg (0.02 mmol) and compound **L2c· 4PF$_6^-$** 19.30 mg (0.02 mmol) and then purified by the same method as complex **2**. The dark green solid was obtained (yield 31%). ^{1}H NMR (400 MHz, CD$_3$CN) δ ppm 9.01 (d, 2H, J=6.1Hz) ppm 8.90 (d, 2H, J=6.9Hz) ppm 8.46 (dd, 4H, J=3.4Hz, J=8.3Hz) ppm 8.39 (d, 4H, J=6.6Hz) ppm 8.35 (s, 2H) ppm 8.33 (s, 2H) ppm 7.92 (t, 4H, J=4.7Hz) ppm 7.86 (m, 4H) ppm 7.81 (m, 4H) ppm 7.63 (m, 4H) ppm 7.47 (d, 2H, J=5.8Hz) ppm 7.43 (d, 2H, J=5.9Hz) ppm 7.28 (m, 8H) ppm 7.16 (m, 4H) ppm 4.65 (m, 4H) ppm 2.87 (m, 4H) ppm 2.60 (s, 3H) ppm 2.53 (s, 3H) ppm 2.10 (m, 4H) ppm 1.81 (m, 4H) ; FT-IR: cm^{-1} found : [O-H stretch, 3489], [C=O, 1736], [C-O, 1216], [C=C, 1590], [C=N, 1637 and 1655], [C-N, 1354] and [C-H bend of aromatic, 839] (Figure 25 and 26).
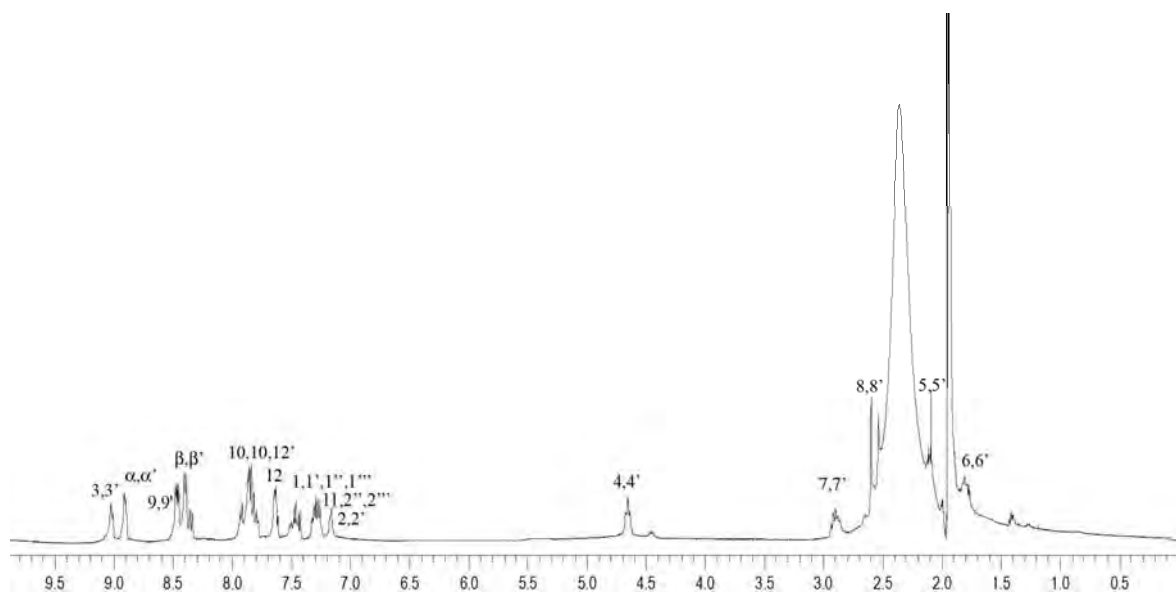
Figure 25. ^{1}H-NMR spectrum of compound **3** in CD_3CN (400 MHz).
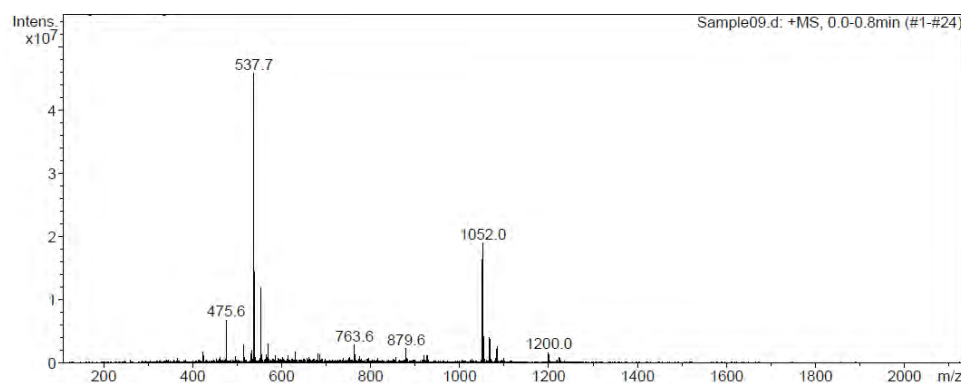
Figure 26. ESI-MS spectrum of compound **3** in acetonitrile.

(12) Synthesis of Co(bpy)$_3$-Viologen

Co(bpy)$_3$-Viologen has been synthesized by reflux compound **a** with Co(bpy)$_2$Cl$_2$ in H$_2$O at 90 $^\circ$C for 5 hours. The reaction mixture was changed to PF$_6$ then purified by silica gel column chromatography. The ^{1}H-NMR and MS show that no desire product was detected. The results indicated that reaction was failed. Thus, no Co complex has been further done.

Results and Discussion

Syntheses. Complexes **1**, **1⊂CB[7]**, **2** and **3** were successfully synthesized following the synthetic pathway as shown in Scheme 1. The preparation of compound **A** and ligands **L1**-**L3** followed the previously developed procedure as discussed above. The complexes **2** and **3** could be synthesized by coordinating **L3a** and **L3b** ligands with

Ru(dcbpy)$_2$Cl$_2$), respectively. While complex **1** was prepared by coordinating **L3b** ligands with [Ru(bpy)$_2$Cl$_2$)] in degassed H$_2$O.

The synthesis of rotaxane **1**⊂CB[7] followed the same procedure as complex **1**, but CB[7] was added to **L3b** ligand prior to the treatment with [Ru(bpy)$_2$Cl$_2$)]. The binding between CB[7] host and **L3b** ligand could be detected by ^{1}H NMR spectroscopy (Figure 17). The solution of **L3b** ligand and Ru(bpy)$_3$Cl$_2$ in the present of CB[7] was stirred for 5 h at 90 °C followed the previous work[7], yielding the crude product **1**⊂CB[7]·6Cl$^-$. The complexes **1-3** were first isolated in Cl$^-$ counter ion form. The complexes were change to PF$_6^-$ and followed by purification with column chromatography on silica gel. The chemical structure of complexes **2**, **3** and rotaxane **1**⊂CB[7] were confirmed by NMR spectroscopy and ESI-MS. Synthetic details for the meal complexes are shown in the supporting information.

Unfortunately, the attempt to synthesize **2**⊂CB[7] and **3**⊂CB[7] using the similar procedure to **1**⊂CB[7] was not successful probably due to the formation of hydrogen bonding between carboxyl group and CB[7].[8] As a result, viologen could not insert into the CB[7] cavity and therefore the inclusion complex of these compounds could not be formed.

Characterization of the complexes. **L1** and **L2a** show the expected [1]H-patterns as previous work.[9] The ^{1}H-NMR spectrum of **L2b** shows the expected pattern of a 2,2'-bipyridine moiety coordinated to Os metal (Figure 15). As a result, a doublet at δ = 7.16 ppm is assigned to H2/H2' whereas two doublets at δ = 7.42 and 7.47 ppm are assigned to H1 and H1', respectively. Two singlets at δ = 8.35 and 8.33 ppm are also assigned to H3 and H3'. After **L2b** connected to the second bipyridine moiety obtaining **L3b**, the signals at δ = 8.66 and 8.61ppm are assigned to H1'' and H1''' whereas H2''/H2''' and H3''/ H3''' are at δ = 7.63 and 8.46 ppm, respectively. The signals of H1/H1' and H2/H2' which connected to Ru metal remain the same position as those of **L2b** (Figure 17).

The ^{1}H-NMR spectrum of complex **1** shows two patterns of two asymmetric 2,2'-bipyridine moieties (Figure 20a). Doublets at δ = 7.26 and 7.18 ppm assigned to H2/H2' and H2''/ H2''', respectively. The signals of proton H1/H1'and H1''/H1''' appear as two doublet of doublets at δ = 7.49-7.45 and 7.59-7.55 ppm, respectively. Two

singlets at δ = 8.37 and 8.39 ppm are also assigned to H3/H3' and H3''/H3''', respectively.

The position of CB[7] host was determined by comparing complex 1⊂CB[7] to compound **1**. The H1/H1' and H3/H3' of bipyridine moiety shift downfield whereas only H2/H2' of substituted bipyridine split to two signals and undergo an upfield shift from δ = 7.18 to 6.90 ppm for H2 and to 6.72 ppm for H2' (Figure 20b). All protons of viologen moiety and butyl chain shift upfield. The α' and β' protons shift from δ = 8.94 and 8.48 to 8.49 and 8.01 ppm, respectively. The H4 and H7 methylene protons shift from δ= 4.68 and 2.95 to 4.36 and 2.57 ppm; the H5 and H6 protons shift from δ =2.13 and 1.83 to 1.71 and 1.39 ppm. All bipyridine protons connected to Os and Ru metals remain at the same position as in complex **1**. The upfield shifts of complexation-induced chemical shift are observed for guest protons that are located in the interior cavity of CB, whereas the downfield shifts are associated with guest protons located near the carbonyl oxygen atom on the CB host.[10] This behavior indicates the formation of the rotaxane with CB[7] residing in the butylmethylene chain in acetonitrile. Since the H2/H2' show the upfield shift whereas H2''/H2''' still remain in the same position as those in complex **1**. The result indicats that CB[7] prefers location near osmium to ruthenium moiety. However, the signals of butyl protons became too board in the presence of CB[7] and are unable to be distinguished between two sides of butyl chain. These results significantly suggest that the host can move dynamically along the entire rotaxane chain with the preferable position with is on the butyl chain of the Os side as discussed above.

The ^{1}H-NMR spectra of complexes **2** and **3** show the similar pattern to a 2,2'-bipyridine moiety in **L3b**. For complex **2**, H1/H1' and H1''/H1''' appear in the same position at δ = 7.57-7.53 ppm as doublet of doublet. The signals at 7.24 and 7.39 ppm are assigned to H2/H2' and H2''/H2''', respectively. The signals of H3/H3' and H3''/H3'' are shown at δ = 8.59 ppm as a broad singlet (Figure 23). In the case of complex **3** (Figure 25), H1/H1' and H1''/H1''' appear at δ = 7.51-7.46 ppm. The signals at δ = 7.28 and 7.16 ppm are assigned to H2''/H2''' and H2/H2', respectively. The proton H3/H3' and H3''/H3''' are completely separated each other which are shown as doublet at δ = 9.01 ppm for H3''/H3''' and 8.33 ppm for H3/H3'. The Hα/Hα' and Hβ/Hβ' protons of **2**

and **3** appear in the same positions at δ = 8.90 and 8.46 ppm, respectively. The butyl protons of both **2** and **3** are shown as board signals.

Electrochemistry. The cyclic voltammogram for complex **1** shows oxidation waves at 0.95 and 0.45 V vs Ag/AgNO$_3$ in acetonitrile as shown in Figure 27a. The first value corresponds to the oxidation of Ru^{2+} to Ru^{3+}, whereas the second value corresponds to Os^{2+} to Os^{3+}.[11] For the inclusion rotaxane **1**⊂CB[7] (Figure 27b), two oxidation waves are also observed. The first oxidation potential of rotaxane **1**⊂CB[7] is 0.35 V versus Ag/AgNO$_3$, corresponding to Os^{3+} to Os^{2+} which is around 100 mV lower than that of **1**, whereas the second oxidation potential is 0.95 V versus Ag/AgNO$_3$, corresponding to Ru^{2+} to Ru^{3+}, which is the same as complex **1**. This result strongly suggests that CB[7] positions on the butyl chain near Os(bpy)$_3$ side. The ^{1}H-NMR spectrum shows a dynamic movement of CB[7] host along the entire chain in preference to the Os side as shown in schemes 2a and 2b. The [Os(bpy)$_3$] moiety is easier to oxidize, probably contact with CB[7] is oxidized first due to the polar cavity edge can stabilize the higher oxidation state Os^{3+}, thus forming a Os^{3+}- CB - V$^{+\bullet}$-Ru^{2+} (Scheme 2c).

(a)

Ru^{2+} V^{2+} Os^{2+}

(b)

Electrochemical oxidation

Ru^{2+} Os^{3+}

(c)
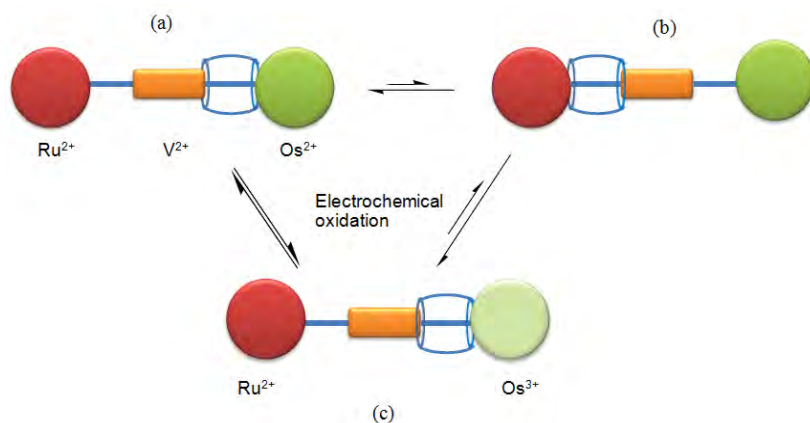
Scheme 2. Selective positioning of the CB[7] host during the oxidation of **1**⊂CB[7] in acetonitrile.

In cathodic scan of complex **1** compared to **1**⊂CB[7], redox couples exhibit two successive one-electron reduction waves (Figure 7a and 7b). The V^{2+} moiety shows two reversible waves. The first wave corresponds to the reversible reduction of V^{2+}→ V$^{+\bullet}$, whereas the second wave shows the reversible reduction of V$^{+\bullet}$ → V^0. For complex **1**, the first and second reduction are observed at -0.75 and -1.15 V, whereas -0.90 and -1.30 V are investigated for **1**⊂CB[7]. These results indicate that the viologen

moiety is more difficult to reduce when the inclusion complex with CB[7] is formed as observed in the previous work. [7]
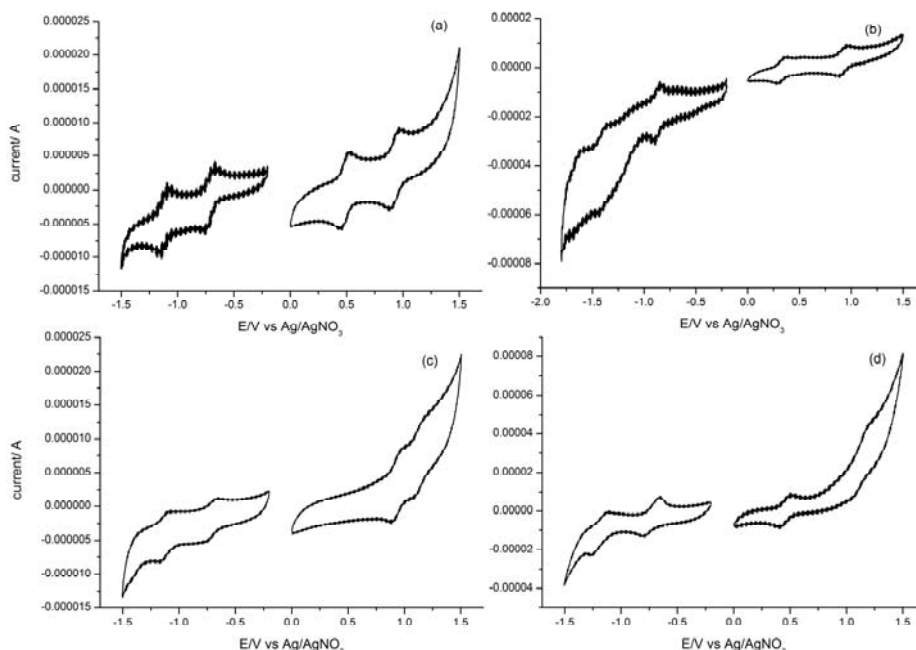
Figure 27. Cyclic voltammograms of (a) complex **1** (b) rotaxane **1**⊂CB[7], (c) complex **2** and (d) complex **3**.

Moreover, the cyclic votammogram of **3** is investigated compared to that of **1** (Figure 27d). The first oxidation potential of Os^{2+} to Os^{3+} is the same as complex **1** at 0.45 V whereas the second oxidation potential of Ru^{2+} to Ru^{3+} is observed at 1.15 V, around 200 mV higher that of **1**. This could be implied that Ru^{3+} with electron withdrawing carboxylic group is more difficult to oxidize. In addition, two reversible cathodic waves are also observed for **3** at -0.75 and 1.15 V corresponding to $V^{2+} \rightarrow V^{+\bullet}$ and $V^{+\bullet} \rightarrow V^{0}$, respectively, which are the same as those of complex **1**. These results suggest that the electron withdrawing carboxylic group has no effect on the reduction property of viologen.

In the case of complex **2** (Figure 27c), the second oxidation potential is also observed at 1.15 V corresponding to the oxidation of $Ru^{2+}COOH$ to $Ru^{3+}COOH$ similar to that of complex **3** whereas oxidation potential of no substituted Ru^{2+} is observed at 0.90 V similar to that of $Ru^{2+}(bpy)_3$-viologen-$Ru^{2+}(bpy)_3$. [7] The cathodic wave pattern is similar

to that of complexes **1** and **3**. Two reversible cathodic processes are observed at -0.75 and -1.15 V.

From the above observations, we can conclude that the reversible potentials for oxidation process of compounds **1-3** are strongly dependent on the central metal ion and the substituent in the bipyridine ligand. The Os complexes are easier to oxidize than their Ru counterparts, which is consistent with the general redox properties of third-row vs second-row transition methal complexes.[12,13]

Absorption and Luminescence. Ru bipyridine complexes exhibit characteristic MLCT absorption band (Ru→bpy) around 450 nm.[14] The Os counterparts also exhibit the MLCT absorption in a similar wavelength. In addition to this spin-allowed transition, Os bipyridine complexes feature spin forbidden MLCT absorption in 500-700 nm region, owing to the heavy atom effect.[13] The electronic absorption spectra for complexes **1-3** and **1**⊂CB[7] in acetonitrile are shown in Figure 28a. Absorption maxima, extinction coefficient and emission quantum yield at room temperature are reported in Table 1. The absorption band at $\lambda \approx$ 450-460 nm of **1-3** is assigned to the MLCT of Ru/Os→bpy transitions and the strong $\pi-\pi^*$ ligand-centered band absorption is observed at 280 nm.[14] The absorption of V^{2+} was found at 250 nm.[13] The absorption spectra of complex **1** and rotaxane **1**⊂CB[7] are similar whereas the Os→bpy MLCT bands of complexes **2** and **3** with attachment of the carboxyl groups is slightly red shifted to 459 and 463 nm, respectively.

The excited state behaviors of these four complexes are also studied using the luminescence emission spectra (Figure 28b). However, the emission intensity of rotaxan **1**⊂CB[7] shows a red shift and increase in the intensity about 4 times compared to that of complex **1**. The blocking the contact between donor and acceptor by CB[7] causes an increase in the distance between Ru(bpy)$_3$ and V^{2+} quencher, thus, the emission quantum yield increases. In addition, the intramolecular electron transfer is hindered by the polar cavities of the host.[9,15] This is also confirmed by electrochemical properties that redox potentials of the viologen are more difficult to reduce when included in the CB[7] host.

Table 1 Photophysical properties of complex 1, rotaxane **1⊂CB[7]** , complexes **2** and **3** in acetonitrile.

compounds	Absorption λ_{max} (nm) ($\varepsilon \times 10^4$ [M^{-1}cm^{-1}])	Emission λ_{max} [nm]	Fluorescence quantum yield (ϕ_f)
1	301 (1.70), 453 (1.57)	617	0.001
1⊂CB[7]	309 (1.56), 452 (1.77)	627	0.004
2	308 (1.78), 455 (1.69)	640	0.002
3	313 (1.82), 475 (1.44)	656	0.002

[a] shoulder. [b] excited wavelength was 450 nm for complex **1**, **1⊂CB[7]** and **2** and 475 nm for complex **3**. [c] {Ru(bpy)$_3$]•2PF$_6$ was used as reference (ϕ_f=0.07).[16]

In the case of complexes **2** and **3**, ruthenium and osmium bipyridine with carboxyl groups show the red shift in absorption and emission spectra due to the extending of π electron from the carbonyl groups. Their emission quantum yields are similar to that of **1**.
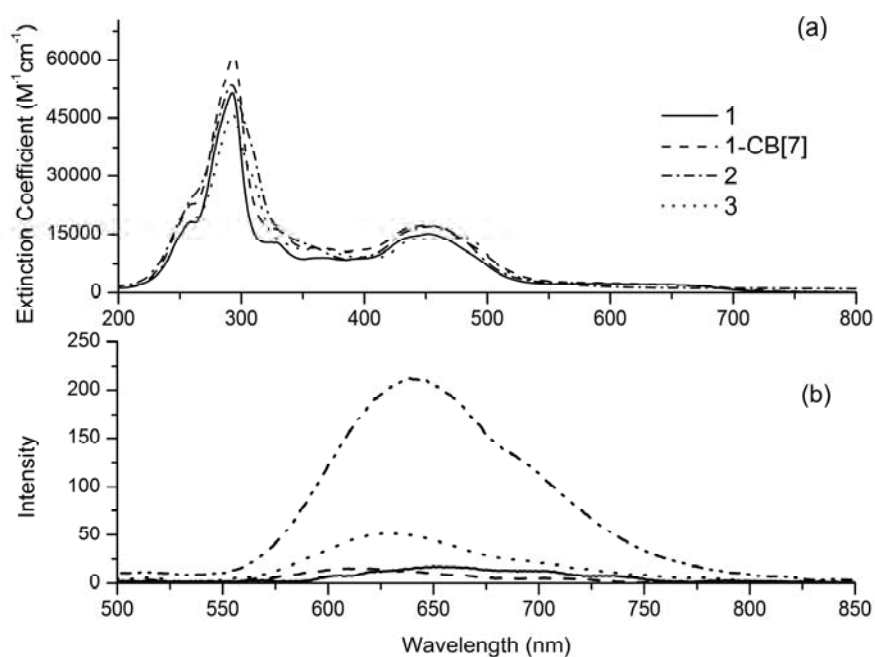

Figure 28. (a) absorption and (b) emission of complex **1-3** and **1⊂CB[7]** in acetonitrile.

Photo-induce formation of viologen radical. The viologen radical formation of all complexes was investigated in acetonitrile by using UV/Vis spectrometry. All complexes were irradiated in the presence of triethanolamine (TEOA) as an external electron donor. When the viologen radical formed, the solution color changed from orange to green. The characteristic absorption peaks of viologen radical at 399 and 603 are observed after 55 min irradiation for complex **1** (Figure 29a).[17] The viologen radical of **1**⊂CB[7] is observed after irradiating for 60 min (Figure 29b). However, the concentration of **1**⊂CB[7] has to be silightly higher otherwise the viologen radical could not be detected. These results suggested that viologen radical in the presence of CB[7] is took a longer time to form in acetonitrile than that of complex **1**. These results are in good agreement with the result from electrochemistry that the viologen with CB[7] is more difficult to reduce.

As shown in Figure 29c and 29d, the viologen radicals of complexes **2** and **3** are formed at 15 and 35 min, respectively. These result suggest that the viologen radical could be stabilized with the carboxylic groups.
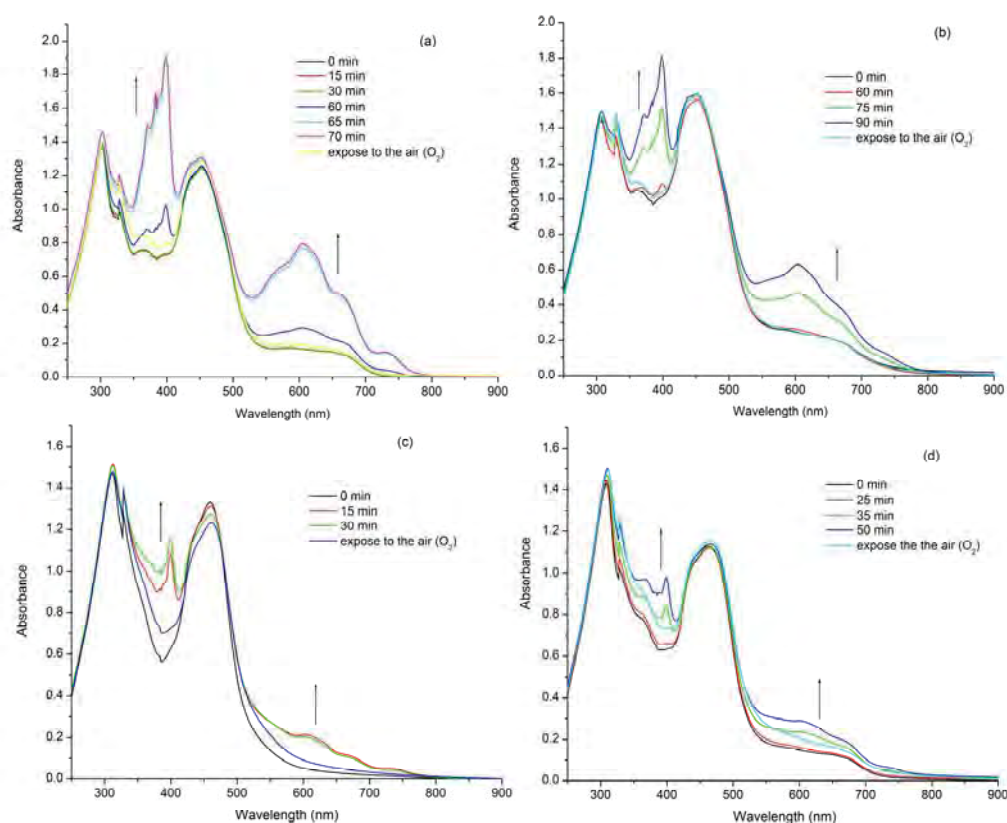
Figure 29. Absorption spectra of photochemical reaction of a) **1**, b) **1**⊂CB[7], c) **2** and d) **3** (8×10^{-3} M) in the presence of TEOA 5×10^{-2} M) in acetonitrile. (The concentration of only **1**⊂CB[7] is 9×10^{-3} M).

Conclusion

The heterodinuclear Ru-Os complexes **1** and its rotaxane **1**⊂CB[7], are synthesized and isolated from non-aqueous solution. Ru and Os complexes with carboxylic acid anchor **2** and **3** are also successfully synthesized. Their photophysical, photochemical and electrochemical behaviors are studied. In the case of rotaxane **1**⊂CB[7], CB[7] prefers to locate on the butyl chain near the Os side in acetonitrile solution. The electrochemical reaction, observed in acetonitrile, showed the same oxidation potential of [Ru(bpy)$_3$] unit in **1** and **1**⊂CB[7] whereas the oxidation potential of [Os(bpy)$_3$] unit in **1**⊂CB[7] was 100 mV lower than that of **1**, confirming that CB[7] located near the [Os(bpy)$_3$] side. The oxidation potential of [Ru(dcbpy)$_3$] in complexes **2** and **3** were higher than **1** and **1**⊂CB[7] due to the electron withdrawing properties of the carboxyl group. In acetonitrile, the formation of the viologen radical from **1**⊂CB[7] is more difficult than complex **1** itself due to the presence of CB[7] in the complex. Moreover, the possibility to from viologen radicals of complexes **2** and **3** was higher than these of **1** and **1**⊂CB[7] because of the presence of carboxylic groups even though they are less stable. When the solution was exposed to air (oxygen), the solution color changed back to the original orange color and the absorption spectrum is restored, indicating that the process is repeatable.

References

[1] L. F. Cooley, S. L. Larson, C. M. Elliott, D. F. Kelley, *J. Phys. Chem*. 1991, **95**, 10694.

[2] D. Zou, S. Andersson, R. Zhang, S. Sun, B. Åkermark, L. Sun, *J. Org. Chem.* 2008, **73**, 3775.

[3] E.M. Kober, J.V. Caspar, B.P. Sullivan and T.J. Meyer, *Inorg. Chem.* 1988, **27**, 4587.

[4] V. Shklover, M. K. Nazeeruddin, S.M. Zakeeruddin, C. Barbé, A. Kay, T. Haibach, W. Steurer, R. Hermann, H.U. Nissen and M. Grätzel, *Chem. Mater.* 1997, **9**, 430; W. J. Youngblood, S. H. A. Lee, Y. Kobayashi, E. A. Hernandez-Pagan, P. G. Hoertz, T. A. Moore, A. L. Moore, D. Gust and T. E. Mallouk, *J. Am. Chem. Soc.* 2009, **131**, 926.

[5] C. Chuy, L.R. Falvello, E. Libby, J. C. Santa-Marı´a, M. Toma´s, *Inorg. Chem.*, 1997, **36**, 2004.

[6] T. Gupta, M. Altman, A. D. Shukla, D. Freeman, G. Leitus, M. E. van der Boom, *Chem. Mater.*, 2006, **18**, 1379.

[7] T. K. Monhaphol, S. Andersson, L. Sun, *Chem. Eur. J.* 2011, **17**, 11604.

[8] P. Thuéry, *Inorg. Chem.*, 2010, **49**, 9078; X. Huang, Y. Tan, Q. Zhou, Y. Wang, Y. Che, *Carbohydr. Polym.*, 2008, **74**, 685.

[9] S. G. Sun, R. Zhang, S. Andersson, J. X. Pan, B. Åkermark, L. Sun, *J. Phys. Chem. B,* 2007, **111**, 13357.

[10] K. Moon, A. E. Kaifer, *Org. Lett.*, 2004, **6**, 185; W. L. Mock, N.-Y. Shih, *J. Org. Chem.*, 1986, **51**, 4440.

[11] J. Otsuki, A. Imai, K. Sato, D.-M. Li, M. Hosoda, M. Owa, T. Akasaka, I. Yoshikawa, K. Araki, T. Suenobu, S. Fukuzumi, *Chem. Eur. J.*, 2008, **14**, 2709; J. L. Chen, Y. Chi and K. Chen, *Inorg. Chem.* 2010, **49**, 823.

[12] S. Baitalik, U. Flörk and K. Nag, Inorg. Chim. Acta., 2002, **337**, 439; P. J. West, T. Schwich, M. P. Cifuentes, M. G. Humphrey, *J. Organomet. Chem.*, 2011, **696**, 2886.

[13] J. N. Demas, G. A. Crosby, *J. Am. Chem. Soc.*, 1971, **93**, 2841; S. Decurtins, F. Felix, J. Ferguson, H. U. Güdel, A. Ludi, *J. Am. Chem. Soc.*, 1980, **102**, 4102.

[29] V. Balzani, G. Bergamini, F. Machioni, P. Ceroni, *Coord. Chem. Rev.*, 2006, **95**, 10694.

[14] A. Juris, V. Balzani, F. Barigelletti, S. Campagna, P. Belser, A.Vonzelewsky, *Coord. Chem. Rev.,* 1988, **84**, 85.

[15] S. G. Sun, R. Zhang, S. Andersson, J. X. Pan, B. Åkermark, L. Sun, *Chem. Commun.*, 2006, **40**, 4195; D. Zou, S. Andersson, R. Zhang, S. Sun, B. Åkermark, L. Sun, *Chem. Commun.*, 2007, **45**, 4734; S. Andersson, D. Zou, R. Zhang, S. Sun, B. Åkermark, L. Sun, *Eur. J. Org. Chem.* 2009, **8**, 1163; S. Sun, S. Andersson, L. Sun, *Chem. Commun.* 2010, **46**, 463.

[16] V. Balzani, G. Bergamini, F. Machioni, P. Ceroni, *Coord. Chem. Rev.*, 2006, **95**, 10694.

[17] H. J. Kim, W. S. Jeon, Y. H. Ko, K. Kim, *Proc. Natl. Acad. Sci. USA*, 2002, **99**, 5007; W. Geuder, S. Hunig, A. Suchy, *Tetrahedron*, 1986, **42**, 1665; R. Kannappan, C. Bucher, E. Saint-Aman, J. C. Moutet, A. Milet, M. Oltean, E. Metay, S. Pellet-Rostaing, M. Lemaire, C. Chaixd, *New J. Chem.* 2010, **34**, 1373; C. Lee, Y.-M. Lee, M. S. Moon, S. H. Park, J. W. Park, K. G. Kim, S.-J. Jeon, *J. Electroanal. Chem.*, 1996, **416**, 139; G. J. Zhao, B. H. Northrop, P. J. Stang, K. L. Han, *J. Phys. Chem.*

A 2010, **114**, 3418; G. J. Zhao, B. H. Northrop, K. L. Han, P. J. Stang, *J. Phys. Chem. A* 2010, **114**, 9007; G. J. Zhao, K. L. Han, *J. Phys. Chem. A,* 2007, **111**, 2469; G. J. Zhao, J. Y. Liu, L. C. Zhou, K. L. Han, *J. Phys.Chem. B,* 2007, **111**, 8940; G. J. Zhao, K. L. Han, *Biophys. J.,* 2008, **94**, 38–46.

Output จากโครงการวิจัยที่ได้รับทุนจาก สกว.

1. ผลงานตีพิมพ์ในวารสารวิชาการนานาชาติ (ระบุชื่อผู้แต่ง ชื่อเรื่อง ชื่อวารสาร ปี เล่มที่ เลขที่ และหน้า) หรือผลงานตามที่คาดไว้ในสัญญาโครงการ

   Narumon Boonyavong,[a] Potjanart Suwanruji,[a] Fei Li,[b] Licheng Sun,[c] Supa Hannongbua,[a] and Thitinun Monhaphol Karpkird*[a] "Synthesis, Electrochemistry and Photo-induce Electron Transfer of Unsymmetrical Dinuclear Ruthenium Osmium 2,2-Bipyridine Complexes" submitted to Photochemical and Photobiological Sciences

2. การนำผลงานวิจัยไปใช้ประโยชน์

   - เชิงวิชาการ (มีการพัฒนาการเรียนการสอน/สร้างนักวิจัยใหม่)

   2.1) สร้างนักวิจัยระดับปริญญาโท 1 คน

   2.2) นำไปใช้เป็นตัวอย่างในการเรียนการสอน วิชา Theoritical Organic Chemistry 01401521 และ Determination of Organic Structures 01403523

3. อื่นๆ (เช่น ผลงานตีพิมพ์ในวารสารวิชาการในประเทศ การเสนอผลงานในที่ประชุมวิชาการ หนังสือ การจดสิทธิบัตร)

   - 4th International Hybrid and Organic Photovoltaics Conference 6-10th May 2012, Uppsala, Sweden under the title "Photo-Induce Electron Transfer of Ruthenium Complexes with One and Two Linked Viologens Trapped CB[7] in Organic Solution"

PROCEEDINGS

PURE AND APPLIED CHEMISTRY INTERNATIONAL

CONFERENCE 2013 (PACCON2013)

Chemical Science for Green Community

January 23-25, 2013
Bangsaen Beach
THAILAND

PROCEEDINGS

PURE AND APPLIED CHEMISTRY INTERNATIONAL

CONFERENCE 2013 (PACCON2013)

**PROFESSOR DR. HER ROYAL HIGHNESS
PRINCESS CHULABHORN MAHIDOL**

Message from the President of The Chemical Society of Thailand under the patronage of Prof. Dr. H.R.H. Princess Chulabhorn Mahidol

Associate Professor Dr. Supawan Tantayanon

On behalf of the Chemical Society of Thailand (CST), I am grateful to Her Royal Highness Princess Chulabhorn for her kindness to graciously preside over, and declare the opening of Pure and Applied Chemistry International Conference 2013 as well as to deliver the special keynote lecture.

The Chemical Society of Thailand has been established in 1980, but not until the year 2002 the first Pure and Applied Chemistry International Conference (PACCON) was organized under the auspice of the CST of which I was the Chair.   However PACCON was not continued in the following years. As the 10th President of the CST (January, 2007-February, 2013), I proposed to have PACCON as one of the annual CST activities and the CST executive board unanimously agreed. Therefore the 2nd PACCON was held in January 2008 and continued with rapid growth every year since then. At the present, PACCON has become well known not only nationally but also internationally.
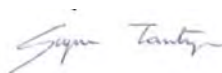
Besides PACCON, the CST has organized many meetings, trainings, seminars, short courses, workshops and other conferences with the aim to disseminate the advancement of chemistry as well as the standard practice for working personnel. It also undertakes many activities that promote education in chemistry in both school and university levels, and public understanding of chemistry. The society has had the strong international collaboration with the Federation of Asian Chemical Societies (FACS) for decades and recently with International Union of Pure and Applied Chemistry (IUPAC). To do all these tasks, the CST certainly requires the strong support and contribution from Thai chemists.

We, therefore look forward to welcoming all Thai chemists becoming our members soon.

As PACCON 2013 is the one of our significant activities, it gives us great honor indeed to co-organize and welcome all of you to this conference. We trust that by sharing and understanding the recent progress in chemistry, we will be updated on the latest trends in chemistry as well as be informed about innovative research strategies to empower our students and people in this world to live well in this fast changing world.

I am very proud of the effort taken by the Faculty of Science, Burapha University as the main organizer in holding this conference. The endeavor taken by the organizing committee in gathering the keynote, plenary and invited speakers as well as the participants nationwide and overseas to address the challenges in establishing the chemical sciences for green community, reflects the commitment given in engaging the scholars, thoughts with tools and technology. I congratulate the organizing committee for the hard work and dedication in making this conference a great success.

I wish all the participants fruitful deliberations and believe that all of you will enjoy the sharing and exchanging of your expertise. I also hope that the conference shall further advance chemistry for life and the future.
Thank you.

Associate Professor Dr.Supawan Tantayanon
President, the Chemical Society of Thailand

Message from the Dean of the
Faculty of Science, Burapha University

Assistant Professor Dr. Usavadee Tuntiwaranurak

On behalf of the faculty of Science, I am very pleased to welcome all participants to beautiful Bangsaen Beach and to this 7th Pure Chemistry International Conference 2013 (PACCON 2013). It is such a great honor and a privilege for hosting this prominent event. This pride overwhelms not only the Department of Chemistry, but also the Faculty of Science as a whole. To serve community towards wholesomeness and sustainability through research as in line with the vision of Burapha University, the PACCON committee has agreed to use the term "Global Chemical Sciences for Green Community" as the theme of the Conference in 2013.

To successfully accomplish in arranging such a significant occurrence in Chemistry with over 1000 registered participants from around the world, I would like to express my gratitude to all organizing staff for their relentless endeavor and their time over the past ten months. I would also like to articulate my appreciation to all speakers, audience, as well as sponsors, who are also keen to make this event happen.

In order to make your stay more enjoyable and remarkable, all participants please take into consideration the fabulous excursions provided by PACCON 2013 to learn more about beautiful Bangsaen Beach and surrounding attractions, including Pattaya, one of the most renowned tourist destinations in Thailand. At last, I hope that your participation in the Conference and your visit to the East Coast of Thailand will truly be worthwhile and unforgettable.

T. Usavadee

Assistant Professor Dr. Usavadee Tuntiwaranurak
Dean of Faculty of Science
Burapha University

COMMITTEE of PACCON2013

Academic Committee

International Academic Advisory Committee:

Prof. Dr.Peter Wolschann	University of Vienna, Austria
Prof. Dr. Seiji Mori	Ibaraki University, Japan
Prof. Dr. Jen-Shinag Yu	National Chiao Tung University, Taiwan
Prof. Dr. Shigeo Goto	Nagoya University, Japan
Prof. Dr. Pierpaolo Zuddas	University Pierre et Marie Curie Paris-Sorborne, France
Prof. Dr. Minoru Isobe	National Tsing Hua University, Taiwan
Prof.Dr. Kato Koichi	Okazaki Institute for Integrative Bioscience, Japan
Prof.Dr. Toshio Nishikawa	Nagoya University, Japan
Prof. Dr. Edman Tsang	University of Oxford, UK
Prof.Dr. Irene K.P. Tan	Institute of Biological Sciences, University of Malaya, Malaysia

Academic Advisory Committee:

Prof. Dr. Somsak Rujiravong	Chulabhorn Graduate Institute
Assoc.Prof. Dr. Surin Laosooksathit	Vice-President of Chemical Society of Thailand, King Mongkut's Institute of Technology North Bangkok
Assoc. Prof. Dr. Supa Hannongbua	Vice-President of Chemical Society of Thailand, Kasetsart University
Assoc. Prof. Dr.Vudhichai Parasuk	Chulalongkorn University

Academic Committee :

Chairperson :	Assoc.Prof.Dr. Thanuttkhul Mongkolaussavarat	Chulabhorn Graduate Institute
Vice-Chairperson :	Dr. Chuleeporn Puttnual	Faculty of Science, Burapha University
	Dr. Chatchawin Petchlert	
	Dr. Anocha Sooksomboon	
Analytical Chemistry	Assoc. Prof. Dr. Orawon Chailapakul	Chulalongkorn University
Inorganic Chemistry	Prof. Dr. Thawatchai Tantulani	Chulalongkorn University
Organic Chemistry and Medicinal Chemistry	Assoc. Prof. Tirayut Vilaivan	Chulalongkorn University
Physical and Computational Chemistry	Assoc. Prof. Dr. Vudhichai Parasuk	Chulalongkorn University
Material Sciences and Technology	Prof.Dr. Jumras Limtrakul	Kasetsart University
Polymer Chemistry	Assoc.Prof.Dr. Ittipol Jangchud	King Mongkut's Institute of Technology Ladkrabang
Petroleum Chemistry and	Assoc. Prof. Dr. Tawan Sooknoi	King Mongkut's Institute of

Catalysis		Technology Ladkrabang
Environmental Chemistry	Prof. Dr. Chongrak Polprasert	Thammasart University
Industrial Chemistry and Innovation	Prof. Dr Suttichai Assabumrungrat	Chulalongkorn University
Cosmetics	Assoc. Prof. Dr Varaporn Junyaprasert	Mahidol University
Chemical Education	Asst. Dr. Ekasith Somsook	Mahidol University
Biological/Biophysical Chemistry and Chemical Biology	Prof. Dr. Piamsook Pongsawasdi	Chulalongkorn University
Bioinformatics	Asst. Prof. Dr. Marasri Ruengjitchatcaahawalya	King Mongkut's Institute of Technology Thonburi
Free radicals / Antioxidants	Prof. Emer. Dr. MaitreeSuttajit	Phayao University
Food safety and Food Chemistry	Assoc. Prof. Dr. SiriratKokpol	Chulalongkorn University

Organizing Committee

Conference Chairman:	Prof.Dr. Sompol Phongthai, M.D	President of Burapha University
Advisory Organizing Committee:	Assoc.Prof.Dr. Supawan Tantayanon	President of Chemical Society of Thailand
	Assoc.Prof.Dr. Surin Laosooksathit	Vice-President of Chemical Society of Thailand
	Assoc.Prof.Dr. Supa Hannongbua	Vice-President of Chemical Society of Thailand
	Assist.Prof.Dr. Usavadee Tantivaranurak	Dean of Faculty of Science, Burapha University
Local Organizing Committee :		
Chairperson:	Assist.Prof.Dr. Usavadee Tantivaranurak	
Committee :	Dr. Chuleeporn Puttnual	
	Dr. Chatchawin Petchlert	
	Asst,Prof.Dr.Prapasiri Barnette	
	Asst,Prof.Dr. Jaray Jaratjaronpong	
	Dr. Nattapong Srisook	
	Dr. Nawasit Rakbamrung	
	Dr. Kanchaya Honglertkongsakul	
	Asst,Prof.Dr.Krisana Chinnasarn	
	Dr. Salil Chanroj	
	Dr. Anocha Suksomboon	
	Dr. Anuttara Udomprasert	
	Assist.Prof Dr. Ekaruth Srisook	
Secretary :		
Assistant Secretary :	Dr. Karaked Tedsri	
	Dr. Panata Wanichwatanadecha	
	Dr. Songklod Sarapusit	
Scientific Committee :	Dr.Pornpen Atorngitjawat	
	Dr.Sirirat Chanvaivit	
	Asst,Prof.Dr.Jittima Charoenpanich	
	Asst,Prof.Dr.Supranee Kaewpirom	
	Dr. Somchart Maenpuen	
	Dr. Chatchawin Petchlert	
	Asst,Prof.Dr.Suchaya Pongsai	
	Asst,Prof.Dr.Ubolluk Rattanasak	
	Asst,Prof.Dr.Rungnapha Saeeng	
	Asst,Prof.Dr.Somsak Sirichai	

Dr. Uthaiwan Siriou
Asst,Prof.Dr.Pitak Sootanan
Asst,Prof.Dr.Klaokwan Srisook
Asst,Prof.Dr.Jomjai Suksai
Asst,Prof.Dr.Orasa Suriyaphan
Dr. Prapapan Techasauvapak
Dr. Karaked Tedsree
Asst,Prof.Dr.Thanida Trakulsujaritchok

Organizers : Faculty of Science, Burapha University

Chemical Society of Thailand

(สำเนา)

คำสั่งมหาวิทยาลัยบูรพา
ที่ ๓๐๒๐ /๒๕๕๕
เรื่อง แต่งตั้งกองบรรณาธิการจัดทำรายงานการประชุมวิชาการนานาชาติ
Pure and Applied International Conference 2013 (PACCON 2013)
....

        ด้วยคณะวิทยาศาสตร์ มหาวิทยาลัยบูรพา ได้กำหนดจัดโครงการการประชุมวิชาการนานาชาติ
Pure and Applied International Conference 2013 (PACCON 2013) ในวันที่ ๒๓ - ๒๕ มกราคม
พ.ศ. ๒๕๕๖ ณ โรงแรม The Tide Resort จังหวัดชลบุรี ดังนั้น เพื่อให้การดำเนินงานเป็นไปด้วยความเรียบร้อย
และเป็นไปตามวัตถุประสงค์ อาศัยอำนาจตามความในมาตรา ๒๖ และมาตรา ๓๒(๓) แห่งพระราชบัญญัติ
มหาวิทยาลัยบูรพา พ.ศ. ๒๕๕๐ จึงขอแต่งตั้งบุคคลต่อไปนี้เป็นกองบรรณาธิการจัดทำรายงานการประชุมวิชาการ
นานาชาติ Pure and Applied International Conference 2013 (PACCON 2013) ดังนี้

บรรณาธิการต่างประเทศ

Prof. Dr. Peter Wolschann	University of Vienna, Austria
Prof. Dr. Seiji Mori Ibaraki	University, Japan
Prof. Dr. Jen-Shinag Yu	National Chiao Tung University, Taiwan
Prof. Dr. Shigeo Goto	Nagoya University, Japan
Prof. Dr. Pierpaolo Zuddas	University Pierre et Marie Curie Paris-Sorborne, France
Prof. Dr. Minoru Isobe	National Tsing Hua University, Taiwan
Prof. Dr. Kato Koichi	Okazaki Institute for Integrative Bioscience, Japan
Prof. Dr. Toshio Nishikawa	Nagoya University, Japan
Prof. Dr. Edman Tsang	University of Oxford, UK
Prof. Dr. Irene K.P. Tan	Institute of Biological Sciences, University of Malaysia, Malaysia
Dr. Ron Beckett	Water Studies Centre, School of Chemistry Monash University

บรรณาธิการที่ปรึกษา

ศาสตราจารย์สมศักดิ์	รุจิรวัฒน์	สถาบันบัณฑิตศึกษาจุฬาภรณ์
รองศาสตราจารย์สุรินทร์	เหล่าสุขสถิตย์	อุปนายกสมาคมเคมีแห่งประเทศไทย, มหาวิทยาลัยเทคโนโลยีพระจอมเกล้าพระนครเหนือ
รองศาสตราจารย์สุภา	หารหนองบัว	อุปนายกสมาคมเคมีแห่งประเทศไทย, มหาวิทยาลัยเกษตรศาสตร์
รองศาสตราจารย์วุฒิชัย	พาราสุข	จุฬาลงกรณ์มหาวิทยาลัย

/บรรณาธิการ...

บรรณาธิการ

รองศาสตราจารย์ธนัฏฐ์คุณ มงคลอัศวรัตน์ สถาบันบัณฑิตศึกษาจุฬาภรณ์

ผู้ช่วยบรรณาธิการ

อาจารย์ชุลีพร พุฒนวล มหาวิทยาลัยบูรพา
อาจารย์ชัชวิน เพชรเลิศ มหาวิทยาลัยบูรพา
อาจารย์อโนชา สุขสมบูรณ์ มหาวิทยาลัยบูรพา

กองบรรณาธิการ

รองศาสตราจารย์อรวรรณ ชัยลภากุล จุฬาลงกรณ์มหาวิทยาลัย
สาขา Analytical Chemistry

ศาสตราจารย์ธวัชชัย ตันฑุลานิ จุฬาลงกรณ์มหาวิทยาลัย
สาขา Inorganic Chemistry

รองศาสตราจารย์ธีรยุทธ วิไลวัลย์ จุฬาลงกรณ์มหาวิทยาลัย
สาขา Organic and Medicinal Chemistry

รองศาสตราจารย์วุฒิชัย พาราสุข จุฬาลงกรณ์มหาวิทยาลัย
สาขา Physical and Computational Chemistry

ศาสตราจารย์จำรัส ลิ้มตระกูล มหาวิทยาลัยเกษตรศาสตร์
สาขา Material Sciences and Nanotechnology

ศาสตราจารย์เปี่ยมสุข พงษ์สวัสดิ์ จุฬาลงกรณ์มหาวิทยาลัย
สาขา Biological/Biophysical Chemistry and Chemical Biology

ผู้ช่วยศาสตราจารย์มารศรี เรืองจิตชัชวาลย์ มหาวิทยาลัยเทคโนโลยีพระจอมเกล้าธนบุรี
สาขา Bioinformatics

รองศาสตราจารย์อิทธิพล แจ้งชัด สถาบันเทคโนโลยีพระจอมเกล้าเจ้าคุณทหารลาดกระบัง
สาขา Polymer Chemistry

รองศาสตราจารย์ตะวัน สุขน้อย สถาบันเทคโนโลยีพระจอมเกล้าเจ้าคุณทหารลาดกระบัง
สาขา Petroleum Chemistry and Catalysis

ศาสตราจารย์จงรัก ผลประเสริฐ มหาวิทยาลัยธรรมศาสตร์
สาขา Environmental Chemistry

ผู้ช่วยศาสตราจารย์เอกสิทธิ์ สมสุข มหาวิทยาลัยมหิดล
สาขา Chemical Education

รองศาสตราจารย์วราภรณ์ จรรยาประเสริฐ มหาวิทยาลัยมหิดล
สาขา Cosmetics

ศาสตราจารย์สุทธิชัย อัสสะบำรุงรัตน์ จุฬาลงกรณ์มหาวิทยาลัย
สาขา Industrial Chemistry and Innovation

ศาสตราจารย์ เกียรติคุณ ไมตรี สุทธิจิตต์ มหาวิทยาลัยพะเยา
สาขา Free radicals/Antioxidants

รองศาสตราจารย์ศิริรัตน์   ก๊กผล   จุฬาลงกรณ์มหาวิทยาลัย

สาขา Food safety and Food Chemistry

ทั้งนี้ ตั้งแต่วันที่ ๑ กันยายน พ.ศ. ๒๕๕๕ ถึงวันที่ ๓๑ มีนาคม พ.ศ. ๒๕๕๖

สั่ง ณ วันที่ ๗ ธันวาคม พ.ศ. ๒๕๕๕

(ลงชื่อ)   สมพล พงศ์ไทย

(ศาสตราจารย์ นายแพทย์สมพล พงศ์ไทย)

อธิการบดีมหาวิทยาลัยบูรพา

สำเนาถูกต้อง

สมฤดี

(นางสาวสมฤดี หวานระรื่น)

นักวิทยาศาสตร์

TABLE OF CONTENT

	PAGE

TABLE OF CONTENT

TABLE OF CONTENT

TABLE OF CONTENT

TABLE OF CONTENT

TABLE OF CONTENT

TABLE OF CONTENT

TABLE OF CONTENT

TABLE OF CONTENT

TABLE OF CONTENT

TABLE OF CONTENT

TABLE OF CONTENT

Analytical Chemistry

SIZE CHARACTERIZATION OF SILVER NANOPARTICLES (AgNPs) PREPARED UNDER VARIOUS CONDITIONS AND UPON INCUBATION IN *IN VITRO* GASTROINTESTINAL DIGESTION

Jakrawan Yostawonkul[1], Juwadee Shiowatana[1], Atitaya Siripinyanond[1*]

[1] Mahidol University /Department of Chemistry and Center of Excellence for Innovation in Chemistry, Faculty of Science, Bangkok 10400, Thailand

[*] Author for correspondence; E-mail: atitaya.sir@mahidol.ac.th, Tel. +66 22015129

Abstract: Silver nanoparticles (AgNPs) were synthesized by using tannic acid as stabilizing and reducing agent. Various sizes of AgNPs can be controlled by varying concentrations of tannic acid. Flow field-flow fractionation (Fl-FFF) with on-line UV-vis spectrophotometer was used for size characterization of tannic acid stabilized AgNPs. Size distributions of AgNPs synthesized by 0.15, 0.30, and 1.50 mM tannic acid at pH 9.0 were about 13, 9.8, and 6.6 nm, respectively. AgNPs were incubated in in vitro gastrointestinal digestion process to mimic the human digestion process for monitoring of changes in tannic acid stabilized AgNPs. Flow field-flow fractionation with off-line graphite furnace atomic absorption spectrophotometer (Fl-FFF-GFAAS) was used for size characterization of gastric digested AgNPs and intestinal digested AgNPs obtained after *in vitro* gastrointestinal process. The result shows that all tannic acid stabilized AgNPs were aggregated upon incubation in gastric digestion step and some aggregated particles were dissociated in intestinal digestion step to a smaller size AgNPs, but the aggregated form was still significantly remained.

1. Introduction

Silver nanoparticles (AgNPs) have been widely used in many consumer products such as toothbrush, detergent, cosmetics, textile and food container [1, 2]. Due to their properties that may differ from bulk material such as antimicrobial property, electronic property and surface property, AgNPs provide novel applications [3]. AgNPs can discharge from the consumer products and enter into human body. Oral is most important way that AgNPs enter to human body but not much is known about the size changing and toxicity of AgNPs in human body.

Previously, AgNPs were synthesized by reduction of Ag-ion to AgNPs by using strong reducing agent such as $NaBH_4$ and aggregation process was prevented by using capping agent or stabilizing agent. Previously, green synthesis of AgNPs has become increasingly interest, because of their environmental friendliness, suitably use for human and biocompatible [4]. Tannic acid was used for synthesis of AgNPs because of it can be hydrolyzed in mild basic condition into glucose and gallic acid. Glucose acts as a good stabilizing agent while gallic acid acts as a good reducing agent. Therefore, tannic acid could act as

green reducing and stabilizing agent for synthesis of AgNPs [5].

The size of AgNPs can affect on absorption and toxicity in human body. Therefore, size changing of AgNPs in human digestion system was studied. *In vitro* gastrointestinal digestion was used for determination of size changing of AgNPs that enter to human body via oral administration [6]. *In vitro* gastrointestinal digestion consists of two digestion steps: gastric and intestinal digestions which have different pH conditions and enzymatic systems. Size of AgNPs after digestion in *in vitro* gastrointestinal digestion can be characterized by many techniques such as transmission electron microscopy (TEM), zetasizer, and flow field-flow fractionation (Fl-FFF) [7, 8].

In this work, AgNPs were synthesized under various tannic acid concentrations. Tannic acid stabilized AgNPs were incubated in *in vitro* gastrointestinal digestion. Flow field-flow fractionation with off-line graphite furnace atomic absorption spectrometer (Fl-FFF-GFAAS) was used for size characterization of tannic acid stabilized AgNPs and size changing of AgNPs upon incubation in *in vitro* gastrointestinal digestion.

2. Materials and Methods

2.1 Chemicals

Silver nitrate was purchased from RCI Labscan (Bangkok, Thailand). Tannic acid, pancreatin, bile extract porcine and pepsin were purchased from Sigma-Aldrich (Steinheim, Germany). Gold nanoparticles (AuNPs) standard of 10 nm diameter (Sigma-Aldrich) was used for Fl-FFF channel calibration. Sodium hydroxide, hydrochloric and sodium azide were purchased form Merck (Darmstadt, Germany). The Fl-FFF carrier was made by 0.02% Fl-70 detergent from Scientific (New Jersey, USA.) with 0.02% sodium bicarbonate from Ajax (New South Wales, Australia). All chemicals were prepared with deioni-zed water.

2.2 Silver nanoparticles synthesis

AgNPs were synthesized by using tannic acid as a stabilizing and reducing agent under various tannic

acid concentrations. Briefly, 25 mL of 0.15, 0.30 and 1.50 mM tannic acid were prepared and adjusted to pH 9.0 (by adding K_2CO_3). Then, 5 mL of 3 mM silver nitrate was mixed together with tannic acid solution under vigorous magnetic stirring at room temperature for 30 min. The yellow-brownish solutions were observed, indicating the formation of different concentrations of tannic acid stabilized AgNPs.

2.3 *In vitro* gastrointestinal digestion

In vitro gastrointestinal digestion was used for determination of size changing of tannic acid stabilized AgNPs. It consists of two major digestion steps: gastric and intestinal digestion steps.

Gastric digestion: 3 mL of tannic acid stabilized AgNPs was added into a conical flask and made up volume to 8 mL with deionized water. Then, the AgNPs solution was adjusted to pH 2.0 by adding hydrochloric acid, and made up volume to 12.5 mL with deionized water. Next, 375 μL of pepsin solution (0.32 g of pepsin was dissolved in 2 mL of 0.1 M hydrochloric acid) was added into AgNPs solution, and incubated in an incubator shaker at 37°C for 2 hours. Mixture was called gastric digested AgNPs.

Intestinal digestion: 5 mL of gastric digested AgNPs was added into a conical flask. Then, 625 μL of pancreatin bile solution (0.02 g pancreatin and 0.125 g bile extract prepared in 5 mL of 1 mM sodium bicarbonate) were mixed together. The mixture was adjusted to obtain pH 7.5 by adding sodium hydroxide. Mixture was incubated in an incubator shaker at 37°C for 2 hours. Finally, the intestinal digested AgNPs sample was obtained.

2.4 Instrumentation

The Fl-FFF system is a PN-1201-FO model from Postnova Analytics (Landsberg, Germany). The Fl-FFF channel dimensions are 27.7 cm length, 2.0 cm wide, and 254 μM thick. A 1 kDa regenerated cellulose membrane (Postnova) was used. The carrier liquid was 0.02 % sodium azide and 0.02 % FL-70 were prepared in deionized water and adjusted to pH 9.3 – 10.0 by sodium hydroxide. 20 μL of sample was introduced into Fl-FFF via Rheodyne injector valve. Channel flow at 1 mL min^{-1} was delivered to Fl-FFF channel by using a high pressure liquid chromatography (HPLC) pump (Model PN 1021, Postnova Analytics, Germany). Cross flow at 2 mL min^{-1} was delivered to Fl-FFF channel by using a high pressure liquid chromatography (HPLC) pump (Model PN 1122, Postnova Analytics, Germany). After fractionation, the sample was directed through a dual wavelength detector (Model 2487 UV-visible detector; Waters corp, USA). The detector was set at 400 nm and 254 nm for detection of AgNPs. The automatic fraction collector (Model FC-204 fraction collector, Gilson, USA) was used to collect fraction from UV-Vis detector outlet. Fraction collector was set at 1 mL min^{-1}. The operating conditions of Fl-FFF are summarized in Table 1.

A Perkin Elmer AAnalyst 100 (Norwalk, CT, USA) with deuterium background corrector was used for detection of collected silver after the UV-vis detector. The Perkin Elmer Model AS – 72 autosamper was used to introduce Ag solution into a graphite tube. The furnace operating condition for silver ion and AgNPs measurement are illustated in Table 2.

Table 1: Fl-FFF condition for size characterization of AgNPs

Fl-FFF: Model PN-1021-FO (Postnova Analytics, Germany)	
Carrier liquid	0.02% Fl-70 + 0.02% NaN$_3$
Cross flow rate/mL min^{-1}	2.0
Channel flow rate/mL min^{-1}	1.0
Equilibration time/min	1.1
Carrier pH	9.3
Membrane	Regenerated cellulose acetate (1 kDa cutoff)

Table 2: GFAAS condition for silver detection

Step	Temperature (°C)	Ramp time(s)	Hold time(s)
Drying	130	20	30
Pyrolysis	800	20	30
Atomization	1800	0	5
Clean up	2600	1	5

3. Results and Discussion

AgNPs were synthesized by using tannic acid. In basic condition, tannic acid can be dissociated into glucose and gallic acid. Glucose acts as a stabilizing agent while gallic acid acts as a reducing agent. Therefore, tannic acid was used as stabilizing and reducing agent for synthesis of AgNPs at pH 9.0. Three different tannic acid concentrations at 0.15, 0.30 and 1.50 mM were used for synthesis of tannic acid stabilized AgNPs. The hydrodynamic diameter of tannic acid stabilized AgNPs were characterized by using Fl-FFF with on-line UV-Vis detector. In Figure 1, hydrodynamic diameter of tannic acid stabilized AgNPs synthesized at 0.15 mM tannic acid was about 13.4 ± 0.1 nm. With higher concentrations of tannic acid, the hydrodynamic diameters of tannic acid stabilized AgNPs were decreased. For 0.30 and 1.50 mM tannic acid, the hydrodynamic diameters of tannic acid stabilized AgNPs were about 9.6 ± 0.1, and 6.6 ± 0.1 nm, respectively. The hydrodynamic diameters of tannic acid stabilized AgNPs synthesized under various concentrations at pH 9.0 are summarized in Table 3.
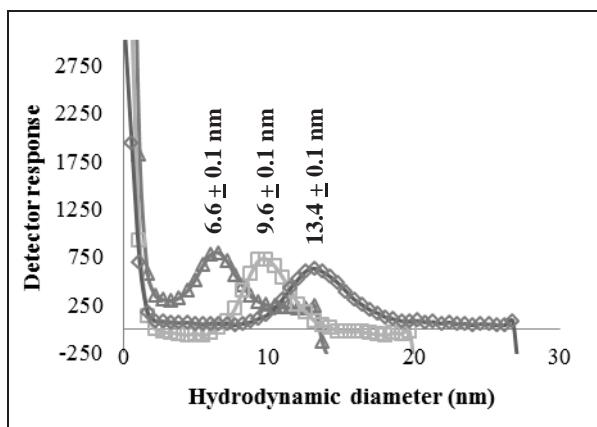
Figure 1. Hydrodynamic diameter of tannic acid stabilized AgNPs synthesized under various concentrations of tannic acid stabilizer at pH 9.0: (—△—) 1.50 mM; (—□—) 0.30 mM; and (—◇—) 0.15 mM.

Table 3: Hydrodynamic size of tannic acid stabilized AgNPs synthesized under various concentrations at pH 9.0.

Tannic acid concentrations (mM)	Hydrodynamic diameter (nm)
1.50	6.6 ± 0.1
0.30	9.6 ± 0.1
0.15	13.4 ± 0.1
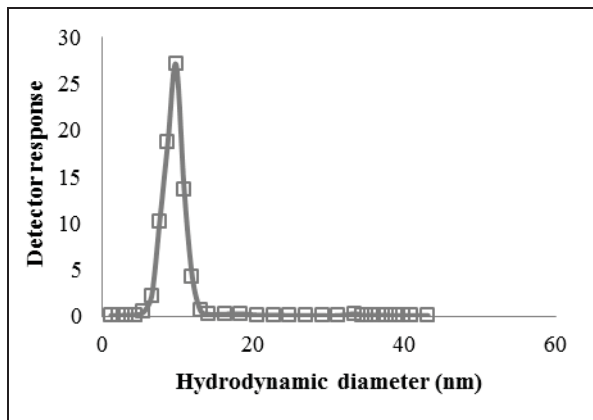
Figure 2. Hydrodynamic diameter of tannic acid stabilized AgNPs synthesized under 0.3 mM tannic acid stabilizer at pH 9.0. The GFAAS was used as an Fl-FFF detector.

3.3 *In vitro* gastrointestinal digestion

In vitro gastrointestinal digestion consists of two digestion steps: *in vitro* gastric and *in vitro* intestinal digestion. Graphite furnace atomic absorption spectrometer (GFAAS) was used as a specific element detector of silver in AgNPs samples fractionated by Fl-FFF and for size characterization of tannic acid stabilized AgNPs and size changing of tannic acid stabilized AgNPs after incubation in *in vitro* gastrointestinal digestion.

First, 0.3 mM tannic acid stabilized AgNPs was synthesized at pH 9.0. The hydrodynamic diameter was characterized by using FlFFF with on-line UV-Vis detector to be about 9.6 ± 0.1 nm (as described in Figure 1). The hydrodynamic diameter from Fl-FFF with on-line UV-Vis detector is in good agreement with the hydrodynamic diameter characterized by using GFAAS as an Fl-FFF detector, as shown in Figure 2. The tannic acid (0.3 mM) stabilized AgNPs was used as initial particles for determination of size changing upon incubation in *in vitro* gastrointestinal digestion.

In vitro gastric digestion was performed, and size changing of AgNPs in human stomach condition was investigated. The initial size of tannic acid stabilized AgNPs (9.6 ± 0.1 nm) was changed. Hydrodynamic diameter of gastric digested AgNPs was characterized by using Fl-FFF with off-line GFAAS. The results show that the peak maximum appeared at larger diameter size, indicating that the tannic acid stabilized AgNPs was aggregated into larger size upon incubation in *in vitro* gastric digestion. The aggregated AgNPs was eluted from Fl-FFF channel after stopping cross flow, as illustrated in Figure 3.
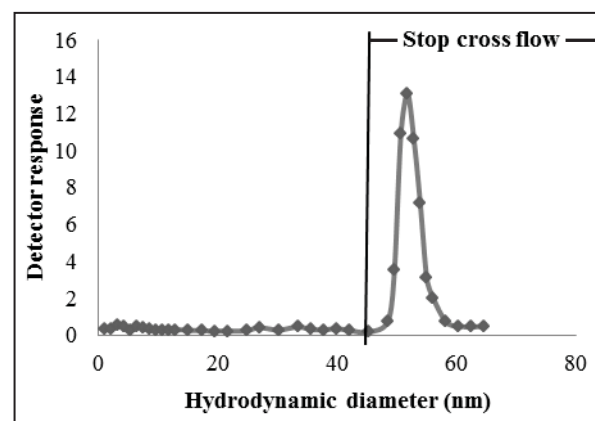
Figure 3. Hydrodynamic diameter of gastric digested AgNPs by using Fl-FFF with off-line GFAAS.

In vitro intestinal digestion was used for determination of size changing of AgNPs in human intestine. The aggregated AgNPs from *in vitro* gastric digestion step was used for characterization of size changing of gastric digested AgNPs upon incubation *in vitro* intestinal digestion step. Hydrodynamic diameter of intestinal digested AgNPs was characterized by using FlFFF with off-line GFAAS. Gastric digested AgNPs were dissociated into two different sizes and almost all are still aggregated. The dissociated AgNPs are smaller than the initial size of tannic acid stabilized AgNPs at about 3.2 and the same size as initial size at about 9.6 nm, respectively, and the aggregated AgNPs was eluted from FlFFF channel after stopping cross flow. From the results, they were shown that the particle size of AgNPs changed upon incubation in in vitro gastrointestinal digestion. They can be classified into three main parts; i.e., smaller than initial size (3.2 nm); the same size as the initial size (9.6 nm); and aggregated particles as shown in Figure 4. Size

changing of tannic acid stabilized AgNPs upon incubation in *in vitro* gastrointestinal digestion are summarized in Table 4.

Conditions	Hydrodynamic diameter (nm)
0.30 mM tannic acid	9.6 ± 0.1
Gastric digestion	> 9.6
Intestinal digestion	3.2, 9.6, aggregated particles (larger than 38.0 nm eluted after stop cross flow)

Table 4: Hydrodynamic size of tannic acid stabilized AgNPs upon incubation in *in vitro* gastrointestinal digestion
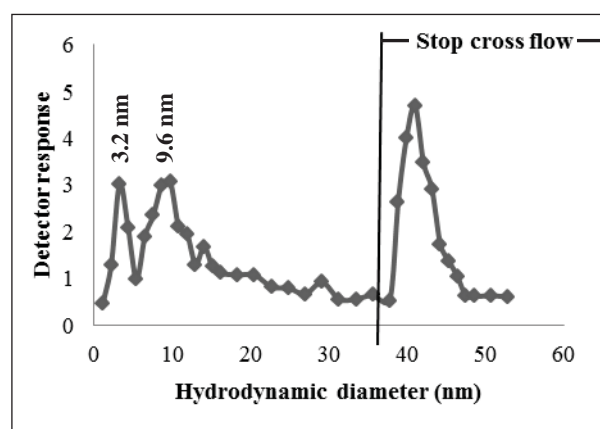
Figure 4. Hydrodynamic diameter of intestinal digested AgNPs by using Fl-FFF with off-line GFAAS.

4. Conclusions

Graphite furnace atomic absorption spectrometry (GFAAS) was used as a silver detector in Ag NPs samples fractionated by FlFFF. Various sizes of AgNPs can be synthesized by using various concentrations of tannic acid. *In vitro* gastrointestinal digestion was carried out to investigate size changing of tannic acid stabilized AgNPs in human digestion condition. Tannic acid stabilized AgNPs were aggregated upon incubation in *in vitro* gastric digestion step. In *in vitro* intestinal digestion step, aggregated AgNPs from *in vitro* gastric digestion step were dissociated into two main different sizes and almost all are still remained.

References

[1] J.P. Shastri, M.G. Rupani, and R.L. Jain, *J. Text.* **103** (2012) 1234-1243.

[2] M. Ahamed, M.S. AlSalhi, and M.K.J. Siddiqui, *Clin. Chim. Acta.* **411** (2010) 1841-1848.

[3] P.K. Jain, *Accounts. Chem. Res.* **12** (2008) 1578-1586.

[4] V.K. Sharma, R.A. Yngard, and Y. Lin, *Adv. Colloid. Interfac.* **145** (2009) 83-96.

[5] Z. Yi, *Colloid. Surface. A.* **392** (2011) 131-136.

[6] J.D. Astwood, J.N. Leach, and R.L. Fuchs, *Nat. Biotechnol.* **14** (1996) 1269-1273.

[7] V. Venkateswarlu, and K. Manjunath, *J. Control. Release.* **95** (2004) 627-638.

[8] S.A. Cumberland, and J.R. Lead, *J. Chromatogr. A.* **1216** (2009) 9099-91

COMPOSITIONAL ANALYSIS OF ESSENTIAL OILS
FROM *ELSHOLTZIA STACHYODES*

Jukreera Panyakaew[1], Nopakarn Chandet[1], Angkhana Inta[2] and Pitchaya Mungkornasawakul[1,3]*

[1] Department of Chemistry, Faculty of Science, Chiang Mai University, Chiang Mai, Thailand
[2] Department of Biology, Faculty of Science, Chiang Mai University, Chiang Mai, Thailand
[3] Environmental Science, Faculty of Science, Chiang Mai University, Chiang Mai, Thailand

*Author for correspondence; E-Mail: pitchaya16@gmail.com, Tel. +66 53 943341-5 ext. 103, Fax. +66 53 892277

Abstract: Essential oils from the aerial parts of *Elsholtzia stachyodes* were collected from the Mae Hong Son region. Those essential oils were extracted by water distillation with 1.31 % yield of *E. stachyodes*. The extracts were analyzed using AT-5MS column for GC-MS analysis with the temperature program. Twenty-five compounds were identified, which main compounds are carvacrol, *γ*-terpinene and *p*-cymeme. It can be concluded that, those oil composition are mainly composed of oxygenated monoterpenes, which are implication of the biochemical markers of various *Elsholtzia* species. However, other chemical components were also acquired such as *α*-terpinene, (*E*)-*β*-ocimeme, *α*-thujene and *β*-myrcene.

Introduction

The genus *Elsholtzia* belongs to the Lamiaceae family and has approximately 40 species worldwide mainly distributed in East Asia. Five species of this genus have been found in Thailand [1]. This genus generally possesses plentiful essential oil, which exerts strong inhibition of central nervous system and takes on definite analgesic effect and shows antibiotic and anti-inflammation relieving fever and analgesic activities [2]. *Elsholtzia stachyodes* is an herb about 0.3-1.0 m. tall where its stem is yellow brown, quadranqular, much branched and leave rhomboid-ovate. It distributed in East Asia, including India, Nepal, China and Thailand, ranging around Northern (Mae Hong Son, Chiang Mai ; Doi Ang kang) [3]. The chemical composition of variuos *Elshotzia* species from different geographaphical origins showed the presence of acylfurans for instance, elsholtziaketone, *α*-dehydroelsholtziaketone, *β*-dehy-droelsholtziaketone and perillene [4-5] and oxy-genated monoterpenoids for instance, 1,8-cineole, linalool, thymol, pinocarvone, geranyl acetate, carvacrol and citral, as representative marker constituents [6-9].

The purpose of this research is identification of the essential oil components of *E. stachyodes* from the Mae Hong Son region by using Gas Chromato-graphy-Mass spectrometry (GC-MS). From our best knowledge, this is the first study on the composition of this unique and endemic species.

Materials and Methods

2.1 Plant Material

The aerial parts of *E. stachyodes* were collected in October 2011 from the Mae Hong region.

2.2 Extraction of the essential oil

Dried leaves of *E. stachyodes* was subjected to water distillation in a Clevenger-type apparatus over 3 hours. The essential oil was obtained with 1.31% (w/w). This material was dried over anhydrous sodium sulphate and stored at 4°C in the dark until used.

2.3 GC-MS analysis

The essential oil was analyzed using an HP-6890 Gas chromatograph equipped with an AT-5MS capillary fused silica column (30 m, 0.25 mm. I.D.; 0.25 μm film thickness) coupled with an HP model 5973 mass selective detector. The oven temperature was initially programmed at 70 $^{\circ}$C for 8 min, then increased at a rate of 5 $^{\circ}$C/min to 200 $^{\circ}$C and maintained for another 8 min. Then, the temperature was continued with a second ramp in by rising at 10 $^{\circ}$C/min to 240 $^{\circ}$C and holding for 4 min. Helium was used as carrier gas with constant flow mode at 1 mL/min. An injection volume of 1 μL with split ratio of 1:200 was used. The injector and detector temperature were 250 and 280 $^{\circ}$C, respectively. Mass spectra were taken at 70 eV. Mass range was from *m/z* 50-550 amu.

The relative percentage amounts of the separated compounds were calculated from total ion chromatography by a computerized integrator.

2.4 Identification of essential oil constituents

Identification of essential oil components was done based on the basis of Retention Index (RI, with respect to homologous series of n-alkanes (C_8-C_{22}) under the same experimental conditions) and comparison of their mass spectra with MS library search (NIST 98 and WILEY), by comparing with the MS literature data [10].

2.5 Statistical analysis

Value dispersion was analysed by one-way analysis of variance (ANOVA) for the quantification of the compounds identified by GC-MS. Results are expressed as mean values ± standard deviation calculated from triplicate determinations. Student's two-tailed *t*-test was used to compare means of two population at the significance level of 5% for the measurement of retention index between retention index on AT-5MS and literature data [10].

Results and Discussion

The GC-MS analyses of the oil showed 25 components were identified, accounting for 99.25% of the total oil. Their retention index and percentage composition are given in Table 1, the values within raw follwed by the same letter are not significantly different at the significance level of 5%. The essential oil components are listed in the order of their elution from AT-5MS column and the total ion chromatogram (TIC) is shown in figure 1. The oil was dominated by the oxygenated monoterpene (49.25%). This follow by monoterpene hydrocarbon (46.76%). Sesquiterpenne were represented in the oil in a small quantity (1.47%). Carvacrol, *γ*-Terpinene and *p*-Cymene were determined as the major compounds of the oil (47.56, 17.12 and 11.36 %).
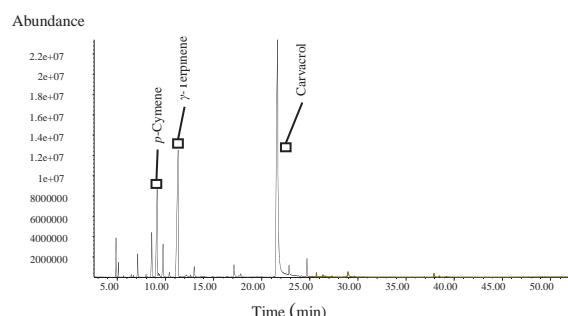
Fig. 1 The total ion chromatograms (TIC) obtained from the essential oil of *E. stachyodes*.

With respect to the knowledge of the essential oil of the studied *Elsholtzia* genus, *E. eriostachya* was dominated by rosefuran epoxide (85.18%), along with germacrene D (3.29%), and rosefuran (1.30%) while the major constituents of the *E. cristata* was mainly characterized by dehydroelsholtzia ketone (86.60%). It is interesting to note that the essential oils from *E. eriostachya* and *E. cristata* were both dominated by acylfurans only, but the marker acylfurans were completely different for the two oils. Furthermore, the *E. pilosa* was comprised of 1,8-cineole (34.37%), along with significant amounts of oxygenated monoterpene [11]. *E. stroblifera* collected from different locations at different stage of growth, showed pinocarvone alone as major compound in the essential oil.

Table 1 Chemical composition (% peak area) of *E. stachyodes* oil.

Compound	RI[a]	RI[b]	%[c]
α-Thujene	922	924	2.57 ± 0.16
α-Pinene	929	932	1.06 ± 0.02
Camphene	945	946	0.13 ± 0.00
Sabinene	968	969	0.22 ± 0.01
β-Pinene	975	974	0.17 ± 0.02
Myrcene	987	988	1.85 ± 0.09
α-Phellendrene	1005	1002	0.40 ± 0.01
α-Terpinene	1017	1014	5.23 ± 0.38
p-Cymene	1025	1020	11.36 ± 1.16
Limonene	1030	1024	0.52 ± 0.04
β-Phellendrene	1031	1025	0.37 ± 0.03
(Z)-*β*-Ocimene	1036	1032	3.64 ± 0.18
(E)-*β*-Ocimene	1048	1044	0.63 ± 0.01
γ-Terpinene	1060	1054	17.12 ± 0.60
cis-Sabinene hydrate	1069	1065	0.62 ± 0.02
Terpinolene	1087	1086	0.23 ± 0.03
p-Cymenene	1093	1089	1.26 ± 0.04
Terpinen-4-ol	1179	1174	1.41 ± 0.05
Cymen-8-ol	1184	1179	0.28 ± 0.01
Elsholtia ketone	1202	1202	0.38 ± 0.03
Carvacrol	1302	1298	47.56 ± 2.51
β-Caryophyllene	1421	1417	1.05 ± 0.06
α-Humulene	1457	1452	0.26 ± 0.00
Germacrene D	1483	1484	0.16 ± 0.02
Caryophyllene oxide	1588	1582	0.77 ± 0.10
Total identified		99.25	
Monoterpene hydrocarbons		46.76	
Oxygenated monoterpenes		49.25	
Sesquiterpene hydrocarbon		1.47	
Oxygenated monoterpene		0.77	
Acylfurans		0.38	
Others		0.62	

RI[a] : Retention index relative to n-alkane on AT-5MS column ; values expressed are means of triplicate.
RI[b] : Retention index relative (literature values (Adams, 2007))
%[c] : Relative percentages of components are calculated on GC peak areas on AT-5MS column ; values expressed are mean values ± standard deviation of triplicate.

However, the oil of *E. stroblifera* Benth. from the Himalayan region, India at an elevation of 2700 m. was characterized by neral (18.3%) and geranial (29.9%) along with significant amounts of monoterpene hydrocarbons [12]. The earlier report [13] had collected the *E. stroblifera* near Nainital region, India at an elevation 2200 m indicated the presence of sabinene (5.6%), *β*-pinene (9.7%) and pinovarvone (51.9%) with an entirely different ecological environment. This might be the reason that the species has adopted changes in the biosynthetic pathways to the secondary metabolites.

According to the previous reports, the chemical compositions of the plant essential oils depend on the species, part of plant, season of harvesting and geographical origin [14-17]. In addition, the extraction method can also influence the type and amount of molecules extracted [18-19].

As far as our literature survy could as certain, the essential oil composition of *E.stachyodes* has not previosly been reported. Data presented here could be assumed as the frst report on this *Elsholtzia* species.

Conclusion

The results from this study indicate that *E. stachyodes* oil was dominated by carvacrol, along with significant amounts of oxygenated monoterpene. As previous studied in literature data [20-21], several compounds found in these essential oils, such as thymol, carvacrol, (-)-camphor, (-)-bornyl acetate, *trans*-caryophyllene and *γ*-terpinene have known antioxidant properties [15]. Hence, the *E. stachyodes* essential oil may provide the evidence required for the utilization of *E. stachyodes* as a kind of herbal drug as well as the possibility of using *E. stachyodes* as a source of low-cost natural antioxidant

Acknowledgements

Address :
Department of Chemistry and Center of Excellence for Innovation Chemistry, Faculty of Science, Mahidol University.

References

[1] C. Ding, L. Zhou, L. Ji, W. Ji, and Y. Ma, *Acta Bot Occident Boreal Sin*. **24** (2004) 1093-1095.

[2] M. Percival, *Clin Nutr Insight*. **1** (1998), 1-4.

[3] B. Bhanubong and C. Pranom, *The Natural History Journal of Chulalongkorn University.* **8(1)** (2008) 1-5.

[4] Y.R. Nave and P. Ochsner, *Composition of Elsholtzia polystachya leaf essential oil*. **43** (1960) 406.

[5] V.N. Vashist and C.K. Atal, *Flavour Ind*. **2** (1970) 47.

[6] C.S. Mathela, A.B. Melkani, J.C. Bisht, A.K. Pant, J.J. Bestmann, U. Kobold, J. Rauser and O. Vostrowsky, *Planta Med* **58** (1992) 376.

[7] N.D. Murari and C.S. Mathela, *J. Indian. Chem. Soc.* **57** (1980) 1003.

[8] R.K. Thappa, S.G. Agrawal, K.L. Dhar and L.H. Hai, *Indian Perfume.* **40** (1996) 31.

[9] N.X. Dung, L.V. Hac, L.H. Hai and P.A. Leclercq, *J. Essent Oil Res.* **8** (1996) 107.

[10] R.P. Adams, *Identification of Essential oil Components by Gas Chromatography/Mass Spectrometry, fourth ed. Allured Publishing Corp., Carol Stream, IL, USA.*

[11] C.S. Mathela, R.C. Padalia, S.C. Joshi, K.K. Singh, D.S. Bisht, A.K. Pant and H. Kharkwal, *Chemical Diversity in Himalayan Elsholtzia species,* **6** (2009)

[12] J.C. Bisht, A.K. Pant, , C.S. Mathela, U. Kobold, O. Vostrowsky, *Planta Med.* (1985) 412–414.

[13] B.M. Anand, D. Vasu, S.B. Philip, N. Anuradha, S.P.S. Mehtaa, K.B. Melkania, *Biochem. Sys & Eco.* **33** (2005) 419–425

[14] F.J. Muller-Riebau, B.M. Berger, O. Yegen and C. Cakor, *J. Agric. Food Chem.* **45** (1997) 4821-4825.

[15] E. Putiecsky, U. Ravid and N. Dudat, *J. Nat, Prod.* **49** (1986) 1015-1017.

[16] A.M. Viljoen, S. Subramoney, S.F.v. Vuuren, K.H.C. Baser and B. Demirci, *J. Food Drug Anal.* **96** (2005) 271-277.

[17] M.J. Jordan, R.M. Martinez, K.L. Goodner, E.A. Baldwin and J.A. Sotomayor, *Ind. Crops Prod.* **24** (2006) 253-263.

[18] F. Bakkali, S. Averbeck, D. Averbeck and M. Idaomar, *Food Chem. Toxicol*. **46** (2008) 446-475.

[19] J. Mejri, M. Abderrabba and M. Mejri, *Ind. Crops Prod*. **32** (2010) 671-673.

[20] M.T. Baratta, H.J.D. Dorman, S.G. Deans, A.C. Figueiredo, J.G. Barroso and G. Ruberto, *Flavour Fragrance J.* **13** (1998) 235-244.

[21] H.F. Wang, K.H. Yih and K.F. Huang, *J. Food Drug Anal*. **18** (2010) 24.33.

DEVELOPMENT OF METAL SENSOR BASED ON TREHALOSE MODIFIED SELF-ASSEMBLED MONOLAYER ON SILICON

Patiya Pasakon[1], Supavadee Kiatisevi[2*]

[1]*Materials Science and Engineering Program, Faculty of Science, Mahidol University, Ratchthewee, Bangkok, Thailand 10400*
[2]*Department of Chemistry, Faculty of Science, Mahidol University, Ratchthewee, Bangkok, Thailand 10400*

[*] Corresponding Author E-Mail Address: supavadee.mon@mahidol.ac.th

Abstract: A simple method to develop a metal sensor based on trahalose modified trichlorosilyl-terminated self-assembled monolayer has been introduced. Starting from the acetoxy terminated monolayer from 11-acetoxyundecyl- l-trichlorosilane was first prepared on Si wafer. Trichlorosilyl terminated monolayer was then produced by reduction of the acetoxy to the hydroxyl group and transformation of the hydroxyl to the trichlorosilyl group by a reaction with tetrachlorosilane. Trehalose was chosen to be chemically coupled to the monolayer because of its good divalent metal ion recognition. Preliminary results based on FTIR spectroscopy and water contact angle measurements indicated that trehalose could successfully be attached to monolayer. In addition, the complexation ability of copper (II) ions towards trehalose base silicon electrode was also investigated by using cyclic voltammetry in applied potential range between -0.7 to 0.5 volt. From these results, the trehalose based silicon electrodes show great potential for their use as metal ion sensors.

Introduction

Heavy metal levels in environmental water sample are generally monitored by atomic absorption spectroscopy (AAS), inductively coupled plasma-mass spectroscopy (ICP-MS), and neutron activation analysis (NAA), but these techniques require sample pretreatment before analysis. This step can be avoided by using highly sensitive metal sensors which provide fast and precise detection. In this report, a new type of metal sensor based on easy-to-prepare trehalose-modified silicon wafers is introduced. Trehalose was employed because of its good divalent metal recognition. Starting from self-assembled monolayers. Trehalose was employed because of its good divalent metal recognition. Starting from self-assembled monolayers (SAMs) of 11-acetoxyundecyl- l-trichlorosilane (**1**) on Si wafer, electrophilic electrodes were fabricated by reduction of the acetoxy to hydroxyl groups and transformation of the hydroxyl to trichlorosilyl groups (figure 1) by a reaction with tetrachlorosilane.
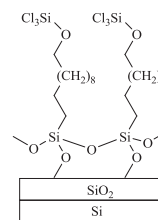
Figure 1: Schematic presentation of trichlorosilyl terminated monolayer on Si electrode.

The trichlorosilyl-terminated monolayers obtained were subsequently used for trehalose deposition. All modification steps aforementioned were followed by FTIR spectroscopy and water contact angle measurements. The chelation between trehalose moieties towards metal ions was finally examined using cyclic voltammetry method.

Materials and Methods

1. Materials

The substrate used for assembly was 12 mm x 15 mm *B*-doped silicon wafer (100) (Wacker-Siltronic, Germany). Prior to SAM preparation, the silicon wafers were cleaned in the mixture of 70% sulfuric acid (Mallinckrodt Baker, Inc.) and 30% hydrogen peroxide (Merck), at 100°C for 45 min, washed with purified water (18 $M\Omega$-cm^{-1}, Millipore-MilliQ water) and dried with nitrogen gas (Thai Industrial Gas (TIG)).

Reagents for fabrication of metal sensor, toluene (Merck), tetrahydrofuran (Fluka), Methylene chloride (Lab-Scan), and *N,N*-dimethyl formamide (Merck) were dried before use. Lithium aluminium hydride (Merck), hydrochloric acid (Lab-Scan), tretrachlorosilane (Sigma Aldrich), and trehalose (Merck) were employed without any purification.

2. Methods

The acetoxy terminated monolayers were first prepared by immersing a silicon wafer into a solution of 0.1 ml compound **1** in 20 ml of dried toluene in a reaction flask under nitrogen gas for 12 h at room

temperature. Subsequently, the reduction of the acetoxy into the hydroxyl terminal groups was carried out by immersing the monolayers on silicon into a solution of 0.7 mM lithium aluminium hydride dissolved in tetrahydrofuran, followed by washing with dil. HCl and purified water. The hydroxyl terminated monolayers were put in a solution of 0.04

M tetrachlorosilane in toluene for 10 min and rapidly immersed in 0.03 M trahalose solution in DMF under nitrogen gas for 12 h at room temperature.

Results and Discussion

1. FTIR characterization

The acetoxy and hydroxyl terminated monolayers were successfully deposited on Si electrodes and characterized by FTIR spectroscopy as presented in Figure 2. The trichlorosilyl terminated monolayers were not analyzed because they were very moisture sentitive, thus they must be immediately used after preparation.
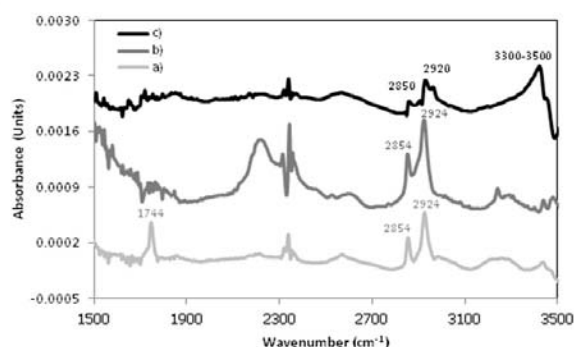
Figure 2: Transmission FTIR spectrum of a) acetoxy; b) hydroxyl; and c) trehalose modified monolayers. Spectrum a and b were substracted from that of blank Si electrode. Spectrum c was substracted from that of a.

IR peaks at 2924 and 2854 cm^{-1} correspond to asymmetric and symmetric stretching of $-CH_2$ groups of monolayers. The C=O vibration of the acetoxy terminal groups appeared at 1744 cm^{-1} (spectrum a). In spectrum C, the IR peaks around 2920 and 2850 cm^{-1} indicate asymmetric and symmetric stretching from $-CH_2$ groups of trehalose moieties. The wavenumber range of 3300-3500 cm^{-1} represents the stretching vibration of hydroxyl groups of trehalose on the surface.

2. Water contact angle measurement

Table 1 shows the results from water contact angle measurements of all modified Si electrodes. The water contact angles obtained are in agreement with the hydrophilic property of each electrode. The trehalose modified electrode exhibited a small contact angle of

51.3 $\pm$ 3.6° comparable to the hydroxyl terminated monolayer (55.3 $\pm$ 3.1°), whereas the acetoxy terminated monolayer exhibited the highest contact angle (66.0 $\pm$ 2.4°) as expected.

Table 1: Water contact angles of a blank Si wafer, the acetoxy and hydroxyl terminated monolayers, and trehalose modified monolayer.

	Water contact angle (°)
blank Si wafer	22.3 $\pm$ 2.5
acetoxy terminated monolayer	66.0 $\pm$ 2.4
hydroxyl terminated monolayer	55.3 $\pm$ 3.1
trehalose modified monolayer	51.3 $\pm$ 3.6

3. Cyclic voltammetry (CV) measurements

The redox reaction of Cu (II) ions interacting with the trehalose modified Si surfaces could be investigated by using cyclic voltammetry (CV) technique. Figure 3 shows the voltammograms of a bare Si wafer, a trehalose modified monolayer before and after exposure to 5 mM copper (II) ion solution. In Figure 3(c), the redox reaction of Cu (II) ions could be observed in applied potential range between -0.7 to 0.5 volt. From the results, the trehalose based Si electrode showed performance in application as metal ion sensors.
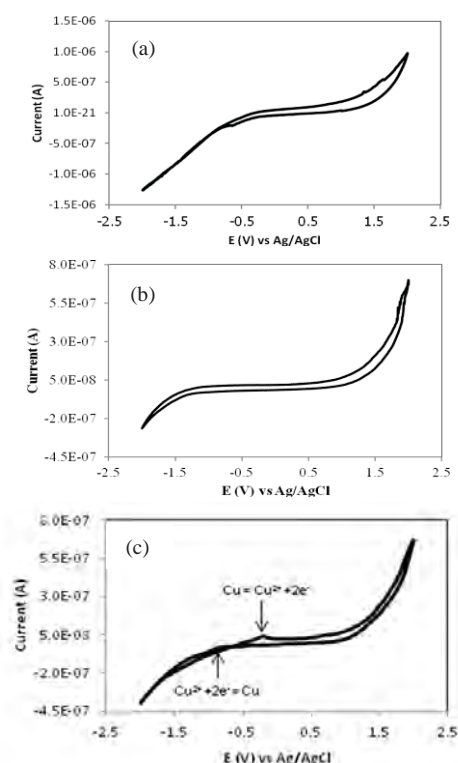
Figure 3: Voltammograms of a) a bare Si wafer, b) a trehalose modified monolayer, and c) a trehalose modified monolayer exposed to 5 mM copper (II) ion solution for 1 h in 15 ml of 0.1 M KH_2PO_4/0.1 M K_2HPO_4 solution with a scan rate of 10 mV/s under nitrogen.

Conclusions

The trichlorosilyl terminated monolayers could be employed to immobilize trehalose on Si electrode as confirmed by FTIR and water contact angle results. Trehalose modified Si electrode exhibited the chelating ability to copper (II) ions as characterized by CV method. These results confirm feasibility of using our electrode as a metal ion sensor. In the future, we plan to study the trehalose modified monolayers in order to detect other metals such as Ni^{2+}, Zn^{2+}, and Pb^{2+}.

Acknowledgements

References

[1] J. Xia, W. Wei, Y. Hu, H. Tao and L. Wu, *J. Anal. Chem.* **20** (2004), pp. 1037-1041.

[2] T. Higashiyama, *J. Pure Appl. Chem.* **7**, (2002), pp. 1263-1269.

[3] Y. E. Alekseev, A. D. Garnovskii and Y. A. Zhdanov, *Russ. Chem. Rev.* **67** (1998), pp. 649-669.

[4] N. K. Singhal, B. Ramanujam, V. Mariappanadar, and C. P. Rao, *Org. Lett.,* **8**, (2006), pp. 3525-3528.

STUDY OF SILVER IONS AND SILVER NANOPARTICLES BINDING WITH BOVINE SERUM ALBUMIN BY USING HOLLOW FIBER FLOW FIELD-FLOW FRACTIONATION COUPLED WITH THERMOSPRAY FLAME FURNACE ATOMIC ABSORPTION SPECTROMETRY

Jaruwan Mettakoonpitak[1], Juwadee Shiowatana[1], Atitaya Siripinyanond[1*]

[1] Department of Chemistry and Center of Excellence for Innovation in Chemistry, Faculty of Science, Mahidol University, Bangkok 10400, Thailand

* E-Mail: atitaya.sir@mahidol.ac.th, Tel. +66 22015129, Fax. +66 23547151

Abstract: Hollow fiber flow field-flow fractionation (Hf-FlFFF) coupled with thermospray flame furnace atomic absorption spectrometry (TS-FF-AAS) has been developed for metal-based particle characterization. In part of Hf-FlFFF, it functions as the separation part of particle size characterization. Many advantages of this striking technique include disposable usage of the membrane, inexpensive channel construction, and simple approach to set up the system. Additionally, it is a home-made device providing a good efficiency for particle separation. In case of TS-FF-AAS, this technique has been used for coupling with Hf-FlFFF as the simultaneous detection part. This developed approach has been applied for studying silver ions and silver nanoparticles binding with bovine serum albumin (BSA). Varying concentration of silver ions and silver nanoparticles at fixed concentration of BSA, silver ions show a capability to bind with BSA until reaching one point in which the concentration of silver ions is maximum that will equivalently bind with BSA. At high concentration of silver ions, the aggregation of particles has occurred affecting decrease of signal as larger particles cannot elute in the experimental condition. In contrast, when the concentration of silver nanoparticles has been increased, the signal has incessantly increased as the signal of silver nanoparticles separated has included with that from silver nanoparticles binding with BSA.

1. Introduction

Hollow fiber flow field-flow fractionation is one of the techniques used for particle separation. This technique has continuously attracted the attention due to many benefits including simple construction, disposable membrane, and inexpensive. Moreover, this outstanding technique provides good efficiency for particle separation. Much research has focused on applying it to separate biological samples such as *E. Coli*, lipoproteins from the healthy person and patient who had the coronary artery and stand, various types of protein from 14.2-670 kDa, urate oxidase (uricase) drug, and phospholipids [1-5]. The separation consists of three steps---injection step, focusing and relaxation step, and elution step. In the injection step, particles are introduced into hollow fiber housing. Then, those particles are focused at one position within that housing by applying carrier from both sides of the hollow fiber housing in opposite direction and relaxation process occurs within a short period of time.

Lastly, particles at accumulation wall of hollow fiber membrane are separated. Two forces of carrier flow are applied. For radial flow, it is applied in perpendicular direction to press particles towards the accumulation wall. The larger particle sizes are forced towards accumulation wall more than the smaller counterparts. In case of axial flow, it functions as carrier flow to take particles reaching to the detector. Therefore, smaller particles move faster than larger particles.

In terms of thermospray flame furnace atomic absorption spectrometry (TS-FF-AAS), it is competent to increase sensitivity for metal determination such as Ag, Bi, Cd, Rb, and Zn [6] compared with regular flame atomic absorption spectrometry.

Additionally, silver ions relate to the public utilities of human. Therefore, many works have reported about the drawbacks of this element affecting to the structure of protein [7-9]. Furthermore, silver in form of nanoparticles has been attracted to widely research both of the advantages and disadvantages. They have been one part of many products assimilated with people from administrative routine to biomedicine such as the antibacterial properties [10]. Therefore, the nanosafety has been monitored such as the study of capability of silver nanoparticles to bind with protein in living body [11].

In this work, Hf-FlFFF technique has been coupled with TS-FF-AAS in order to determine metal based particles---bovine serum albumin (BSA)-silver ions binding and bovine serum albumin (BSA)-silver nanoparticles binding. Hf-FlFFF functions as the separation part of these binding molecules while TS-FF-AAS acts as the detection part to determine silver ions and silver nanoparticles binding with BSA. In order to study the tendency of binding ratio between bovine serum albumin and silver, Hf-FlFFF is used to characterize BSA and TS-FF-AAS is used to detect silver ions and silver nanoparticles for quantitative analysis.

2. Materials and Methods

2.1 Hf-FlFFF Coupled with TS-FF-AAS

Home-Made Hollow Fiber Housing: polysulfone hollow fiber membrane (30000 M_r cutoff) with internal diameter of 0.5 mm and 22 cm in length was inserted in two pieces of hollow fiber tubes made from PFA tube with 1/8 inch outer diameter and 22 cm in length. Two hollow fiber tubes were connected with stainless steel tees fitting 1/8 inch (Alltech, Illinois, USA). One piece of PFA tube of 5 cm in length was linked with that stainless steel tees fitting at T-shaped position.

Instrumental Set-Up: One side of the hollow fiber housing is connected with an HPLC pump (Model 2800, BIO-RAD, Philadelphia, USA) by PFA tube with 1/16 inch and 30 cm in length. Another side of this housing was connected with 4-way diagonal flow switching valve linked to UV detector (UV-2075, Jasco, Tokyo, Japan) and another pump (Model 2800, BIO-RAD, Philadelphia, USA). The micro-metering valve (IDEX Health & Science, Washington, USA) was connected with housing at the T-shaped position in order to adjust radial flow rate. That UV detector was linked to atomic absorption spectrometer (iCE 3000 series AA spectrometry, Thermo SCIENCTIFIC, Massachusetts, USA). For thermospray flame furnace atomic absorption spectrometry technique, nickel tube (with Mount for T cell and STAT, Thermo SCIENCTIFIC, Massachusetts, USA) was put on a burner of the device and sample solution was introduced through ceramic tube into nickel tube. The set up is similar to what was reported by Berndt *et al.* [6]. Silver hollow cathode lamp was used as a light source for this technique. Figure 1 shows the instrumental set-up. BSA was detected at 280 nm while silver ions and silver nanoparticles were investigated from TS-FF-AAS. The condition for separation is shown in Table 1.

2.2 Reagent

Silver nanoparticles 3.4 nm: They were prepared from 500 ppm AgNO$_3$ (ACI Labscan, Bangkok, Thailand) stabilized by 0.453 mM tannic acid (Fluka, Missouri, USA) and adjusted pH to 10 by using 0.1 M potassium carbonate (CARLO ERBA Reagents, Rodano, Italy). Then, they were characterized by using flow field-flow fractionation.

BSA-silver ions binding: 2000 ppm BSA (Molecular weight of 67 kDa) was incubated with 5-500 ppm silver ions at 37^{0}C for 24 hr.

BSA-silver nanoparticles binding: 2000 ppm BSA (Molecular weight to 67 kDa) was incubated with 50-400 ppm silver nanoparticles and 500 ppm BSA (Molecular weight of 67 kDa) was incubated with 10-220 ppm silver nanoparticles at 37^{0}C for 24 hr.

30 mM Tris-buffer pH 8.8 was used as a carrier liquid.

3. Results and Discussion

3.1 BSA-silver ions binding

The occurrence of the BSA-silver ions binding was suggested by the closeness between the retention time observed by UV detection and that by TS-FF-AAS. Retention time of BSA detected by using UV-detection appeared at 9 min approximately (Figure 2a) while that from silver ions determined by using TS-FF-AAS occurred at 12 min roughly (Figure 2b). The retention time from TS-FF-AAS delayed a little bit because of dead volume between UV-detector and TS-FF-AAS. Therefore, BSA-silver ions binding occurred. However, the retention time in which concentration of silver ions more than 100 ppm would shift to longer time because larger binding molecule occur at high concentration of silver ions (Figure 2c). This phenomenon corresponded to the previous study that silver ions at high concentration had capability to change BSA molecular structure into a larger extent and assembled together to form conglomeration [7]. Therefore, concentration of silver ions affected the size of binding molecule. From this experimental section, it indicated that silver ions had capability to bind with BSA until reaching one point in which the concentration of silver ions was maximum that would equivalently bind with BSA. At higher concentration of silver ions, the aggregation of binding molecules occurred leading to the decrease of signal as larger particles could not elute in this condition (Figure 2d). In addition, the precision of measurement was poor at high concentration of silver ions because of uncertain amount of aggregation of larger binding molecules in each replicate.
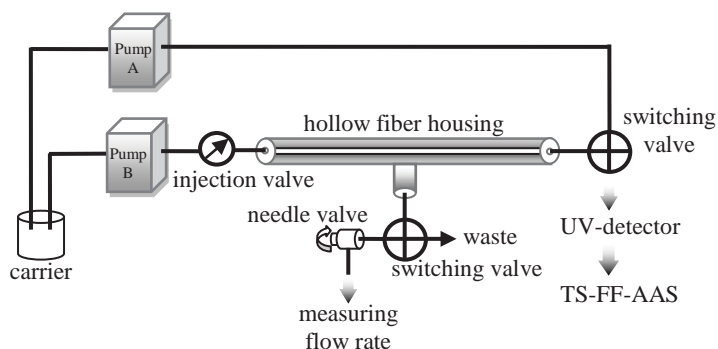
Figure 1. Hf-FlFFF coupled with TS-FF-AAS set-up

Table 1: Condition Used in Hf-FlFFF System

Parameter	Optimum Condition
Focusing time	5 min
Radial flow rate	0.2 mL/min
Axial flow rate	0.3 mL/min
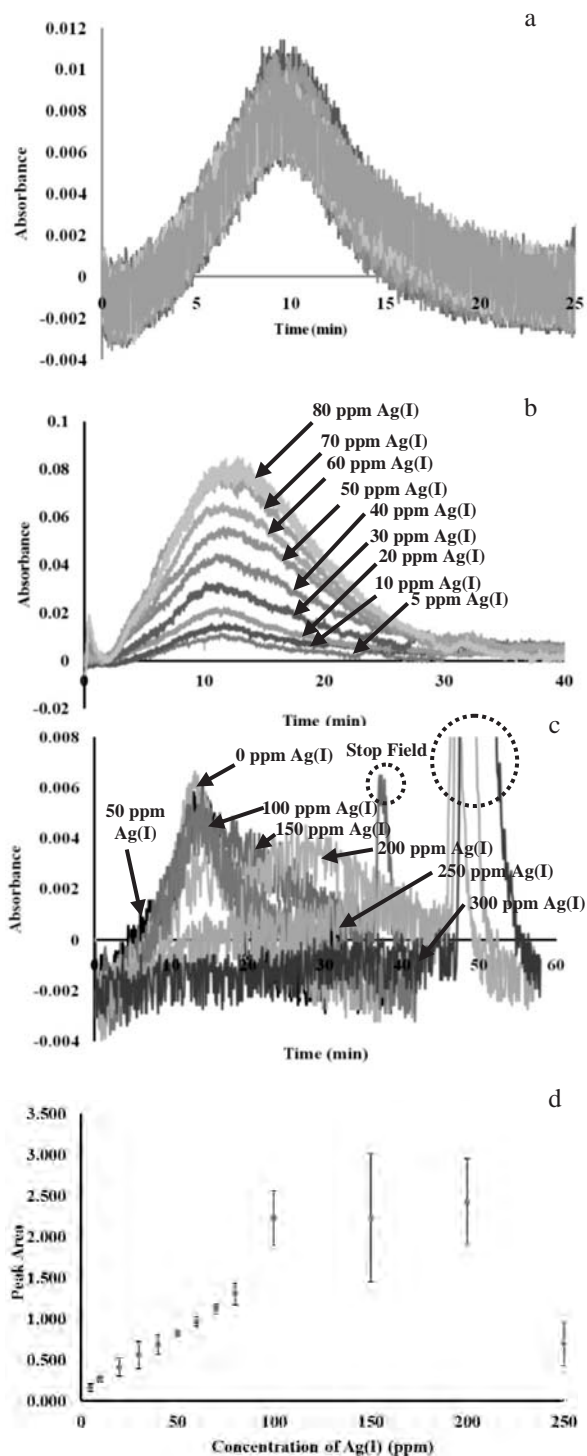
Figure 2. (a) Fractogram from UV-detection for 5-80 ppm silver ions binding with 2000 ppm BSA (b) Fractogram from TS-FF-AAS detection for 5-80 ppm silver ions binding with 2000 ppm BSA (c) Fractogram from UV detection for 0-300 ppm silver ions binding with 2000 ppm BSA (d) Relationship between peak area from TS-FF-AAS detection and concentration of silver ions

Figure 3. (a) Fractogram from UV-detection for 0-400 ppm silver nanoparticles binding with 2000 ppm BSA (b) Fractogram from TS-FF-AAS detection for 0-400 ppm silver nanoparticles binding with 2000 ppm BSA (c) Relationship between peak area from TS-FF-AAS detection for 0-400 ppm silver nanoparticles binding with 2000 ppm BSA (d) Relationship between peak area from TS-FF-AAS detection for 10-220 ppm silver nanoparticles binding with 500 ppm BSA

3.2 BSA-silver nanoparticles binding

To confirm the binding between BSA and silver nanoparticles, the retention time from UV detection (for BSA determination) should be close to that from

TS-FF-AAS detection (for silver nanoparticles detection). Retention time for BSA detection (from UV detection) was approximately 13 min (Figure 3a) while that for silver nanoparticles was about 15 min (Figure 3b). The delay time caused from dead volume

between UV detector and TS-FF-AAS. Additionally, the absorbance of UV detection that should be only originated from BSA increased when increasing concentration of silver nanoparticles.

In terms of signal from TS-FF-AAS, the binding behavior between BSA and silver nanoparticles differed from that between BSA and silver ions. The signal from TS-FF-AAS incessantly increased through high concentration of silver nanoparticles was added (Figure 3c). This phenomenon was confirmed by changing concentration of silver nanoparticles to 500 ppm (Figure 3d). This might be due to the fact that under this experimental condition, silver nanoparticles and BSA-silver nanoparticles coeluted as their particle sizes were quite close. Alternatively, the increase in silver signal as observed by TS-FF-AAS might be due to the binding between silver nanoparticles and BSA, as the binding between silver nanoparticles and BSA was already documented [11]. Therefore, the signal from UV detection and TS-FF-AAS would increase when increasing concentration of silver nanoparticles.
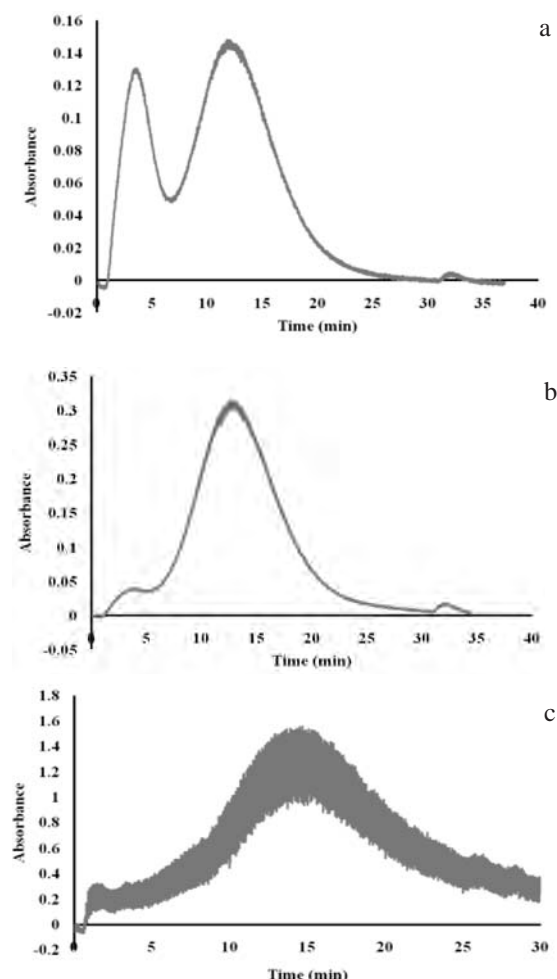
Figure 4. (a) Fractogram from UV-detection at 254 nm of 100 ppm silver nanoparticles (b) Fractogram from UV-detection at 400 nm of 100 ppm silver nanoparticles (c) Fractogram from TS-FF-AAS of 100 ppm silver nanoparticles

To confirm this presumption, individual injection of silver nanoparticles was performed. As the results, they agreed with the assumption that Hf-FlFFF can separate silver nanoparticles providing the close retention time to that of BSA-silver nanoparticles binding molecules (Figure 4a). Moreover, void peak might come from tannic acid stabilizer because it absorbed light at 254 nm.

4. Conclusions

The developed system, Hf-FlFFF coupled with TS-FF-AAS, has been competent to use in characterization of metal based particles. BSA-silver ions binding and BSA-silver nanoparticles binding were studied in order to demonstrate the system. In case of BSA-silver ions, they have been able to bind together until reaching one point. After that, the binding phenomenon would change to aggregation of BSA molecules. However, in terms of BSA-silver nanoparticles, signal from TS-FF-AAS incessantly increased even though it was performed at high concentration of silver nanoparticles because signal from silver nanoparticles separated included that of silver nanoparticles binding with BSA.

References

[1] P. Reschiglian, A. Zattoni, B. Roda, L. Cinque, D. Meluccim, B. R. Min and M. H. Moon, *J. Chromatogr. A* **985** (2003) 519-529.
[2] I. Park, K. Paeng; D. Kang and M. H. Moon, *J. Sep. Sci.* **28** (2005) 2043–2049.
[3] R. Zhu, W. Frankema, Y. Huo and W. T. Kok, *Anal. Chem.* **77** (2005) 4581-4586.
[4] A. Roda, D. Parisi and M. Guardigli, *Anal. Chem.* **78** (2006) 1085-1092.
[5] LeeaJ. Y. Lee, H. K. Min, D. Choi, and M. H. Moon, *J. Chromatogr. A* **1217** (2010) 1669- 1666.
[6] J. Davies and H. Berndt, *Anal. Chim. Acta* **479** (2003) 215-223.
[7] X. Zhao, R. Liu, Y. Teng and X. Liu. *Sci Total Environ.* **409** (2011) 892–897.
[8] V. W.-M. Lee and H. Li, *J. Am. Soc. Mass Spectrom.* **9** (1998) 760-766.
[9] X.-C. Shen, H. Liang, J.-H. Guo, C. Song, X.-W. He and Y.-Z. Yuan, *J. Inorg. Biochem.* **95** (2003) 124-130.
[10] S. Shrivastava, T. Bera, S. K. Singh, G. Singh, P. Ramachandrarao and D. Dash, *ACS Nano.* **3** (2009) 1357-1364.
[11] J. Mariam, P. M. Dongre and D. C. Kothari, *J. Fluoresc.* **21** (2011) 2193-2199.

COMPARATIVE STUDY OF CHROMATOGRAPHIC SEPARATION MODE FOR THE DETERMINATION OF GLYPHOSATE, GLUFOSINATE, AND THEIR METABOLITES BY LIQUID CHROMATOGRAPHY-TANDEM MASS SPECTROMETRY

Walaiporn Chanchanasophon, Siripastr Jayanta, Natchanun Leepipatpiboon*

Chromatography and Separation Research Unit, Department of Chemistry, Faculty of Science, Chulalongkorn University, Bangkok 10330, Thailand.

*Author for correspondence; E-Mail: natchanun.l@chula.ac.th, Tel. +66 22187608, Fax. +66 22187598

Abstract: A liquid chromatography–tandem mass spectrometry (LC-MS/MS) method for simultaneous determination of glyphosate, glufosinate, and their metabolites (aminomethylphosphonic acid (AMPA), 3-(methylphosphinico) propionic acid (3-MPPA), and *N*-acetyl-glufosinate) was developed. A comparative study of various chromatographic separation modes such as hydrophilic interaction liquid chromatography (HILIC), reversed phase liquid chromatography (RPLC), and ion chromatography (IC) were undertaken. Parameters affecting chromatographic separations such as type, concentration, and pH of the mobile phase were studied and optimized separately. Broad peak shapes and tailing of glyphosate and AMPA peaks were observed in HILIC mode using Acquity UPLC BEH amide column. Good resolution and symmetric peak shapes were observed on Zorbax RRHD Eclipse Plus C18 (RPLC) and Dionex IonPac AS11 (IC). The analysis time for the herbicides in HILIC, RPLC, and IC modes was 10 min, 2 min, and 11 min, respectively. The linearity was achieved in the range of 0.01-1.00 mg/L and 0.005-0.250 mg/L with acceptable values of coefficient of determination, $r^2 > 0.98$ and 0.92 for RPLC and IC mode, respectively. The lowest calibration levels (LCL) were 0.01 mg/L and 0.005 mg/L for RPLC and IC modes, respectively. The comparative result showed that two of three studied LC modes are suitable for the separation of glyphosate, glufosinate and their metabolites. The chromatographic conditions in two selected modes were simple, fast, and required no derivatization step commonly required for these analytes. Tandem mass spectrometry provides excellent analyte selectivity and improved method sensitivity.

1. Introduction

Herbicides are widely applied in agriculture for the control of weeds. Applications of herbicides allow farmers to timely and effectively control weeds with minimum cost and labor. Glyphosate and glufosinate are most widely used herbicides globally including Thailand. National import statistics indicated that glyphosate and glufosinate toped the imported list of the country hazardous substances since 2002. Glyphosate was number one agricultural substance in 2009 when eighty-five thousand tons of herbicides were imported [1, 2]. These agricultural substances are sources of chemical residues with adverse affect to human and the environment. For these reasons, the European Union (EU) regulates herbicide residues in vegetables and fruits. The maximum residue limit (MRL) is set at 0.01 mg/kg depending on particular herbicide and matrix type [3].

Glyphosate is mainly decomposed to aminomethyl phosphonic acid (AMPA). While *N*-acetyl-glufosinate and 3-(methylphosphinico) propionic acid (3-MPPA) are the degradation products of glufosinate. Glyphosate, glufosinate and their metabolites are very difficult to analyze due to their extreme polarity. Their molecular structures contain both positive and negative ions (zwitterionic) and therefore, have extreme water solubility. Other properties that contribute to their analytical difficulty are low volatility, and lack of chromophore or fluorophore. Chemical structures of these herbicides are illustrated in Figure 1.
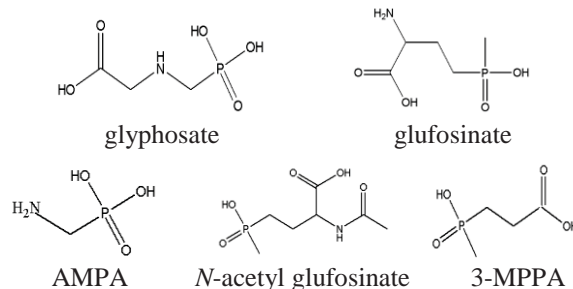
Figure 1. Chemical structures of glyphosate, glufosinate and their metabolites.

There are many analytical methods for glyphosate and glufosinate. The U.S. Environmental Protection Agency (U.S.EPA) recommends a HPLC post-column derivatization fluorescence detection procedure for the analysis of glyphosate in drinking water. (EPA method 547) [4]. Derivating reagents were ortho-phthalaldehyde (OPA) and 2-mercaptoethanol. Association of Official Analytical Chemists (AOAC) recommends ion-exchange chromatography with UV-visble detection for glyphosate in water (AOAC official method 996.12) [5]. EU recommends for the analysis of glyphosate, glufosinate, and their metabolites in vegetables and fruits by LC-MS/MS [6]. Other published works employed both pre- and post-column derivatization for determination glyphosate, glufosinate and their metabolites using different derivatizing reagents were reported, such as 9-

fluorenylmethylchloro formate (FMOC-Cl) [7,8], OPA, and Thiofluor (*N*, *N*-dimethyl-2-mercaptoethylamine hydrochloride) [9]. Different analytical techniques were also employed, e.g., LC-fluorescence [9], LC-UV [10], ion chromatography-conductivity [11], capillary electropholysis (CE) [12], gas chromatography-mass spectrometry (GC-MS, GC-MS/MS) [13, 14], LC-mass spectrometry (LC-MS, LC-MS/MS) [7, 8]. The most effective method for the analysis of glyphosate, glufosinate, and their metabolites are pre- or post-column derivatization process due to the high polarity and their lack of chromophores and fluorophore. Derivatizing procedure often employs toxic chemical and is complex, time consuming, and expensive.

Hydrophilic interaction chromatography (HILIC) is an alternative option for polar compounds. The procedure was successfully employed for glyphosate, glufosinate, and their metabolites (HILIC-MS/MS) in human serum [15] and in vegetables and fruits [16]. The coupling of HILIC and coulometric detection were employed for these herbicides in fruits juice [17].

The aim of this paper is identify simple and fast analytical method that requires no derivatizing step for the analysis of glyphosate, glufosinate, and their metabolites. For this, we compare several chromatographic separation modes (HILIC, RPLC, IC) using LC-MS/MS.

2. Materials and Methods

2.1 Chemicals and reagents

Glyphosate (96%) and AMPA (99%) reference standards were purchased from Aldrich (WI, USA). Glufosinate-ammonium (97.5%) and glufosinate-*N*-acetyl (98%) were obtained from Dr Ehrenstorfer (Augsburg, Germany). 3-MPPA was purchased from Fluka (Buchs, Switzerland). Methanol (MeOH) and acetonitrile (MeCN) were LC/MS grade from J.T. Baker (Deventer, The Netherlands). Ammonium acetate and ammonium hydroxide were analytical grade from J.T. Baker. Ammonium formate, citric acid monohydrate and dimethylamine (DMA) were analytical grade from Fluka. Sodium hydroxide was analytical grade from Carlo Erba Reagents (Rodano, Italy). Acetic acid and formic acid were analytical grade from Merck (Damstadt, Germany) and Fisher Scientific (Leicestershire, UK), respectively. Water was purified from Milli-Q purification system (Millipore, Billerica, MA, USA) at 18.2 MΩ cm^{-1} resistivity.

2.2 Stock solutions and working standard solutions

Stock standard solutions of individual analyte at final concentration of approximately 100 mg/L were prepared in Milli-Q water. All stock standard solutions were stored in plastic bottles. For the optimization of MS/MS parameters (tuning), individual standard solution was prepared at 10 mg/L in MeOH. For comparative study modes, a mixture of standards solution was prepared at 1 mg/L in MeOH. For

standard calibration curves, a mixture of stock standards was prepared at 1 mg/L, this solution was diluted to desired concentrations.

2.3 Instrumentation

The LC-MS/MS system consisted of an Agilent Technologies (CA, USA) 1290 series separation module interfaced with an electrospray ionization (ESI) 6490 triple quadrupole mass spectrometer was employed throughout. The data were acquired and processed using the MassHunter software.

2.3.1 Hydrophilic interaction liquid chromatography (HILIC)

LC separation was performed on an Acquity UPLC BEH amide column (2.1 x 100 mm, 1.7 µm) (Waters, Dublin 9, Ireland). The column was kept at 40 °C. The injection volume was 5 µL and the flow rate of mobile phase was 0.1 mL/min. The optimized mobile phase composition was 10mM ammonium acetate in water at pH 8.5 (adjust with ammonium hydroxide) (mobile phase A) and MeCN (mobile phase B). A mobile phase gradient program was started at 55% B (held for 2.5 min), 10% B at 2.6 min (held for 7.4 min). The analysis time was 10 min and post time 5 min. The MS instrument was performed by electrospray ionization in positive mode (ESI+) for glufosinate and negative mode (ESI-) for glyphosate, AMPA, *N*-acetyl glufosinate and 3-MPPA. The MS conditions used in this study were as follows: capillary voltage of ±1500 V, nozzle voltage of 0 V, gas temperature of 200 °C, gas flow of 17 L/min, nebulizer pressure of 50 psi, sheath gas temperature of 400°C, sheath gas flow of 12 L/min, fragmentor of 380 V and dwell time 100 ms for each MRM transition.

2.3.2 Reversed phase liquid chromatography (RPLC)

LC separation was performed on a Zorbax RRHD Eclipse Plus C18 (2.1 x 50 mm, 1.8 µm) (Agilent Technologies, CA, USA). The column was kept at 35 °C. The injection volume was 5 µL and the flow rate of mobile phase was 0.3 mL/min. The optimized mobile phase composition was 0.2 M formic acid in water (mobile phase A) and MeOH (mobile phase B). A mobile phase isocratic program was 95% A: 5% B. The analysis time was 2 min. The MS instrument was performed by electrospray ionization in negative mode (ESI-). The MS conditions used in this study were as follows: capillary voltage of -4000 V, nozzle voltage of -500 V, gas temperature of 150 °C, gas flow of 19 L/min, nebulizer pressure of 50 psi, sheath gas temperature of 400 °C, sheath gas flow of 12 L/min, fragmentor of 380 V and dwell time 50 ms for each MRM transition.

2.3.3 Ion chromatography (IC)

LC separation was performed on a Dionex IonPac™ AS11 (2 x 100 mm, 13 µm) with a guard column Dionex IonPac™ AG11 (2 x 50 mm) (Thermo

Scientific, Sunnyvale, CA). The column was kept at 35 °C. The injection volume was 20 μL and the flow rate of mobile phase was 0.3 mL/min. The optimized mobile phase composition was water (mobile phase A) and 1mM citric acid in water at pH 11(adjust with DMA) (mobile phase B). A mobile phase gradient program was started at 0% B, 50% B at 8 min (held for 3 min). The analysis time was 11 min and post time 7 min. The MS instrument was performed by electrospray ionization in negative mode (ESI-). The MS conditions used in this study were as follows: capillary voltage of -4000 V, nozzle voltage of -500 V, gas temperature of 200 °C, gas flow of 17 L/min, nebulizer pressure of 50 psi, sheath gas temperature of 400 °C, sheath gas flow of 12 L/min, fragmentor of 380 V and dwell time 100 ms for each MRM transition.

3. Results and Discussion

3.1 Mass spectrometry optimization

The LC-MS/MS was operated in the multiple reaction monitoring (MRM). Two precursor/product ion transitions were monitored for each target. The target ion transition with the highest intensity was used for quantification, while the second target ion transition was used for confirmation. Optimization of collision energy (CE) and cell accelerator voltage (CAV) for each compound are showed in Table 1. All compounds in RPLC and IC modes were analyzed in negative ion mode. HILIC mode, glyphosate, AMPA, *N*-acetyl glufosinate, and 3-MPPA were analyzed in negative ion mode. The response of glufosinate in positive ion mode showed greater sensitivity than signal in negative mode because the molecular structure of this compound is easily protonated.

3.2 Liquid chromatography optimization

3.2.1 Optimization of the HILIC mode

The Acquity UPLC BEH amide column contains trifunctional amide bonded to ethylene bridge hybrid (BEH) stationary phase which enable the phase to retain high polarity compounds. MeCN was employed as mobile phase B due to its good miscibility with water, offered good HILIC retention, and suitable viscosity. The mobile phase A was ammonium acetate. The mobile phase system was tested at pH 2.5, 4.5, 6.6, 8.5, and 10.5 and at ion strength of 5, 10, 15, and 20 mM, respectively. It was observed that retention time increased with increasing ionic strength, the optimum sensitivity was observed at 10 mM. Poor peak separation was observed at pH 2.5 and 4.5. Optimum separation was observed at pH 8.5, however, peak shape of glyphosate and AMPA were broad and tailing was observed (Figure 2).
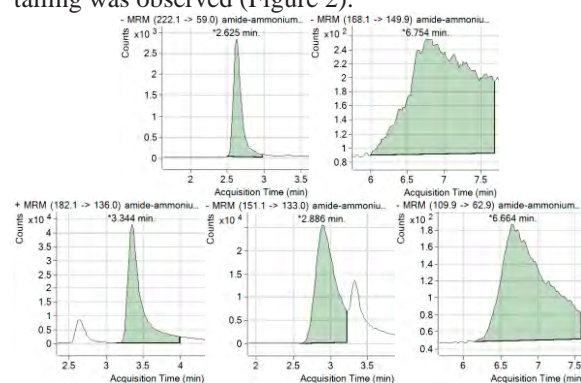
Figure 2. Chromatograms of all compounds analyzed in HILIC mode. (from top left to bottom right are *N*-acetyl glufosinate, glufosinate, glyphosate, 3-MPPA and AMPA, respectively)

3.2.2 Optimization of the RPLC mode

RPLC mode is a common chromatographic separation. The stationary phase less polar than the mobile phase so the polar compound will elute first. In the mobile phase, 10 mM ammonium acetate, 10 mM ammonium formate, 0.1% formic acid-MeCN and 0.2 M formic acid-MeOH were tested. It was found that 0.2 M formic acid-MeOH provided optimum chromatographic separation for all compounds (Figure 3).

Table 1: Molecular weights (M.W.), retention times (t_R), ion transition and optimized MS/MS parameters in three chromatographic separation modes.

Mode	Compound	M.W.	t_R (min)	Quantification Transition (m/z)	CE (V)	CAV (V)	Confirmation Transition (m/z)	CE (V)	CAV (V)
HILIC	*N*-acetyl glufosinate	223.16	2.593 ± 0.045	222.1 > 59.0	5	5	222.1 > 136.1	5	5
	3-MPPA	152.09	3.120 ± 0.252	151.1 > 133.0	8	3	151.1 > 107.0	14	3
	glufosinate	181.13	3.348 ± 0.042	182.1 > 136.0	11	5	182.1 > 56.1	29	5
	AMPA	111.04	6.671 ± 0.079	109.9 > 62.9	20	3	109.9 > 79.0	29	3
	glyphosate	169.07	6.820 ± 0.190	168.1 > 149.9	8	3	168.1 > 63.0	23	3
RPLC	AMPA	111.04	0.486 ± 0.007	109.9 > 62.9	20	3	109.9 > 79.0	29	3
	glufosinate	181.13	0.511 ± 0.004	180.1 > 136.1	14	3	180.1 > 85.1	17	3
	glyphosate	169.07	0.537 ± 0.008	168.1 > 149.9	8	3	168.1 > 63.0	23	3
	3-MPPA	152.09	0.670 ± 0.004	151.1 > 133.0	8	3	151.1 > 107.0	14	3
	N-acetyl glufosinate	223.16	0.691 ± 0.004	222.1 > 136.1	5	5	222.1 > 59.0	5	5
IC	AMPA	111.04	3.581 ± 0.060	109.9 > 79.0	29	3	109.9 > 62.9	20	3
	glufosinate	181.13	3.601 ± 0.026	180.1 > 136.1	14	5	180.1 > 85.1	17	5
	N-acetyl glufosinate	223.16	3.818 ± 0.046	222.1 > 136.1	5	5	222.1 > 59.0	5	5
	3-MPPA	152.09	4.098 ± 0.074	151.1 > 133.0	8	3	151.1 > 107.0	14	3
	glyphosate	169.07	8.577 ± 0.017	168.1 > 149.9	8	3	168.1 > 63.0	23	3
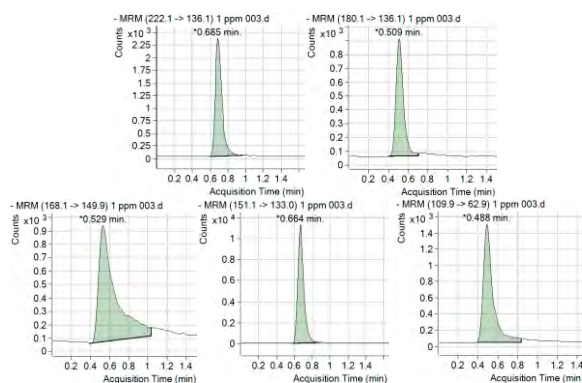
Figure 3. Chromatograms of all compounds analyzed in RPLC mode. (from top left to bottom right are *N*-acetyl glufosinate, glufosinate, glyphosate, 3-MPPA and AMPA, respectively)

3.2.3 Optimization of the IC mode

An anion exchange column, Dionex IonPac AS11, was employed. Poor peak shapes were observed when the mobile phase pH was below 11. Type of solvents for preparing mixed-standards solution were investigated. MeOH provided greatest sensitivity and peak shape, followed in order of decreasing sensitivity by MeCN, 1% formic acid in MeCN, water and 1% formic acid in MeOH. The optimum conditions of this mode were selected and the best chromatographic separation of all targets compounds was shown in Figure 4. It should be noted that the column should be flushed after 100-150 injection with 30 mM NaOH for 1 hour at a flow rate of 0.3 mL/min. After flushing, NaOH should be removed from the system to protect MS ion source by flushing mobile phase at a flow rate of 0.3 mL/min for 30 min.
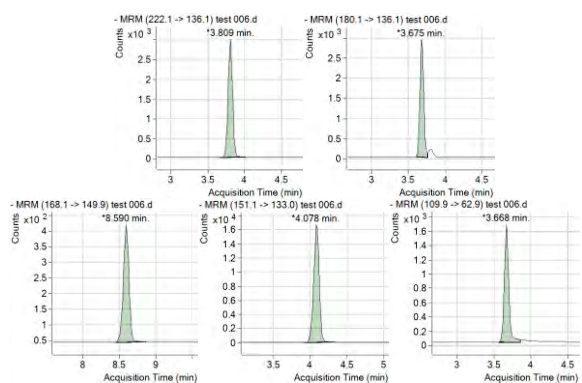
Figure 4. Chromatograms of all compounds analyzed in IC mode. (from top left to bottom right are N-acetyl glufosinate, glufosinate, glyphosate, 3-MPPA and AMPA, respectively)

3.3 Method validation

The linearity was achieved in the range of 0.01-1.00 mg/L and 0.005-0.250 mg/L with acceptable values of coefficient of determination, $r^2 > 0.98$ and 0.92 for RPLC and IC mode, respectively. The lowest calibration levels (LCL) were 0.01 mg/L for RPLC and 0.005 mg/L for IC modes.

4. Conclusions

We have successfully demonstrated comparative chromatographic separation study for the determination of glyphosate, glufosinate, and their metabolites. RPLC and IC modes are suitable for the separation of these analytes, good resolutions and symmetric peak shapes were observed. RPLC procedure was faster and easier in comparison to the IC procedure. However, both were suitable for the analyses of these herbicides with detection sensitivity in sub mg/L level. Coupling to the tandem mass spectrometry further enhanced analyte selectivity and improved the method sensitivity. The proposed procedures were simple, fast, and required no derivatization step.

Acknowledgements

References

[1] http://www.oae.go.th/ewt_news.php?nid=146 (Retrieved November 1, 2012)
[2] http://www. Hiso.or.th/hiso/analystReport/picture/5_lesson2.doc (Retrieved November 1, 2012)
[3] *Commission of the European Communities (2005/396/EC)*, Brussels, (2005).
[4] T.W. Winfield, W.J. Bashe and T.V. Baker, *U.S. Environmental Protection Agency Method 547*, Cincinnati,Ohio, (1990).
[5] L.W. Morlier and D.F. Tomkins, *J. AOAC Int.* **464** (1997) 464-468.
[6] M. Anastassiades, D.I. Kolberg and D. Mack, *EU Reference Laboratory for Single Residue Methods*, Fellbach, (2010).
[7] M. Ibanez, O.J. Pozo and J.V. Sancho, *J. Chromatogr. A* **1134** (2006) 51-55.
[8] L. Grey, B. Nguyen and P. Yang, *J. AOAC Int*. **84** (2001) 1770-1780.
[9] M. Piriyapittaya and S. Jayanta, *J. Chromatogr. A* **1189** (2008) 483-492.
[10] K. Qian, S. He and T. Tang, *Food Chem*. **127** (2011) 722-726.
[11] I.K. Dimitrakopoulos and N.S. Thomaidis, *J. Chromatogr. A* **1217** (2010) 3619-3627.
[12] H.H. See and P.C. Hauser, *J. Chromatogr. A* **1217** (2010) 5832-5838.
[13] M. Motojyuku and T. Saito, *J. Chromatogr. B* **875** (2008) 509-514.
[14] A. Royer and S. Beguin, *J. Agric. Food Chem.* **48** (2000) 5184-5189.
[15] N. Yoshioka, M. Asano and A. Kuse, *J. Chromatogr. A* **1218** (2011) 3675-3680.
[16] X. Li, J. Xu and Y. Jiang, *Acta Chromatogr*. **21** (2009) 559-576.
[17] C.F.B. Coutinho, L.F.M. Coutinho and L.H. Mazo, *Anal. Chim. Acta* **592** (2007) 30-35.

DETERMINATION OF TOTAL ANTIOXIDANT CAPACITY OF HERBS INFUSIONS BY SEQUENTIAL INJECTION ANALYSIS WITH AMPEROMETRIC DETECTION

Pachara Meanha[1], Rasamee Chaisuksant[1]*

[1] *Department of Chemistry, Faculty of Science, Silpakorn University, Nakorn Pathom, 73000 Thailand*
Corresponding Author: E-mail rasamee@su.ac.th

Abstract: Sequential injection analysis (SIA) was developed for determination of total antioxidant capacity (TAC) of herbs infusions by 2,2′-azino-bis(3-ethylbenzothiazoline-6- sulfonic acid) (ABTS) assay with electrochemical detector (ECD). The ABTS reagent acts as an electroactive species at the glassy carbon electrode in phosphate buffer pH 7.0. The decrease of cathodic current signal from ABTS•+ radical after reaction with antioxidants can be monitored. The SIA system was designed to be semi-automatic controlling of the bi-directional Masterflex peristaltic pump (model 77521-40) with small scale and low-cost electrochemical flow-cell. The standard antioxidant, gallic acid showed linear calibration curve in the concentration range of 0-70 ppm (R^2 = 0.9940). Different Thai herbs infusions were determined by the proposed SIA-ECD method and compared with ABTS assay by classical spectrophotometric method. The results were reported in gallic acid equivalent (GAE mg g^{-1} sample) unit. Results from the proposed method were in good agreement with the classical method. The SIA-ECD method provided satisfactory precision (0.60-3.61% RSD) with rapid sample throughput (20 samples h^{-1}) and the consumption of the expensive ABTS reagent was greatly reduced.

1. Introduction

Natural antioxidants from fruits, vegetables and herbs have drawn a great deal of attention due to scientific evidences for health benefits[1]. Research on antioxidants in numerous natural foods and biological samples are increasing in number along with the development of fast screening methods for antioxidant capacity test. Many kinds of herbs are processed to be instant herbal drinks. Information of antioxidant capacity of the manufacturing products should be used to guarantee the quality of the products as well as for the process monitoring.

Ginger contains pungent phenolic substances with antioxidative, anti-inflammatory, anti-tumor, anti-carcinogenic and anti-mutagenic activities [2–4]. Natural ginger has been processed into instant ginger tea or ginger infusion powder and is one of the popular beverages in Asian countries. Cinnamon has been used for centuries a flavor modifier to make food more palatable. Cinnamon possesses numerous pharmacological activities including antioxidant, antimicrobial, antipyretic, antiulcerous, antiallergic, anti-inflammatory effects and treat for diabetic [5-7].

Various of methods to evaluate total antioxidant capacity (TAC), including 2, 2′-azinobis (3-ethylbenzothiazoline-6-sulfonic acid) (ABTS) assay, 2, 2-diphenyl-1-picrylhydrazyl (DPPH) assay, ferric reducing antioxidant power (FRAP) has been review [8]. One of the most common methods for assessing the antioxidant capacity is the ABTS assay based on scavenging of 2,2′-azinobis-(3- ethylbenzothiazoline-6-sulphonate) radical cation. By classical spectrophotometry, the sample to be tested is added to a solution containing a certain amount of $ABTS^{o+}$. After 30 min, the concentration of the remaining $ABTS^{o+}$ is determined via absorption at wavelength 734 nm [9]. Although the classical ABTS assay is uncomplicated, it is time consuming in order to reach the equilibrium state. In 2007, Milardovic et al. [10] reported the use of a flow injection analysis (FIA) system with biamperometric detection for determination of TAC which analysis rates were 30 samples h^{-1}. However, continuous flow system requires large reagent consumption and waste. Recently an automated $ABTS^{o+}$ assay by sequential injection analysis (SIA) was developed by Chan-Eam, et al. [11] using amperometric detection on glassy carbon electrode for analysis of TAC in instant ginger infusions. The SI-amperometric technique using syringe pump provided satisfactory precision (4.11% RSD) with rapid sample throughput of 40 samples h^{-1}. Later, the SIA-ECD using peristaltic pump with the Pump Drive Controller (PDC) program version 1.0 was developed [12] for antioxidant capacity test of the ginger samples by ABTS assay which provided the ability of using the less expensive instrument and achieved the significant reduction of reagent and sample consumption. The PDC software version 1.0 was written in Processing Language to monitor the pump drive for switching on/off and the voltage was applied in Pulse Width Modulation (PWM) mode to drive the eight rollers of the pump head at the corresponding speed. The speed of the pump was then, calibrated to the solution flow rate in mL/min. The sample throughput rate of the SIA system was 9 samples h^{-1} at the constant solution flow rate of 2.0 mL/min.

In order to adjust, the PDC program version 1.2 was developed from the previous PDC program version 1.0. In this version, the flow rate of each step in the SIA system as required. Thus, the sample

throughput rate could be increased. The ABTS assay by the proposed SIA-ECD was performed and compared with classical spectrophotometry.

2. Materials and Methods

2.1 Reagents and chemical

All the reagents used were of analytical grade. 2, 2′-azinobis-(3-ethylbenzothiazoline-6-sulfonic acid) diammonium salt (ABTS) was from Fluka. Potassium persulfate was from Merck. The antioxidant standard was 98% gallic acid (GA) monohydrate from Riedel-de-Haen. Aqueous solutions of GA standard were prepared daily using deionized water. The $ABTS^{o+}$ cation radical solution was prepared by oxidation the ABTS reagent with potassium persulfate as previously described [11]. The concentration of $ABTS^{o+}$ solution determined from spectrophotometry was 0.20 mM. A 0.50 mM phosphate buffer pH 7.0 prepared from 98% $Na_2HPO_4.2H_2O$ and 98% $NaH_2PO_4.H_2O$ from Fluka was used as supporting electrolyte and carrier in all electrochemical measurements.

Instant ginger powder and cinnamon sticks were purchased from local supermarkets. For ginger infusion, accurate weight (1.XXXX g) of sample powder was added to 25 mL deionized water and heated up to 70 °C in water bath for 30 min. The residue was filtered off through 11 μm Whatman® filter paper and the volume of the supernatant was made to 25 mL with deionized water. For cinnamon, the sample sticks were cut in to tiny pieces ∼ 1 cm long and 1.XXXX g of cinnamon was weight and infusion was prepared in the same procedure as ginger powder. Then the cinnamon infusions was three-fold diluted before analysis by the SIA-ECD method. For classical spectrophotometric method, sample infusions were further ten-fold diluted from before analysis.

2.2 Apparatus

The SIA system was designed to enable the ABTS assay as shown in Figure 1. The SIA module was assembled from a six-port valve (V-341, Upchurch Scientific, USA) with the bi-directional peristaltic pump of Masterflex (Cole-Parmer Instrument Co. USA). The bi-directional peristaltic pump comprised of the pump drive model 77521-40, pump head 07519-10 and cartridges 07519-85. The cartridge tubing was the two-stop Tygon tubing of 1.02 mm i.d. which connected to the holding/mixing coil of 1.07 mm i.d., 200 cm length PTFE tubing.

Electrochemical measurements were carried out with a potentiostat, Autolab PGSTAT30 and controlled by the GPES software version 4.9.007 (Eco Chemie, The Netherlands) for applying potential and data processing in the chrono-amperometry mode. The SIA system was furnished with an in-house electrochemical flow-cell (made of acrylic resin with cell volume of 350 μL) and three-electrode system composed of the working electrode (WE) was a glassy carbon electrode (GCE) (3mm-diameter disk), the reference electrode (RE) was a Ag/AgCl (sat. KCl)

and another GCE served as a counter electrode (CE). Pretreatment of the GCEs was done by polishing with alumina on a damp polishing cloth (Metrohm, The Netherlands) before fixing to the flow cell. A pH-meter (Mettler Toledo 320, USA) was employed for pH adjustment of the buffer solution.

The classical spectrophotometric batch method was carried out as described by Chaiyan [13]. The $ABTS^{o+}$ reagent was prepared and diluted to give absorbance ∼ 0.7. The assay was 2 mL of $ABTS^{o+}$ mix with 2 mL antioxidant. After 30 min reaction time, the absorbance was measured at 730 nm with a double-beam Lambda 35 UV/Vis Spectrophotometer. TAC values were calculated with calibration curve of GA in the concentration range 0-1 ppm and expressed in GAE unit (mg g^{-1} sample).
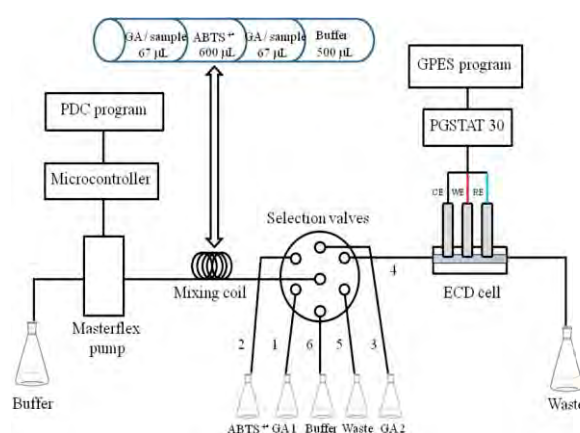
Figure 1. Schematic diagram of the SIA system for the evaluation of TAC with an in-house flow-through ECD. CE=counter electrode; WE = working electrode; RE = reference electrode.

2.3 SIA-ECD Procedure

As shown in Table 1 for the ABTS assay, the sequential injection procedure composed of six main steps in one cycle. The aspirated steps into the holding/mixing coil are follows: antioxidant standard/ sample was aspirated in two segments (step 1 and 3) and the $ABTS^{o+}$ radical solution was aspirated as the middle segment between the standard/sample segments (step 2). The phosphate buffer carrier solution was aspirated to finish the segment sequence (step 4). Then, the direction of the flow was changed forward and backward for mixing the solutions (step 5) before the solution was propelled to the ECD cell (step 6). The analytical signal of amperometric detection was the cathodic current of the $ABTS^{o+}$ radical from reduction at the applied potential -0.10 V vs Ag/AgCl on the GCE working electrode. The peak current from antioxidant sample was calibrated with the calibration curve of standard GA in concentration range 0-70 ppm. The antioxidant capacity results were expressed in the GAE unit.

Table 1: SIA protocol sequence for the ABTS assay.

Step	Valve position	Volume (μL)	Time (s)	Flow rate (mLmin⁻¹)	Flow direction	Event
1	1	67	2	2	Reverse	Std./sample zone 1 aspirated
2	2	600	12	3	Reverse	Reagent zone aspirated
3	1	67	2	2	Reverse	Std./sample zone 2 aspirated
4	6	500	10	3	Reverse	Carrier aspirated
5	6	-	8	2	Forward	Zones mixing
		-	8	2	Reverse	
		-	8	2	Forward	
		-	8	2	Reverse	
		-	8	2	Forward	
		-	8	2	Reverse	
6	4	-	100	3	Forward	Zones sent to ECD

3. Results and Discussion

3.1 Analytical Performance

The volume of ABTS^{o+} at 600 μL was selected to cover the GA concentration range 0-70 ppm for the least volume of a sample segment at 67 μL (2 s of aspiration time with the constant flow rate 2.0 mL/min). Response signals of standard GA was measured under the optimum condition at room temperature (25 ^{o}C) and calibration curve was shown in Figure 2. The inset shows a calibration graph of linear equation Y = (-0.0036 ± 0.0157) X + (0.3081 ± 0.0003$_8$) with R^2 = 0.9940; where Y = peak current in nA, X = GA concentration in ppm. At higher concentration of GA more than 70 ppm resulted in decreasing of the peak current of ABTS^{o+}. The peak current of ABTS^{o+} without reaction with antioxidant show good precision of 1.64 % RSD (n = 10). Limit of detection was 79.8 ppm, calculated as the concentration of GA which gave the signal three times standard deviation of blank signal.
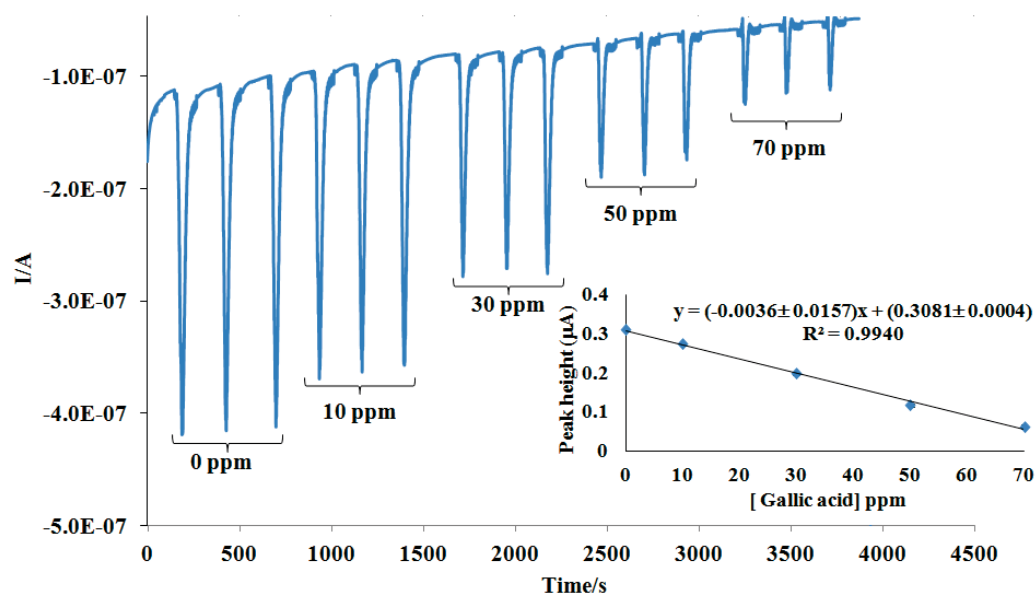
Figure 2. Signal profiles of the SIA-ECD system obtained for injections of each concentration of GA and calibration curve. Three consecutive signals of each GA concentration were used to construct the calibration graph (inset).

Sample analysis time was 174 s, so that the throughput of 20 samples h^{-1} was achieved. This sample throughput was about 2 fold higher than the previous SIA-ECD using PDC program version 1.0 [12].

3.2 Evaluation of total antioxidant capacity of herbs infusions

The proposed SIA-ECD for ABTS assay was applied to evaluate TAC of three ginger and a cinnamon infusions. Comparative of the GAE values obtained by the proposed SIA-ECD method and those from classical spectrophotometric method are shown in Figure 3. The cinnamon sample provided has antioxidant capacity about 3-4 fold higher than ginger sample. Using the paired t-test [14], the results from both methods have no significant difference with t_{stat} of A= 0.10, B= 2.02, C= 2.45 and D=3.46 which t_{crit} = 4.3 at 95% level of confidence. The consumption of ABTS^{o+} using in SIA-ECD and classical spectrophotometry was 69 and 206 μg for each measurement, respectively which means that by the proposed method, the expensive reagent could be reduced. Moreover, colored samples interfere spectrophotometric technique but no effect on the detection by the SIA-ECD.
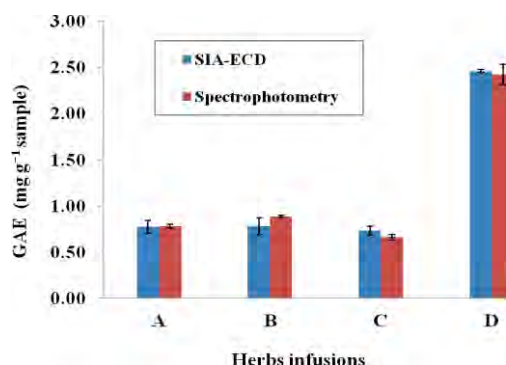
Figure 3. TAC values for extracts of ginger infusions (A-C) and cinnamon infusions (D) obtained from the SIA-ECD and the classical spectrophotometric methods.

4. Conclusions

The SIA-ECD method using peristaltic pump was developed for the estimation of TAC in herbs infusions by ABTS assay with collaboration of researchers from chemistry and computer science. Good linearity was obtained for gallic acid antioxidant standard in the range of 0-70 ppm (R^2 = 0.9940). The proposed method provided satisfactory precision (0.60-3.61% RSD) with rapid sample throughput (20 samples h^{-1}). The main merit of the SIA assay compared to the classical method in significant reduction of reagent and sample consumption was achieved.

References

[1] Y. Z. Fang, S. Yang, and G. Wu, *Nutrition.* **18** (2002) 872-879.
[2] Y. Shukla and M. Singh, *Food Chem. Toxicol.* **45** (2007) 683-690.
[3] K. Park, K. Chun, J. Lee, S.S. Lee and Y. Surh, *Cancer Lett.* **129** (1998) 139-144.
[4] I. Stoilova, A. Krastanov, A. Stoyanova, P. Denev and S. Gargova, *Food Chem.* **102** (2007) 764-700.
[5] A. Sangal, *Adv. Appl. Sci. Res.,* **2** (4) (2011) 440-450.
[6] B. Shan, Y. Z. Cal, J. D. Brooks and H. Corke, *J. Agric. Food Chem.* **55(2007) 5484**-5490.
[7] A. Al-Jamal and I. N. Rasheed, *Afr. J. Food Sci.* **4(9)** (2010) 615-617.
[8] L. M. Magalhaes, M. Santos, M. A. Segundo, S. Reis, and J.L.F.C. Lima, *Talanta.* **77** (2009) 1559-1566.
[9] M. J.T.J. Arts, J. S. Dallinga, H.P. Voss, G. R.M.M. Haenen, and A. Bast, *Food Chem.* **88** (2004) 567–570.
[10] S. Milardovic, L. Kerekovic´,and V. Rumenjak, *Food Chem.* **105** (2007) 1688–1694.
[11] S. Chan-Eam, S. Teerasong, K. Damwan, D. Nacapricha, and R. Chaisuksant, *Talanta.* **84** (2011) 1350-1354.
[12] J. Kongkedsuk, A. Hongwitayakorn, W. Bootnapang, N. Boonto, and R. Chaisuksant, *Chiang Mai J. Sci.* (2012) (in press)
[13] C. Boonyuen, S. Wangkarn, O. Suntornwat, R. Chaisuksant, *Kasetsart J. Nat. Sci.***43** (2009) 21-27.
[14] J.N. Miller, J.C. Miller, *Statistics and Chemometrics for Analytical Chemistry,* 5th ed. Pearson Education Limited, UK, (2005), pp. 40-41.

ANALYSIS OF PETROLEUM PRODUCTS BY NUCLEAR MAGNETIC RESONANCE (NMR) SPECTROSCOPY

Wachirapun Punkrawee and Anuttra Nuamthanom *

Chemistry Program, Department of Science Service, Ratchathewi, Bangkok, 10400 Thailand

*E-mail: Anuttra@dss,go.th

Abstract: According to the European Union (EU) Directive number 2005/69/EC, a tire may not be put on sale in the market if the percentage of bay region hydrogens (% H_{bay}) in oil of valcanized rubber exceeds the limit of 0.35% as measured by the ISO 2146 test method. The major aim of this research is to compare the methylene chloride-d_2 (CD_2Cl_2) with chloroform-d_1 ($CDCl_3$), a solvent basicaly use in the previously mentioned ISO 2146 test method as Nuclear Magnetic Resonance (NMR) solvent. The use of CD_2Cl_2 in this work is intended to better determine the %H_{bay}, using a NMR spectroscopy technique. As a standard test method, the signal of chloroform (Chemical shift = 7.2 ppm) must be subtracted from the signal of an aromatic (Chemical shift = 6-9.5 ppm) due to its peak overlapped in this region. However, when using CD_2Cl_2, the interference has not been observed, and thus a solvent peak is not included in the calculation. The calculation of % H_{bay} found in the proposed method is comparable to the conventional ISO test method, using the t-test analysis.

1. Introduction

Nowadays many toxic contaminants have been widespread in the environment. Polcyclic aromatic hydrocarbons (PAHs) for example, are one of the organic pollutants since they are not only widely spread, but also carcinogenic[1]. PAHs can be formed in the environment through a natural process (volcanic eruption or forest fire) or a combustion (vertical exhaust pipe, cooking). PAHs consist of carbon and hydrogen atoms, which contain two or more aromatic rings. In recent years, the EU REACH regulation[2] has restricted the use of PAHs in tire and extender oil to protect a human healths and environments.The restricted PAHs and their chemical structure are listed in Table 1. Tires and extender oil may not be placed in the market if 1) they contain more than 1 mg/kg of BaP and/or 2) they contain more than 10 mg/kg of the sum of the contents of all eight PAHs. Or the percentage of bay hydrogen (%H_{bay}) in a tire exceeds 0.35% as measured by the ISO 21461 test method[4]. In the case of extender oil, these restrictions must be maintained if the weight of oil extract using dimethyl sulfoxide (DMSO) is less than 3%. However, using this method cannot identify any type of carcinogen or non-carcinogen. Another problem with DMSO extract is that it may not contain only PAHs but also other chemical substances (e.g. sulfur, nitrogen, naphthens).

D.T.Coker et.al.[3] improved NMR method for measure bay hydrogen. The DMSO extraction from oil was analysed by NMR spectroscopy using $CDCl_3$:CCl_4 (1:4) as a NMR solvent.

Bay region hydrogen is a hydrogen atom in three-sided concave polycyclic aromatic hydrocarbons as shown in table 1. The percentage of bay hydrogen (%H_{bay}) in tire must be less than 0.35% as measured and calculated by ISO test method number 21461[4] to pass the EU regulation. In this method, oil was extracted from the tire. Then, the %H_{bay} in extracted oil was measured by NMR technique using $CDCl_3$ as a solvent. However, the signal of $CDCl_3$ interferes with the aromatic signal from oil, resulting in a subtraction of solvent signal (7.2 ppm) from the aromatic area (6-9.5ppm).

In this work, the %H_{bay} protons in spiking oil samples were measured using CD_2Cl_2 and $CDCl_3$ as NMR solvent . Then results were compared by t-test analysis.

2. Materials and Methods

2.1 Oil Sample

Extender oil used in this research was provided by the Thai Lube Base Public Co., Ltd.

2.2 Reagents

Deuterated Methylene chloride was obtained from Cambridge Isotope Laboratory Inc. (Andover, Massachusetts, USA). Deuterated Chloroform was obtained from Merck (Darmstadt, Germany). n-hexane was purchased from RCI Labscan. Benzo(a)pyrene (BaP), Benzo(a)anthracene (BaA), Chrysen (CHR), Benzo(b)fluoranthene (BbFA), Benzo(j)fluoranthene (BjFA), Benzo(k)fluoranthene (BkFA) and Dibenzo (a, h) anthracene (DBahA) were purchased from Cerilliant Co.(Round Rock Texas, USA). Benzo(e)pyrene (BeP) was obtained from Dr.Ehrenstorfer (Augsburg Germany).

2.3 Preparation of PAHs solution
2.3.1 Preparation of individual PAHs

Weighed 0.04 g of each PAH in glass vials and dissolved them separately in 1.52 ml n-hexane. Then, put the glass vials into an ultrasonic bath and sonicated them for 10 minute until all solid were dissolved.

Table 1: The structures of eight polcyclic aromatic hydrocarbons (PAHs) studied in this research.

Name	Abbreviation	Structure*
Benzo(a)pyrene	BaP	
Benzo(e)pyrene	BeP	
Bebzo(a)anthracene	BaA	
Chrysen	CHR	
Benzo(b)fluoranthene	BbFA	
Benzo(j)fluoranthene	BjFA	
Benzo(k)fluoranthene	BkFA	
Dibenzo(a,h)anthracene	DBahA	

* Hydrogens in the cycles are those found in the bay region.

2.3.2 Preparation of eight PAHs mixed
Pipetted 200 µl of each PAH and mixed them uniformly in an amber glass bottle.

2.4 Preparation of spiked samples
2.4.1 BaP
Pipetted 40 µl of BaP solution (from 2.3.1) into 0.1 ml extender oil and shook it vigorously.

2.4.2 Eight PAHs
Pipette 80 µl of mixed PAHs solution (from 2.3.2) into 0.1 ml extender oil and shook it vigorously.

2.5 NMR measurement
2.5.1 Prepared individual PAHs in $CDCl_3$ and CD_2Cl_2
Pipetted 50 µl of each PAH solution from 2.3.1 in a 5 mm NMR tube. Then, added $CDCl_3$ and CD_2Cl_2 as NMR solvent, respectively.
2.5.2 Prepared the spiked BaP oil sample in $CDCl_3$
Pipetted 50 µl of spiked sample from 2.4.1 in a 5 mm NMR tube then add $CDCl_3$ and shook it vigorously. Prepared other four NMR tubes using the same procedure.
2.5.3 Prepared the spiked BaP oil sample in CD_2Cl_2
Five tubes of spiked oil sample in CD_2Cl_2 were prepared as described for $CDCl_3$.
2.5.4 Preparation of spiked eight PAHs mixed oil sample in $CDCl_3$
Pipetted 50 µl of spiked oil sample from 2.4.2 in a 5 mm NMR tube, then added $CDCl_3$ and shook it vigorously. Prepared other four NMR tubes using the same procedure.
2.5.5 Prepared the spiked eight PAHs mixed oil samples in CD_2Cl_2
Five tubes of spiked oil samples in CD_2Cl_2 were prepared as described for $CDCl_3$.
2.5.6 ^{1}H-NMR spectroscopy
The ^{1}H NMR spectra were measured, using a 400 MHz NMR spectrometer as found in the following conditions : pulse 90° of 2 µs, spectral width of 5.6 kHz, relaxation delay for 2 second, LB (Line Broadening) of 0.3 Hz, 256 transients and reference by its solvent.

2.6 Calculation
The formula used for the calculation of %H_{bay} for $CDCl_3$ and CD_2Cl_2 were shown in Equation 1[5] and 2, respectively.

For $CDCl_3$
$$\%H_{bay} = \frac{I_1}{(I_2 - I_3) + I_4} \times 100 \qquad Eq.1$$

For CD_2Cl_2
$$\%H_{bay} = \frac{I_1}{I_2 + I_4} \times 100 \qquad Eq. 2$$

Where;

I_1 = Bay region area (8.3-9.5 ppm)
I_2 = Aromatic area (6.0-9.5 ppm)
I_3 = $CDCl_3$ signal (7.2 ppm)
I_4 = Aliphatic area (0.2-5.8 ppm)

3. Results and Discussion

The ^{1}H NMR spectra of each of PAHs in CDCl$_3$ and CD$_2$Cl$_2$ are shown in Fig. 1 and 2, respectively. The aromatic protons of these compounds were revealed in the chemical shift between 7-9.5 ppm, and the aromatic signals from BbFA and BjFA were close to the signal of CDCl$_3$ (7.2 ppm), which led the difficulties identifying the CDCl$_3$ area. All of these had effected the calculation of % H$_{bay}$ region.
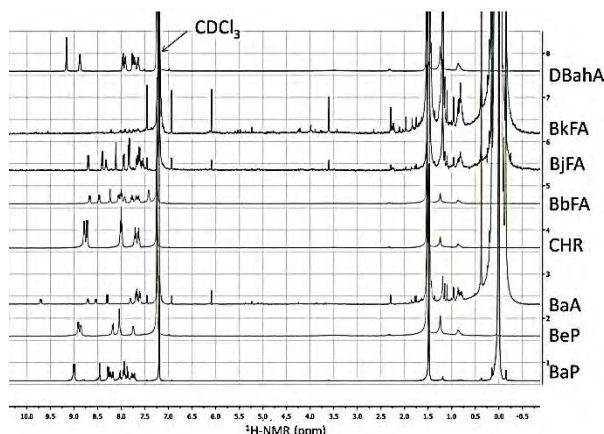
Figure 1. ^{1}H-NMR spectra of each PAH with CDCl$_3$ as NMR solvent
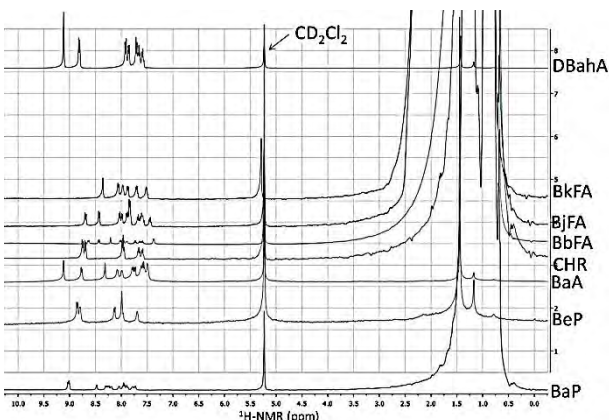
Figure 2. ^{1}H-NMR spectra of each PAH with CD$_2$Cl$_2$ as NMR solvent

Fig. 3 and Fig. 4 show the ^{1}H-NMR spectrum of spiked oil samples, using CDCl$_3$ and CD$_2$Cl$_2$ as NMR solvent. The integration area used for the calculation of %H$_{bay}$ protons were also shown in these figures, and the expansion of aromatic area was inserted on the top of the figures. As shown in Fig. 3, the signal of CDCl$_3$ (the chemical shift = 7.2 ppm) was overlapping with the signal of aromatic protons (the chemical shift between 6.0-9.5 ppm). Therefore, when calculating the %H$_{bay}$ protons the integration of the solvent peak needs to be subtracted from the integration of the aromatic area. Making a wrong integration of solvent peak may influence the results of the %H$_{bay}$ protons. In case of CD$_2$Cl$_2$ (Fig. 4), its signal CD$_2$Cl$_2$ (chemical shift = 5.3 ppm) was separated from the aromatic area. Thus, it is not necessary to subtract the solvent peak in the calculation.

Table 2 shows the calculation of the %H$_{bay}$ protons in spiked oil samples, using CDCl$_3$ and CD$_2$Cl$_2$ as NMR solvents.

The data from CD$_2$Cl$_2$ and CDCl$_3$ were compared using t-test analysis at the 99.0% confidential level to proof the differentiation between them.
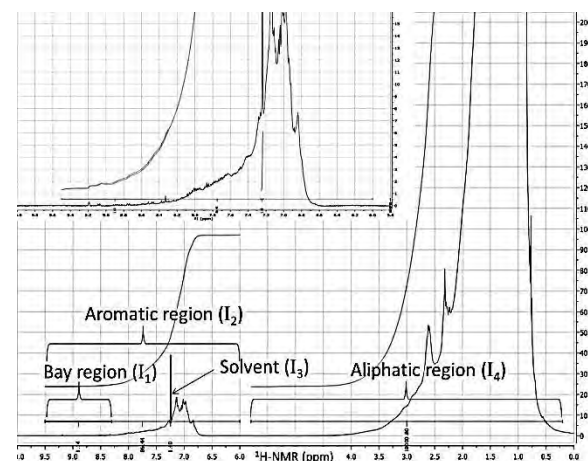
Figure 3. The ^{1}H-NMR spectra of spiked oil sample using CDCl$_3$ as NMR solvent. The insertion is an expansion of the aromatic region.
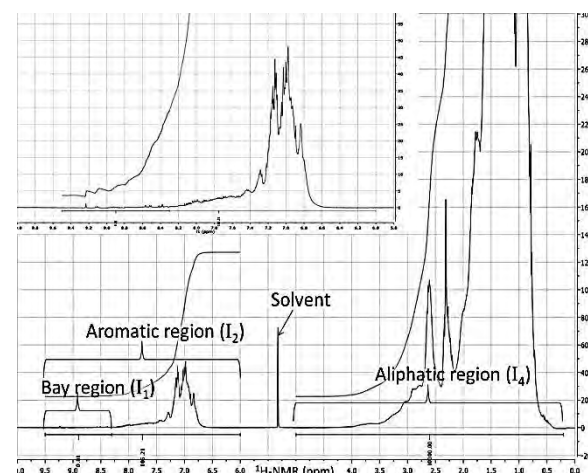
Figure 4. The ^{1}H-NMR spectra of spiked oil sample using CD$_2$Cl$_2$ as NMR solvent. The insertion is an expansion of the aromatic region.

The %H$_{bay}$ results of spiked BaP samples showed that there was not significantly different between CDCl$_3$ (Mean = 0.021, S.D. = 0.0005) and CD$_2$Cl$_2$ (Mean = 0.0195, S.D. = 0.0012) at condition t = 2.53, degree of freedom = 8, p = 0.035. For the spiked eight PAHs, the %H$_{bay}$ results showed that there was not significantly difference between CDCl$_3$ (Mean = 0.011, S.D. = 0.0005) and CD$_2$Cl$_2$ (Mean = 0.0103, S.D. = 0.0011) at condition t = 1.56, degree of freedom = 8, p = 0.157.

Table 2: The percentage of bay hydrogen (% H_{bay}) of spiked oil samples, using $CDCl_3$ and CD_2Cl_2 as NMR solvents.

No.	%H_{bay}			
	BaP		Eight PAHs	
	$CDCl_3^a$	$CD_2Cl_2^b$	$CDCl_3^a$	$CD_2Cl_2^b$
1	0.0206	0.0207	0.0112	0.0090
2	0.0215	0.0178	0.0103	0.0117
3	0.0214	0.0198	0.0116	0.0109
4	0.0210	0.0187	0.0116	0.0101
5	0.0204	0.0205	0.0110	0.0098
Average	**0.0210**	**0.0195**	**0.0111**	**0.0103**
SD	0.0005	0.0012	0.0005	0.0011
%RSD	**2.2581**	**6.2722**	**4.7016**	**10.2409**

[a] Calculated by Eq. 1
[b] Calculated by Eq. 2

4. Conclusions

The t-test analysis showed that the results of %H_{bay} between two solvents are not significantly different. However, replacing the $CDCl_3$ NMR solvent with CD_2Cl_2 proves useful for defining the integration area for the % H_{bay} calculation. Using CD_2Cl_2 as an NMR solvent provides a great way of not interfering with the aromatic area if compared to the $CDCl_3$. As a result of this, the solvent signal needs not to be subtracted from the aromatic signal in the calculation formula.

References

[1] E. Manoli, S.C.I. Konstantinou, T. Albanis, *Polycyclic aromatic hydrocarbons in the bulk precipitation and surface waters of Northern Greece*, Chemosphere, **41**, pp. 1845-1855.

[2] *REACH Annex XVII Restrictions Polycyclic-Aromatic Hydrocaron (PAHs)*, guidance note part 1, October 2010.

[3] D.T. Coker, A.G. King, D.L. Mumforb, C.S. Nessel, *Carcinogenic assessment of petroleum products by nuclear magnic resonance*, Anal Commu, May 1997, **Vol 34**, pp.137-140.

[4] ISO 21461 : *2009 Rubber determination of aromaticity of oil valcanized rubber compound*.

[5] ISO/TC 45/SC 3 N *Rubber-Determination of aromaticity of oil by NMR spectroscopy*.

EFFECT OF ACID-HEAT TREATMENT ON COENZYME Q$_{10}$ EXTRACTION EFFICIENCY FROM *ARTEMIA*

Nirundorn Raekasin[1], Thitima Rujiralai[1*], Wilairat Cheewasedtham[2],
Chonlatee Cheewasedtham[3]

[1] Department of Chemistry and Center of Excellence for Innovation in Chemistry, Faculty of Science,
Prince of Songkla University, Hat Yai, Songkhla, 90112 Thailand
[2] Department of Science, Faculty of Science and Technology, Prince of Songkla University,
Pattani campus, Muang, Pattani, 94000 Thailand
[3] Department of Technology and Industry, Faculty of Science and Technology,
Prince of Songkla University, Pattani campus, Muang, Pattani, 94000 Thailand

[*] Author for correspondence; Email: thitima.r@psu.ac.th, Tel. +66 74288445, Fax. +66 74558841

Abstract: Extraction of coenzyme Q$_{10}$ (CoQ$_{10}$) from *Artemia* has been rarely reported. We firstly investigated the acid-heat treatment for cell lysis of CoQ$_{10}$ from *Artemia*. Parameters, *i.e.*, type of solvents and concentration of acids, were optimized to obtain the highest yield of CoQ$_{10}$, followed by the extraction with hexane. The extract was analyzed by high performance liquid chromatography with the ZORBAX Eclipse XDB-C18 column coupled with a diode array detector set at 275 nm. CoQ$_{10}$ was eluted with methanol-ethanol (5:95, v/v) at a flow rate of 1.0 mL min^{-1}. The yield of CoQ$_{10}$ in *Artemia* was found the highest at 95.9±10.9 μg g^{-1} on a dry weight basis (n=5) when 75% (wt/wt) acetic acid was used under the temperature at 84°C for 35 min. The performance of detection was also performed. The calibration of CoQ$_{10}$ was found to be linear in the range of 1.0-50.0 μg mL^{-1} with the correlation coefficient (r) of 0.999. The limit of detection and limit of quantification were achieved at 0.3 and 1.1 μg mL^{-1}, respectively. The advantages of the optimized acid-heat method were low cost consuming, simple and fast to release CoQ$_{10}$ from *Artemia*.

1. Introduction

Coenzyme Q$_{10}$ is a vitamin-like substance and also called ubiquinone-10, ubidecarenone or CoQ$_{10}$. Its structure is shown in Figure 1. CoQ$_{10}$ can be dissolved in the intermediate polarity solvents such as chloroform, benzene, diethyl ether, hexane, acetone and slightly soluble in ethanol but practically insoluble in water [1]. CoQ$_{10}$ involves with the production of energy (ATP) in mitochondrial electron transport chain and promotes antioxidant properties [2-3]. The utility of CoQ$_{10}$ is the prevention for aging and therapeutic such as cardiac disease and parkinson's disease [4-5]. It is synthesized naturally in human body, but its rate of production decreases with age. Therefore, humans can gain CoQ$_{10}$ from food or nutraceutical dietary supplement [6]. The upper level uptake of CoQ$_{10}$ for supplement is 1200 mg day^{-1} [7]. The important sources of CoQ$_{10}$ are the microorganisms such as *Agrobacterium tumefaciens*, photosynthetic bacteria *Rhodospirillum rubrum* and also found in pelagic fish tissues, bee pollen, palm oil, tobacco leaves and litchi pericarp [8-14].

Artemia or brine shrimp is the invertebrate animal identified as Crustacea class like crab and shrimp, but it has no shell. *Artemia* has the short life cycle and its food is microorganisms. *Artemia* is commonly used for food of nursery fish as it contains good nutrients related to its diets such as fat, protein and carbohydrate [15]. Furthermore, the diguanosine tetraphosphate (GP4G) compound in the *Artemia* extract was found to be the high energy intermediate source in biochemical process [16].

Many analytical procedures have been reported for the extraction of CoQ$_{10}$ including the saponification process of *Sphingomonas* sp. ZUTE03 before solvent extraction [17], the accelerated solvent extraction (ASE) of bee pollen [11] and the lysing cell step following by the ultrasonic assisted extraction [14] or the acid-heat treatment [18] before solvent extraction. However, the partial CoQ$_{10}$ could be damaged by an alkali condition used in the saponification process [17]. Moreover, the ASE and ultrasonication method are not suitable for the large scale preparation for industrial scale. Up to date, the source of CoQ$_{10}$ as *Artemia* which can be cultivated within 2 weeks and easier to be harvested than bacteria is rarely reported and there is no suitable preparation method for CoQ$_{10}$ from *Artemia* yet. Therefore, the aim of this work is to investigate the application of weak acid, acetic acid, together with heat treatment in *Artemia* cell lysis and CoQ$_{10}$ extraction with hexane. The extraction efficiency was investigated by means of high performance liquid chromatography with diode array detection (HPLC-DAD).
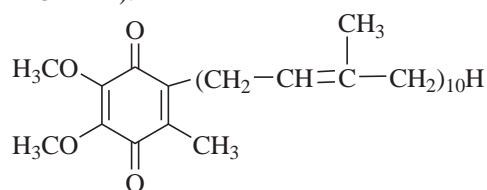
Figure 1. Structure of coenzyme Q$_{10}$.

2. Materials and Methods

2.1 Materials

Coenzyme Q_{10} standard was purchased from Sigma (St. Louis, MO, USA). A stock standard CoQ_{10} at 100 μg mL^{-1} was prepared in absolute ethanol and stored at -20°C within 3 months when not in use. The calibration curve of CoQ_{10} was prepared at concentration of 1.0, 2.5, 5.0, 10.0, 20.0, 30.0, 40.0 and 50.0 μg mL^{-1}. All reagents used were of analytical grade. The deionized (DI) water was obtained from Maxima ultrapure water instrument (ELGA, England).

2.2 Sample preparation

Fresh *Artemia* samples were collected from the Ecological Aquaculture Research Unit at Department of Technology and Industry, Faculty of Science and Technology, Prince of Songkla University, Pattani campus. After that, samples were washed with DI water about 10 mL g^{-1} sample and kept in a plastic bottle at 4°C before analysis. Moisture content of sample was analyzed by AOAC 930.15 method. The CoQ_{10} yield was calculated based on *Artemia* dry weight.

2.3 Extraction of CoQ_{10} from *Artemia*

The extraction method was modified from Tian *et al*. (2009). One gram of fresh *Artemia* sample was weighed into a 60-mL test tube and 75% (wt/wt) acetic acid was added, following by the gentle shaking. Sample was then incubated in water bath at 84°C for 35 min. After cooling at room temperature, sample was vigorously mixed by vortex mixer for 1 min. The extraction was performed by adding 5 mL of ethanol and 10 mL of hexane, followed by vigorously vortex mixing for 1 min. After allowance to settle for equilibrium at room temperature, the upper phase was pipetted into a round bottom flask. The extraction of aqueous phase was repeated and the extracted solution was combined and evaporated to dryness by a rotary evaporator (EYELA Rotary evaporator N-1001, China). The residue was re-dissolved with 2 mL ethanol and filtered through 0.2 μm Nylon membrane before HPLC analysis as mentioned below.

2.4 Analysis of CoQ_{10}

The yield of CoQ_{10} from *Artemia* was analyzed on Agilent 1200 HPLC system (Agilent Technologies, USA) through an Agilent ZORBAX Eclipse XDB-C18 column (150 mm × 4.6 mm, 5 μm thickness). The column temperature was set at 27°C. The mobile phase consisted of methanol and ethanol (5:95, v/v) with the isocratic elution at the flow rate of 1.0 mL min^{-1}. The diode array detection was set at 275 nm.

2.5 Statistical analysis

The experimental results obtained were expressed as mean±SD (n=5). Statistical analysis was performed by using ANOVA at 95% confident level. Microsoft Excel version 2007 was used for data analysis.

3. Results and Discussion

3.1 Quantitative analysis of CoQ_{10}

As shown in Figure 2, the retention time of CoQ_{10} is about 6.300 ± 0.008 min in both of standard and *Artemia* extracts and clearly separated from other signal caused by other substances in the matrix. Therefore, the external standard can be used for determination of CoQ_{10}.
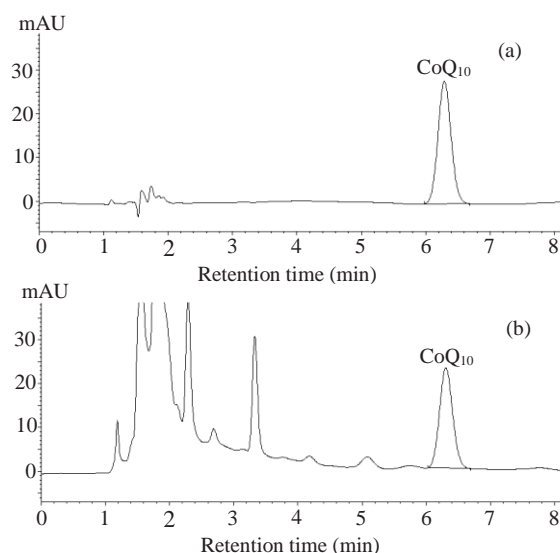
Figure 2. Typical HPLC chromatogram of CoQ_{10} at 20 μg mL^{-1} in (a) CoQ_{10} standard (b) *Artemia* extract.

3.2 Linearity, limit of detection (LOD) and limit of quantification (LOQ)

The calibration curve of CoQ_{10} was found to be linear in the range of 1.0-50.0 μg mL^{-1} (Figure 3). The linearity relation was y=20.230x(±0.043)-0.763(±1.068) with a correlation coefficient (r) of 0.999. The LOD and LOQ were calculated at the signal to noise ratio at 3 and 10 and achieved at 0.3 and 1.1 μg mL^{-1}, respectively [19].
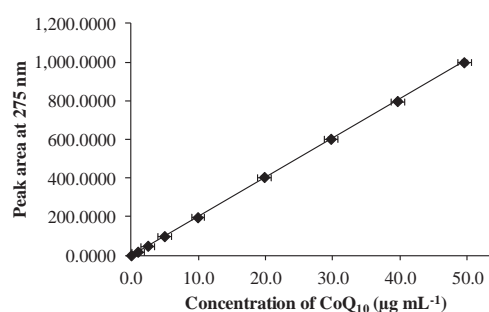
Figure 3. The calibration curve of CoQ_{10}.

3.3 Optimization of extracting CoQ_{10} from *Artemia*

The cell disruption step is necessary for the extraction of CoQ_{10} from animal tissues. Tian *et al.* (2009) studied the cell lysis of *Agrobacterium*

tumefaciens and found that the highest content of CoQ_{10} was obtained when using 3 M (~9%) hydrochloric acid (HCl) under the incubation at 84°C for 35 min before the solvent extraction. Therefore, we also studied the cell lysis of *Artemia* with HCl as mentioned by Tian *et al.* (2009). The concentrations of HCl used were at 0.1% and 9% (wt/wt). Moreover, other types of solvents, *i.e.*, DI water, 70% and 100% (v/v) ethanol and glacial acetic acid were also studied for cell lysis. All treatments were carried out for 35 min at 84°C. The result is shown in Figure 4. The highest of CoQ_{10} content at 130.4±3.4 µg g^{-1} was obtained by glacial acetic acid since this weak acid could gently lyse cell membrane of *Artemia* to release CoQ_{10}. Although glacial acetic acid provided the best result, it would not be appropriate for the CoQ_{10} production when using a lot of raw material of *Artemia* due to its smell. Therefore, the concentration of acetic acid was studied in the range of 5 to 100% (wt/wt). As shown in Figure 5, the yield of CoQ_{10} increased and reached the highest when 75% (wt/wt) acetic acid was used. After that, its yield was found to be constant. The concentration of acetic acid at lower than 75% (wt/wt) provided the incomplete separation between organic phase and aqueous phase, resulting in low efficiency extraction. Therefore, 75% (wt/wt) acetic acid was chosen in this work. Our preliminary studied indicated that the acid-heat treatment suitable for CoQ_{10} extraction. However, the reduction of energy is more required that the other parameters such as various incubation temperature, incubation time or the number of extraction will be further investigated.

4. Conclusions

Determination of CoQ_{10} by HPLC-DAD was found to be a reliable method with the linearity concentration in the range of 1.0-50.0 µg mL^{-1}. The LOD and LOQ of the determination were achieved at 0.3 and 1.1 µg mL^{-1}, respectively. Among CoQ_{10} extractants; DI water, ethanol, hydrochloric acid and acetic acid, using 75% (wt/wt) acetic acid under the incubation at 84°C for 35 min was found to be the optimal condition for cell lysis of CoQ_{10} from *Artemia*. Under these optimal conditions, CoQ_{10} could be extracted at 95.9±10.9 µg g^{-1} dry weight of *Artemia*. The acid-heat method was advantageous in terms of low cost consuming, simple and fast to release CoQ_{10} from *Artemia*.

Acknowledgements
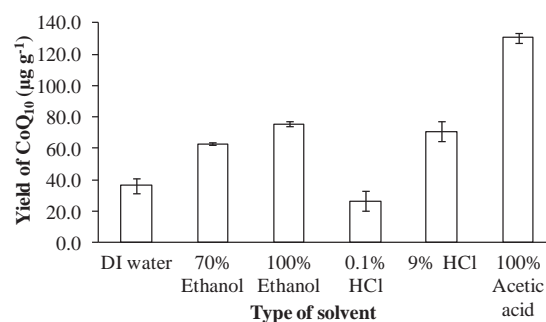
Figure 4. The effect of types of solvent at 84°C on yield of CoQ_{10} (µg g^{-1} on a dry weight basis).
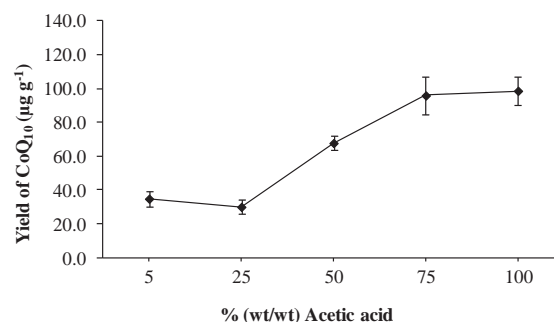
Figure 5. The effect of the acetic acid strength on yield of CoQ_{10} (µg g^{-1} on a dry weight basis).

References

[1] O. Monica, K. S. Santosh and J. Q. Peter, *Biosci. Rep.* **6** (1986) 783-796.

[2] L. Giorgio, F. Romana, F. Gabriella and L. G. Maria, *Mitochondrion.* **7S** (2007) S8-S33.

[3] B. Magnus, B. Kerstin and D. Gustav, *Mitochondrion*. **7S** (2007) S41-S50.

[4] K. Adarsh, K. Harharpreet, D. Pushpa and M. Varun, *Pharmacol. Ther.* **124** (2009) 259-268.

[5] W. S. Clifford, *Pharmacol. Ther.* **107** (2005) 120-130.

[6] R. Nageswara Rao, M. V. N. Kumar Talluri and D. D. Shinde, *J. Pharm. Biomed. Anal.* **47** (2008) 230-237.

[7] N. H. John and S. Andrew, *Regul. Toxicol. Pharmacol.* **45** (2006) 282-288.

[8] H. Suk-Jin, K. Sang-Yong, S. Jin-Ho, O. Deok-Kun and L. Jung-Kul*, Appl. Microbiol. Biotechnol*. **74** (2007) 974-980.

[9] T. Yuting, Y. Tianli, Y. Yahong, K. S. Pavan, D. W. Patrick, A. M. Peter, F. Hong, J. K. Robert, W. Cheng-I and L. Y. Martin, *Bioresour. Technol.* **101** (2010) 7877-7881.

[10] S. Nathalie and L. Serge, *J. Food Compos. Anal.* **20** (2007) 403-410.

[11] X. Xiaofeng, Z. Jing, C. Lanzhen, Z. Jinhui, Y. Bing, L. Yi, W. Liming and L. Fengmao, *Food Chem*. **133** (2012) 573-578.

[12] H. N. Mei, M. C. Yuen, N. M. Ah, H. C. Cheng and H. M. Ali, *Am. J. Appl. Sci.* **3(7)** (2006) 1929-1932.

[13] Z. Yuangang, Z. Chunjian, L. Chunying and Z. Lin, *J. Sep. Sci.* **29** (2006) 1607-1612.

[14] R. Guohua, S. Guanglin and X. Guang, *J. Food Process Eng*. **34** (2011) 671-681.

[15] P. Léger, D. A. Bengtson, P. Sorgeloos, K. L. Simpson and A. D. Beck, in: P. Sorgeloos, D. A. Bengtson, W. Decleir, E. Jaspers (Eds.), *Ecology, Culturing, Use in aquaculture*, Universa Press, Wetteren, Belgium, (1987), pp. 357-372.

[16] A. H. Warner, *Isolation, purification and some properties of P^1, P^4-diguanosine 5´-tetra phosphate asymmetrical-pyrophosphohydrolase from brine shrimp eggs*, Doctor of Philosophy Dissertation, Southern Illinois University, (1964).

[17] W. Zhong, J. Fang, H. Liu and X. Wang, *J. Ind. Microbiol. Biotechnol.* **36** (2009) 687-693.

[18] T. Yuting, Y. Tianli, P. Jinjin, Y. Yahong, L. Juhai and L. Y. Martin, *Food Sci. Technol. Int*. **16** (2010) 195-203.

[19] J. N. Miller and J. C. Miller, *Statistics and Chemometrics for Analytical Chemistry*, 5th ed., England (2005), pp. 121-124.

TRACE ELEMENTS DETERMINATION IN HUMAN MILK SAMPLES BY INDUCTIVELY COUPLED PLASMA MASS SPECTROMETRY

Usana Thiengmanee[1], Juwadee Shiowatana[1], Waret Veerasai[1], Oraporn Dumrongwongsiri[2], Areeporn Sangcakul[3], Atitaya Siripinyanond[1,*]

[1]Department of Chemistry and Center of Excellence for Innovation in Chemistry, Faculty of Science, Mahidol University, Bangkok 10400, Thailand
[2]Department of Pediatrics, Faculty of Medicine, Ramathibodi Hospital, Mahidol University, Bangkok 10400, Thailand
[3]Research Center, Faculty of Medicine, Ramathibodi Hospital, Mahidol University, Bangkok 10400, Thailand

*Author for correspondence; E-mail: atitaya.sir@mahidol.ac.th, Tel. +66 22015129

Abstract: Trace elements (Ca, Fe, Cu, Zn, and I) in human milk samples donated from volunteer's mothers of Ramathibodi Hospital were determined by ICP-MS. Pior ICP-MS determination of trace elements, human milk samples were digested by using HNO_3 in the closed vessel under microwave radiation. Appropriate volume ratio of nitric acid to human milk was examined, which was found to be 1 mL of human milk to 3 mL of nitric acid for about 40 minutes. The microwave operating conditions were as follows: temperature 145 ºC, 170 ºC, and 190 ºC for step 1-3, respectively, and pressure 50 bars in all steps. The recovery was 82-111% with a limit of detection of 198, 0.067, 0.0014, 0.25, and 0.0058 mg/L for Ca, Fe, Cu, Zn, and I, respectively. For 35 human milk samples, the concentrations were found to be in range of 200-360 mg/L for Ca, 1.3-3.0 mg/L for Fe, 0.1-0.35 mg/L for Cu, 0.5-3.2 mg/L for Zn, and 0.01-0.85 mg/L for I.

1. Introduction

Human breast milk is a dietary source of nutrients providing the normal growth to human and relates to the development during infant age from the early stages of birth to the stages initiatively having a capability to consume food. All macronutrients (such as proteins, lipids, and carbohydrates) and micronutrients (such as vitamins, enzymes, minerals and trace elements) are contained in breast milk [1, 2]. Although infant bodies need these nourishments at low level, it will have detrimental impact on unusual development of infants if they lack these nutrients. In addition, minerals and trace elements such as calcium (Ca), iron (Fe), copper (Cu), zinc (Zn) and iodine (I) play important roles in human health, especially at the infant stage in order to develop several functions, organs and systems in infant's bodies, therefore lack of these elements will cause deficiencies [3, 4]. Thus, the study about methods for determination of trace elements in human breast milk is important to indicate a level of these elements. Several techniques have been employed for determination of trace elements in breast milk samples, including neutron activation analysis (NAA) but this technique has been utilized primarily for trace elements speciation, is more time consuming, and requires relatively extensive sample preparation. Atomic spectrometry is the well-known technique for trace elements analysis such as flame atomic absorption spectrometry (FAAS), graphite furnace atomic absorption spectrometry (GFAAS), and flame emission spectrometry (FES), inductively coupled plasma spectrometry (ICPs) [5, 6].

Inductively coupled plasma mass spectrometry (ICP-MS) is one of techniques for determination of trace elements. It is outstandingly used in multi-elemental analysis, due to rapid and sensitive detection, simple method of monitoring trace element isotopes in milk, and simple sample pretreatment [7, 8]. Before trace elements analysis, breast milk samples were prepared for introduction into ICP-MS because they contain macromolecules such as lipid or fat causing the large droplet size, causing incomplete atomization or ionization of trace elements. Therefore, the study of sample preparation method for determination of trace elements in breast milk samples before ICP-MS analysis is conducive to solve this problem [9]. Microwave digestion is an approach used for digestion of all macromolecules and matrix interferences in breast milk and trace elements are not lost because this process occurs in a closed system and this method can also increase the efficiency of oxidation and reduce the time of digestion [10].

In this work, microwave digestion method was examined for its sutibility as samples preparation method for determination of trace elements in breast milk samples. The method is then applied to determine trace elements in 35 human breast milk samples.

2. Materials and Methods

2.1 Human breast milk samples

35 volunteer's mothers of Ramathibodi Hospital mothers in Bangkok (Thailand) agreed to join the research. They were between sixteen to thirty-five years old. Milk samples were collected from both breasts with breast pump, and then the samples were immediately transferred to a PET bottle and sent to the laboratory. Collected human breast milk samples were frozen and kept at -20 ºC until analysis.

2.2 Reagents and standard solutions

Water purified with a Milli-Q deionized water system (Barnstead EASYpureII, Illinois, USA) was employed for preparing standard solutions and sample

solutions in this experiment. KH_2PO_4 was obtained from Ajax Finechem (Auckland, New Zealand), KIO_3, $Fe(NO_3)_3 \cdot 9H_2O$, $Cu(NO_3)_2 \cdot 2.5H_2O$, $Ca(NO_3)_2 \cdot 4H_2O$, and $Zn(NO_3)_2$ were purchased from Sigma-Aldrich (Steinheim, Germany). All of standards for calibration were prepared in ultrapure water and kept in polypropylene containers previously leached in 10% HNO_3.

2.3 Human breast milk preparation

1 mL of human breast milk and 3 mL concentrated nitric acid are added into DAK-100/4 vessel (Berghof Products + Instruments GmbH, Eningen, Germany) and digested for about 40 minutes by microwave digestion. The samples are directly heated through the absorption of the microwave radiation by microwave digestion. Upon complete digestion the solution was made up volume to contain 10% nitric acid.

2.4 Instrumentation

Microwave digestion system is a speedwave 4 model (Berghof Products + Instruments GmbH, Eningen, Germany). The temperature program for microwave digestion is shown in Table 1.

The ICP-MS instrument is Perkin-Elmer Sciex ELAN6000 model (Shelton, CT, USA). After sample preparation, samples in 10% nitric acid are introduced into ICP-MS. The instrument conditions used for determination of breast milk are shown in Table 2.

Table 1 Temperature program for microwave digestion (SPEED*WAVE* 4)

Step	T (ºC)	P (bar)	Power (%)	Ta (min)	Time (min)
1	145	50	70	2	5
2	170	50	80	5	10
3	190	50	90	2	15

Table 2 The instrument conditions for ICP-MS operation

RF power	1200 W
Carrier gas flow	0.9 L min^{-1}
Resolution	0.3-3.0 amu
Detector	Dual-stage discrete dynode electron multiplier
Mass filter	Quadrupole
Isotope monitored	^{42}Ca, ^{43}Ca, ^{44}Ca, ^{54}Fe, ^{57}Fe, ^{63}Cu, ^{65}Cu, ^{66}Zn, ^{68}Zn, ^{127}I

3. Results and Discussion

3.1 Optimization of the volume ratio between nitric acid and human breast milk on microwave digestion

For the preparation of human breast milk samples, the volume ratio of nitric acid with human breast milk on microwave digestion were varied for using the least volume of nitric acid to digest the most volume of human breast milk. Various volume ratio of nitric acid with human breast milk (nitric acid (A) : milk (M) = 3

: 1, 4 : 1, 5 : 1, 3 : 0.5, 4 : 0.5, and 5 : 0.5 mL) were tested using microwave digestion for about 40 minutes and were made up to 10% nitric acid for ICP-MS analysis. From the results (Figure 1) , the optimum volume ratio of nitric acid to human breast milk is 3:1 because complete digestion was obtained with the highest milk:acid ratio.
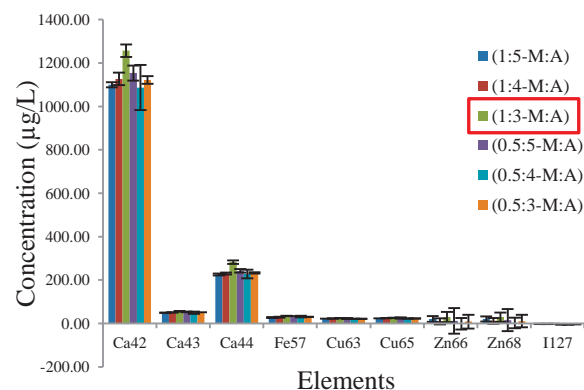
Figure 1. The concentration of trace elements in human breast milk.

3.2 Analytical performance

The analytical performance such as sensitivity (S), accuracy (recovery), and limit of detection (LOD) were evaluated for the proposed method. Sensitivity was established from the mean value of the slopes of the external standard (ICP-MS).

Recovery was determined by spiking standard solutions into human breast milk samples and calculated follow equation below. Three replicate measurements were made on each solution.

$$\% \text{ Recovery} = [(C_{sp}-C_s)/C_a] \times 100$$

C_{sp}= Concentration of standard solution spiked into sample
C_s= Concentration of samples
C_a= Concentration of standard solution

Limit of detection defined as the analyte concentration in micrograms per liter of human breast milk which provides an intensity reading statistically different from that of the blank, was calculated by dividing 10 times the standard deviation of the intensity readings of the reagent blanks by the sensitivity.

$$\text{LOD} = 3 \times SD_{blk}/\text{Slope}$$

The recovery was 82-111% with a limit of detection of 198, 0.067, 0.0014, 0.25, and 0.0058 mg/L for Ca, Fe, Cu, Zn, and I, respectively as shown in Table 3

Table 3 Limit of detection and %recovery for trace elements in breast milk by ICP-MS

Elements	LOD (mg/L)	%Recovery		
		S6	S3	S5
Ca	0.17	111	97	86
Fe	0.07	108	99	108
Cu	0.0007	105	98	86
Zn	0.53	90	82	106
I	0.0054	99	104	105

S3, 5, 6 = Sample 3, 5, 6

3.3 Determination of trace elements in human breast milk

Human breast milk samples from 35 volunteer's mothers of Ramathibodi Hospital mothers were prepared with microwave digestion method and trace elements were determined by ICP-MS. The concentrations of human breast milk were found to be in range of 200-360 mg/L for Ca, 1.3-3.0 mg/L for Fe, 0.1-0.35 mg/L for Cu, 0.5-3.2 mg/L for Zn, and 0.01-0.85 mg/L for I, respectively (Figure 2a-2e).
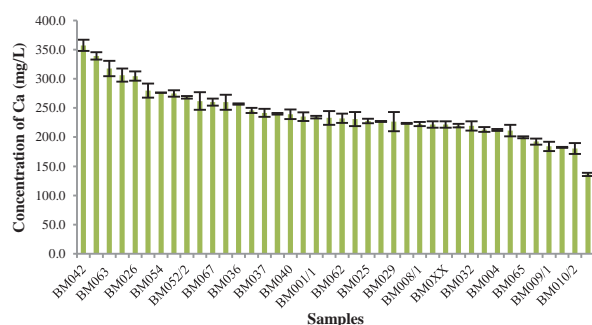
Figure 2a. Concentration of Ca in human breast milk BM001-BM070
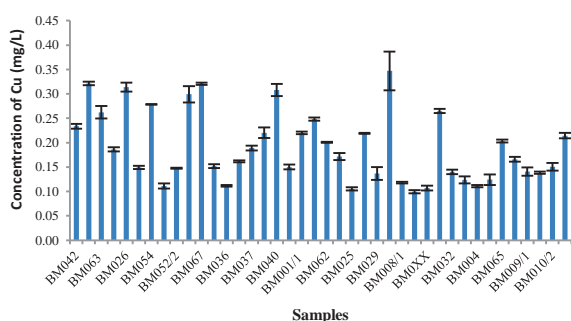
Figure 2b. Concentration of Cu in human breast milk BM001-BM070
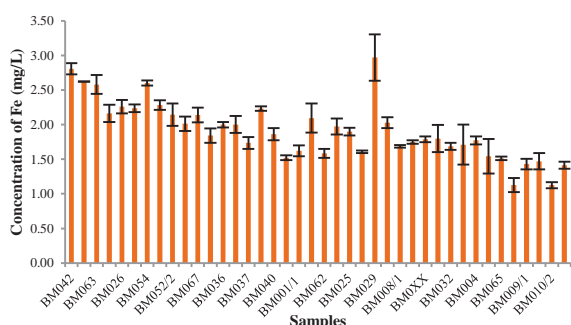
Figure 2c. Concentration of Fe in human breast milk BM001-BM070
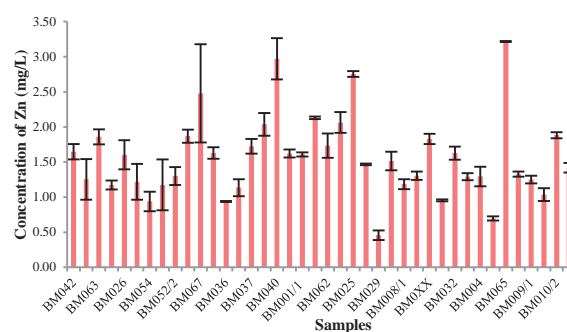
Figure 2d. Concentration of Zn in human breast milk BM001-BM070
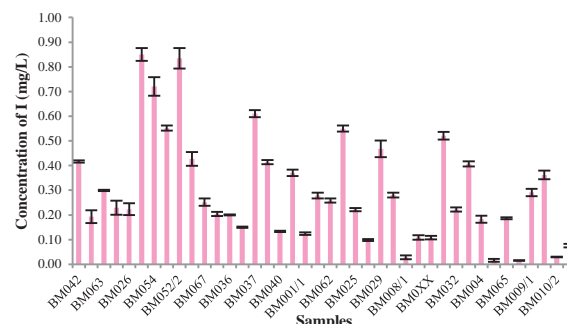
Figure 2e. Concentration of I in human breast milk BM001-BM070

4. Conclusions

Trace elements in breast milk samples donated from volunteer's mothers of Ramathibodi Hospital were analyzed by ICP-MS. The microwave digestion should be used as a sample preparation method because it can increase the efficiency of oxidation as this process occurred in a closed system. In addition, this preparation method can also reduce time and nitric acid volume of digestion and trace elements are not lost. Under microwave digestion milk samples were digested by using HNO_3 in the closed vessel. In addition, analytical performance (recovery and limit of detection) was studied. The recovery was 82-111% and the limit of detection of 0.17, 0.07, 0.0007, 0.53, and 0.0054 mg/L for Ca, Fe, Cu, Zn, and I respectively.

References

[1] Y. D. Shi and et al. *Food Chemistry.* **127** (2011) 1193–1198.

[2] L.Yang, M. Zhang, S. Lin, D. Chen and M. Zheng. *Microchim. Acta.* **142** (2003) 85–88.

[3] N. Yamawaki and et al. *Journal of Trace Elements in Medicine and Biology*. **19** (2005) 171–181.

[4] F. A. R. Martino, M. L. F. Sánchez and A. Sanz-Medel, *Analytica Chimica Acta*. **442** (2001) 191–200.

[5] P. J. Mc. Kinstry, H. E. Indyk and N. D. Kim. *Food Chemistry*. **65** (1999) 245-252.

[6] H. Vanhoe, F. V. Allemeersch, J. Versieck and R. Dams**.** *Analyst***. 118** (1993) 1015-1019.

[7] H. J. Reid and et al. *Talanta*. **75** (2008) 189–197.

[8] S. Sturup and A. Buchert. *Fresenius J Anal Chem*. **354** (1996) 323-326.

[9] P. Brätter, I. N. Blascob, V. E. N. Brätter and A. Raab. *Analyst*. **123** (1998) 821–826.

[10] É. M. M. Flores, J. S. Barin, M. F. Mesko and G. Knapp. *Spectrochimica Acta Part B*. **62** (2007) 1051–1064.

AN INEXPENSIVE AND DISPOSABLE PENCIL-LEAD ANTIMONY-FILM ELECTRODE FOR THE DETERMINATION OF TECTILON YELLOW 3R BY DIFFERENTIAL PULSE VOLTAMMETRY

Sangprakay Siri , Winai Oungpipat [*]

Division of Chemistry, Department of Science, Rajamangala University of Technology Krungthep, 2 Nang Linchi Road, Sathron, Bangkok 10120, Thailand

[*] E-Mail: winai_o@hotmail.com

Abstract: This paper describes the fabrication, characterization and application of an inexpensive and disposable pencil-lead antimony-film electrode for the electrochemical determination of azo dye, Tectilon Yellow 3R. The antimony-film on the surface of pencil-lead substrate was deposited ex situ from a solution containing 0.6 mg/L antimony and 0.01 M hydrochloric acid at -1.4 V (vs. SCE) for 210 seconds. Several parameters were studied and optimized, including preparation of antimony-film electrode and differential pulse voltammetric settings. Tectilon Yellow 3R was determined on this electrode by differential pulse voltammetry. The electrode exhibited highly linear behaviour in the examination range of 0.05-10.0 mg/L, with the detection limit (3σ) of 0.05 mg/L for Tectilon Yellow 3R. Good reproducibility of 3.2% relative standard deviation for 5 mg/L Tectilon Yellow 3R (n = 10) was achieved. The results confirm that the pencil-lead antimony-film electrode offers high-quality performance and provides an attractive alternative to others types of carbon electrodes by virtue of its high electrochemical reactive, good mechanical rigidity, low cost and ease of modification.

1. Introduction

Azo dyes are synthetic colors that contain an azo (-N=N-) linkage as part of the structure (Figure 1). They are the largest group of organic dyes for their widespread applications in many areas of dye-stuff industry, pharmacy and dosimetry. However they also represent a human hazard because their degradation products including amines are carcinogenic. Therefore, many countries and health organizations have published guidelines to control the use, purity and permitted amounts of such dyes in foods and also to specify permitted percentages of soluble and insoluble colorant materials. Thus, a rapid and accurate method is needed to identify and quantify of the dyes.

Due to the above reason, many analytical methods have been developed to characterize and determine azo dyes. So far, azo dyes have already been determined by using chromatography [1-2], spectrophotometry [3] and electrochemical methods [4-10]. As advanced electrochemical techniques still allure considerable attention in modern analytical chemistry, the development of novel electrode surfaces, sensors and associated sensing approaches is still one of the most captivating topics in many electroanalytical laboratories.

In the search for a mercury-free electrode used for voltammetric analysis, bismuth film electrodes (BiFEs) and antimony film electrodes (SbFEs) were introduced, respectively. Different materials have been used as substrates for BiFEs and SbFEs, including glassy carbon [11-14], wax impregnated graphite[15], carbon paste [16-18], noble metals[19], screen-print [20-21] and carbon-fibers [22]. Pencil-lead graphite has been employed as an electrode material in different applications for voltammetric analysis [23-24]. The main attractions of this material are its low-cost, high electrical conductivity, low background current and fast and easy pretreatment.

As there have not yet been any literature reports about the use of pencil-lead antimony film electrodes (PSbFEs) to detect azo dyes, in this work, PSbFEs were prepared by ex situ depositing antimony onto pencil-lead rods for the determination of azo dye, Tectilon Yellow 3R.

TY3R   M = 539.56

Figure 1 Molecular structure of Tectilon yellow 3R.

2. Materials and Methods

2.1. Reagents and apparatus

Antimony chloride (1000 mg/L) was purchased from Fisher Chemical (United Kingdom). Tectilon Yellow 3R (200%) was purchased from Ciba (Germany). All other chemicals used were of analytical grade. Ultra-pure water used for standard and buffer solutions was prepared by a Milli-Q system (Millipore, Bradford, USA). Standard solutions were prepared

daily by diluting the stock solution with a supporting electrolyte just before use.

A modular electrochemical system AUTOLAB equipped with PGSTAT12 and ECD modules (Eco Chemie, Utrecht, Netherlands) was used in combination with GPES software (Eco Chemie). The voltammetric cell was a 50 ml glass vial (Metrohm, Switzerland) equipped with a pencil-lead antimony-film working electrode, SCE reference electrode and a Pt counter electrode.

The pencil-lead rods were Pilot HB (0.5 mm in diameter and 6 cm in length) purchased from a local bookstore. The pencil-lead rod was coated with an insulator so that the length of 0.5 cm at both ends of the rod was exposed. One of the exposed ends of the rod was used for electrical connection. Prior to use, the electrode was rinsed with 4 mol/L HNO_3, gently rubbed with a clean soft tissue and rinsed with ultra-pure water.

2.2 Fabrication of the pencil-lead antimony-film electrode (PSbFEs)

The pencil-lead rod was used as the substrate for deposition of the antimony film. The pencil-lead rod was immersed into the plating solution containing 0.01 M HCl and 0.6 mg/L Sb(III). The antimony film was then deposited ex situ onto the supporting pencil-lead rod surface in the presence of dissolved oxygen by applying a constant potential of -1.4 V for 210 s. Finally, the PSbFEs was rinsed with ultra-pure water and was ready to use.

2.3 Renewal of the PSbFEs

The renewal of PSbFEs for repeatedly identical fresh antimony-film surface could be done by the following electrochemical procedure. An electrochemical cleaning step was firstly introduced in order to remove the antimony film by applying a potential of $+0.5$ V for 15 s in an acidic solution of 0.01 mol/L HCl, after which the deposition of a fresh antimony film was carried out by applying a constant potential of -1.4 V for 210 s.

2.4 Electroanalytical measurements

The pencil-lead antimony-film electrode (PSbFE) the reference and counter electrodes were immersed into an electrochemical cell containing 25 mL of pH 4.70 acetate buffer and appropriate amounts of Tectilon yellow 3R. Current measurements were performed using differential pulse voltammetry in the potential range between -0.1 and -0.6 V. To record differential pulse voltammograms, the following instrument parameters were used: step potential 0.00495 V, modulation amplitude -0.0499 V. All electroanalytical measurements were made at room temperature.

3. Results and Discussion

3.1. Electrochemical behavior of Tectilon yellow 3R at PSbFE and PE

A comparison of differential pulse voltammograms obtained at PE and PSbFE for electrochemical reduction of 5 mg/L Tectilon yellow 3R were illustrated in Figure 2. A well-defined reduction peak of Tectilon yellow 3R was observed at -0.35 V for PE and -0.34 V for. PSbFE. However, the current density obtained at PSbFE was higher than that obtained at PE. Therefore, the PSbFEs appears to be suitable for determination of Tectilon yellow 3R as it enhances the sensitivity of the method.
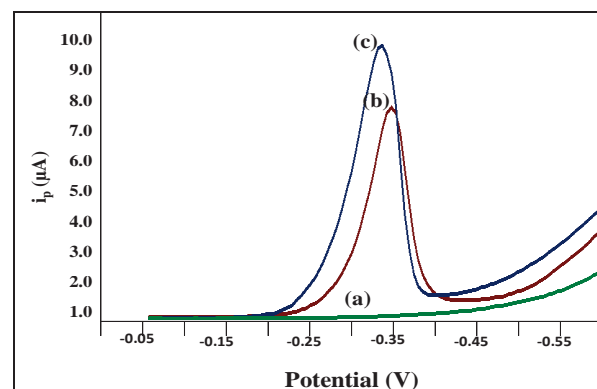
Figure 2 Differential pulse voltammograms in acetate buffer solution (pH 4.70) in the absence of Tectilon Yellow 3R at PSbFE (a) and in the prescence of 10 mg/L Tectilon Yellow 3R at PE (b) and PSbFE (c). Differential pulse settings: modulation amplitude of -0.0499 V, step potential of 0.00495 V.

3.2 Optimization of parameters for ex situ antimony plating onto the PE

The effects of preplating of the antimony film conditions, including plating potential, antimony concentration, plating time and acidic solutions concentration were studied.

The effect of plating potential was tested between -0.8 V and -1.6 V. It could be seen from Figure 3(a) that the current peak of Tectilon yellow 3R increased with increasing plating potential and provided the highest response at -1.4 V. Increasing potential higher than this value resulted in the decrease in the current peak. Therefore the potential -1.4 V was used as the plating potential.

The effect of antimony concentration in the range from 0.3 - 1.0 mg/L on current peak of Tectilon yellow 3R is shown in Figure 3(b). The current response of Tectilon yellow 3R increased with increasing antimony concentration and reached the maximum at antimony concentration of 0.6 mg/L. Slightly decrease in the current response was observed at the antimony concentration higher than 0.6 mg/L. This may be ascribed to the saturation of antimony in the film formed on the PE. Consequently, the antimony concentration of 0.6 mg/L was selected as the optimum value.

Plating time also has the profound effect on the Tectilon yellow 3R current response. Figure 3(c) shows the optimization of the plating time. The peak

current increased with plating time up to plating time 210 s and then decreased gradually. The rapid and highly accumulation was attributed to the strong interaction between PSbFE and Tectilon yellow 3R. Thus, 210 s of plating time was employed.

The effect of type and concentration of the supporting electrolyte for plating solution on the current peak was investigated. Three acidic solutions including hydrocholric acid (HCl), nitric acid (HNO_3) and acetic acid (CH_3COOH) were chosen for this purpose. The result revealed that HCl resulted in the best current obtained. Therefore, the effect of HCl concentration was then studied. It can be seen from Figure 3 (d) that 0.01 mol/L of HCl was the best supporting electrolyte for plating solution. It is most likely due to the stability of PSbFE at 0.01 mol/L HCl.
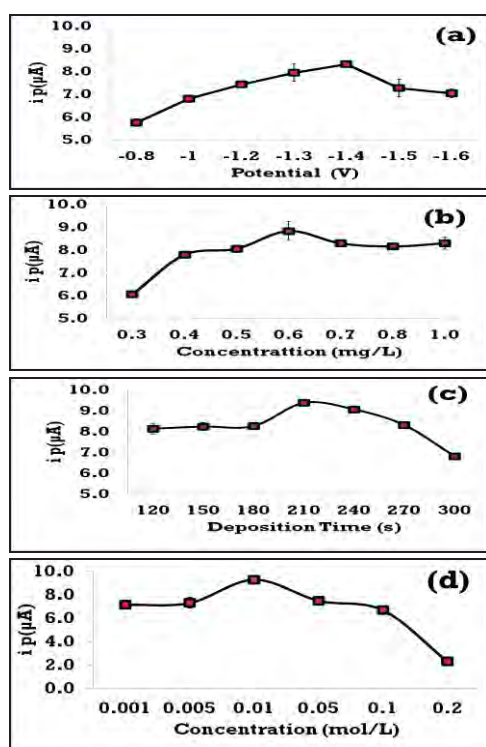
Figure 3 Effect of the ex situ antimony film plating potential (a), antimony concentration (b), plating time (c), concentration of the supporting electrolyte (d) on the differential pulse voltammetric response of 10 mg/L Tectilon yellow 3R at PSbFE. Differential pulse settings: modulation amplitude of -0.0499 V, step potential of 0.00495 V.

3.3 Optimization of parameters for differential pulse measurements

The effect of pH of the supporting electrolyte and modulation amplitude and step potential upon the differential pulse signals were conducted.

Figure 4(a) shows the effect of pH of the supporting electrolyte upon the differential pulse signal. As can be seen in the figure, the signal increased gradually with increasing pH from 4.0- 4.7 and then decreased sharply at pH value higher than 4.7.

As a result, pH 4.7 was chosen to use for further studies.

Figure 4(b) illustrates the effect of modulation amplitude in the range -0.01– (-0.40) V on differential pulse signal. The peak current obtained increased with increasing modulation amplitude up to -0.0499 V. At higher modulation amplitude value, the peak current decreased and peak became broader and ill defined. Thus, modulation amplitude of -0.0499 V was used as the optimum conditions.

The step potential in the range 0.001-0.010 V was optimized by observing the variation on the peak current and peak shape. The results were shown in Figure 4 (c). As can be seen from Figure 4(c), the best peak was observed at 0.00495 V.
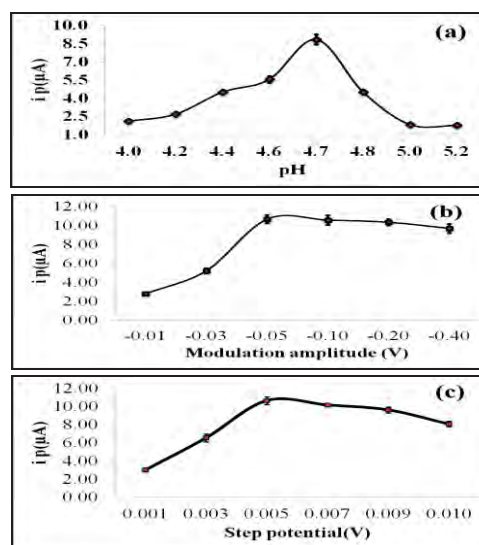
Figure 4 Effect of the pH of the supporting electrolyte (a), modulation amplitude (b), step potential (c), on the differential pulse voltammetric response of 10 mg/L Tectilon yellow 3R at PSbFE.

3.4 Validation of analytical procedure

The increase in the current density with Tectilon yellow 3R concentration was investigated in the 0.05-15 mg/L range by differential pulse voltammetry at PSbFE under the optimum experimental conditions. Figure 5 displays the obtained voltammograms. Well–defined and sharp reduction peaks were obtained at -0.35 V with the current density increasing proportionally to the Tectilon yellow 3R concentration. Figure 5 inset shows the corresponding calibration curve. Linear relationship in the range of 0.05-10 mg/L with the equation of y = 1.0178x - 0.0299 and correlation coefficient of 1.0 was noticed. The sensitivity of the PSbFE was found to be 1.0178 µA L/mol. The limit of detection (LOD) calculated from the equation LOD = 3SD/B, where SD is the standard deviation of the peak current and B is the slope of the calibration curve was 0.05 mg/L. The limit of quantification (LOQ) calculated from the equation LOQ = 10SD/B was 0.17 mg/L.

The reproducibility of PSbFE was investigated for 5mg/L Tectilon yellow 3R. The peak current responses

of Tectilon yellow 3R were determined with ten electrodes which produced under the same conditions. The responses of peak current showed a relative standard deviation of 3.2%. This confirmed that the results were reproducible. The repeatability of PSbFE was studied for ten repetitive measurements of 5mg/L Tectilon yellow 3R under the same conditions. The relative standard deviation of the responses obtained was 1.9%.
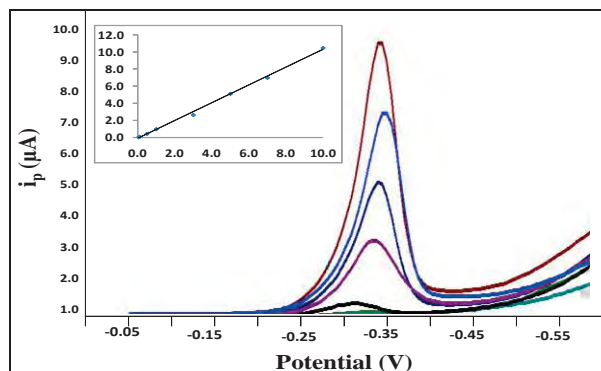
Figure 5 Differential pulse voltammetric responses of Tectilon Yellow 3R with different concentrations in acetate buffer (pH 4.70) at PSbFE under optimized conditions from 0.00, 0.05, 0.50, 1.00, 5.00 and 10.00 mg/L. The inset shows the calibration curve for Tectilon Yellow 3R determination.

To further demonstrate the practicality of the proposed method, the recovery test was conducted by adding three different amounts of Tectilon Yellow 3R into waste water samples. The results obtained were summarized in Table 1. The recoveries in the range of 97.4-101.5% indicated that the proposed method was highly accurate, precise and reproducible. Moreover, the high percentage of recovery signifies that the coexisting species in the sample did not significant interfere in the analyte signal produced by the electrochemical reduction of Tectilon Yellow 3R.

Table 1: Recovery study for Tectilon Yellow 3R determination in waste water samples.

Original (mg/L)	Added (mg/L)	Found (mg/L)	RSD (%)	Recovery (%)
0.00	1.00	1.02	4.0	101.5
0.00	3.00	3.04	2.9	101.5
0.00	5.00	4.87	4.0	97.4

4. Conclusions

In this study, the PSbFE, a metallic mercury- free and environmentally friendly electrode has been developed and successfully employed for the determination of Tectilon yellow 3R. The results confirm that the PSbFE offers high-quality performance and provides an attractive alternative to others types of carbon electrodes by virtue of its high electrochemical reactive, good mechanical rigidity, low cost and ease of modification. This proposed method can also be used for the direct detection of other relevant azo dyes.

References

[1] C. Long, *Food Chemistry* **126** (2011) 1324-1329.
[2] M. Fuh and K.J. Chia, *Talanta* **56** (2002) 663–671.
[3] H.M. Pinheiro, E. Touraud and O. Thomas, *Dyes and Pigments* **61** (2004) 121–139.
[4] S. Combeau, M. Chatelut and O. Vittori, *Talanta* **56** (2002) 115–122.
[5] E. Ungureanu, *Electrochimica Acta* **53** (2008) 7089–7099.
[6] S. Chanlon, L. Joly-Pottuz, M. Chatelut, O. Vittori and J.L. Cretier, *Journal of Food Composition and Analysis* **18** (2005) 503–515.
[7] A. Rahim H.M. Yusoff , A. G. Fogg and R. Ahmad, *Talanta* **47** (1998) 797–801.
[8] C. Guaratini, A. Fogg, M. Valnice and B. Zanoni, *Dyes and Pigments* **50** (2001) 211–221.
[9] A. G. Fogg, A. Rahim, H.M. Yusoff and R. Ahmad, *Talanta* **44** (1997) 125 129.
[10] M.V.B. Zanoni, A.G. Fogg, J. Barek and J. Zima, *Analytica Chimica Acta* **349** (1997) 101-109.
[11] X.Y. Xie, H.Q. Luo and N.B. Li, Journal of *Electroanalytical Chemistry* **639** (2010) 175-180.
[12] B. Claux and O. Vittori, *Electroanalysis* **19**, 2007, No. 21, 2243 – 2246.
[13] B. Nigovic and S.B. Hocevar , *Electrochimica Acta* **58** (2011) 523– 527.
[14] V. Guzsvany, H. Nakajima, N. Soh, K. Nakano and T. Imato, *Analytica Chimica Acta* **658** (2010) 12–17.
[15] H. Li., *Journal of Hazardous Materials* **191** (2011) 26–31.
[16] L. Cao, J. Jia and Z. Wang, *Electrochimica Acta* **53** (2008) 2177–2182.
[17] A. Ashrafi and K. Vytras, *Electrochimica Acta* **73** (2012) 112– 117.
[18] H. Sopha, *Electrochimica Acta* **55** (2010) 7929–7933.
[19] C. Kokkinos, A. Economou, I. Raptis and T. Speliotis, *Electrochemistry Communications* **11** (2009) 250-253.
[20] X. Niu, H. Zhao and M. Lana, *Electrochimica Acta* **56** (2011) 9921– 9925.
[21] J. Quintana, *Analytica Chimica Acta* **707** (2011) 171–177.
[22] R. Alcantara, *Carbon* **42** (2004) 2153–2161.
[23] D. Demetriades, A. Economou and A. Voulgaropoulos, *Analytica Chimica Acta* **519** (2004) 167–172.
[24] A. Bond, P. Mahon, J. Schiewe and V. Vicente-Beckett, *Analytica Chimica Acta* **345** (1997) 67-74.

INVESTIGATING THE INFLUENCE OF CAPSAICINOIDS AND PHENOLIC COMPOUNDS FROM HOT PEPPER EXTRACTS ON DECELERATION OF AUTOOXIDATION OF MYOGLOBIN

Chatrachatchaya Choichayapong[1*] ,Pimpanitpa Kunthadong[1], Warunee Thongdee[2] , Weeranuch Khottawong[2], Saksit Chanthai[2]

[1] Applied Chemistry Program, Faculty of Sciences and Liberal Arts, Rajamagala University of Technology Isan, Muang, Nakorn Ratchasima, 30000 Thailand
[2] Department of Chemistry, Faculty of Science, Khon Kaen University, Muang, Khon Kaen, 40002 Thailand

[*] Author for correspondence; E-Mail: Chatrachatchaya.ch@rmuti.ac.th, Tel. +66 44233000 ext 4013

Abstract: Capsaicinoids was extracted from ground dried-hot peppers by magnetic stirring method at 60°C using 90% methanol as solvent. The content of capsaicinoids in the extract of 8 hot pepper samples was found in the range of 63.76 – 106.62 dry weight (mg/g DW). Interestingly, the phenolic compounds were also presented in the methanol extracts in the range of 16.56 – 21.91 mg/g DW. For phenolic compounds extraction, these samples were extracted at room temperature by the same method but using methanol: 0.05%HCl (90:10) as solvent. The content of phenolic compounds was found in the range of 27.99 – 39.03 mg/g DW. While those of capsaisinoids were also presented in the acidified methanol extracts in the range of 59.02 – 113.81 mg/g DW. It was noted that the capsaisinoids content that present in the acidified extracts were higher than those of the methanol extracts. Autooxidation kinetics of oxymyoglobin in the presence of both capsaicinoids and phenolic compounds obtained from these hot peppers was investigated. The metmyoglobin was reduced and re-oxygenated to be oxymyoglobin and it was then measured the absorbance at 581 nm at 37 °C for 2 hours. The results showed that hot pepper extracts including both capsaicinoids and phenolic compounds could decelerate autooxidation of the oxymyoglobin. The k_{obs} values for autooxidation of oxymyoglobin in the presence of the sample extract for capsaicinoids and phenolic compounds were in the range of 0.384 – 0.503 hr^{-1} and 0.293 – 0.478 hr^{-1}, respectively compared to k_{obs} values of oxymyoglobin without the addition of these antioxidants.

1. Introduction

Hot peppers are known to be good sources of phyto-compounds including vitamin C, E and A, alkaloid, flavonoids, and carotenoids [1]. Capsaicinoids, the pungent alkaloids, are the main active component of hot peppers. The naturally occurring capsaicinoids present in hot pepper are capsaicin and four structurally related compounds, namely dihydrocapsaicin, nordihydrocapsaicin, homocapsaicin and homodihydrocapsaicin [2]. Capsaicin and dihydrocapsaicin are responsible for approximately 80-90% of the total capsaicinoids present and contribute greatly to overall pungency [3]. The capsaicinoids accumulate in the pericarp and placenta of hot pepper and their concentrations vary, depending on hot pepper's species, growing conditions and the harvested time. Capsaicinoids have many of useful properties, especially antioxidant properties. Many reports reveal substantial antioxidant activity of hot pepper extracts and capsaicinoids [4-7].

Phenolic compounds in hot pepper include simple phenols, flavonoids [8]. Phenolic compounds are antioxidants which can retard or inhibit lipid oxidation by acting scavengers and, protect against propagation of the oxidative chain like capsaicinoids [9, 10].

On the basis of antioxidant properties of capsaicinoids and phenolic compounds, these compounds were extracted from various hot pepper samples and their concentrations were evaluated. In addition, one goal of this study was to investigate the influence of both compouds in hot pepper samples on autooxidation of myoglobin.

2. Materials and Methods

2.1 Materials

Chemicals and reagents: All the reagents used were analytical reagent (AR) grade including dihydrocapsaicin, gallic acid monohydrate, sodium dithionite, Tris, sodium carbonate and horse heart myoglobin (Sigma-Aldrich, Germany); Folin-Ciocarteu phenol reagent, methanol, hydrochloric acid (Carlo Erba, Italy).

Hot pepper samples: Eight samples (green, orange and red pepper fruits as labelled sample A-H) used in this study were randomly purchased from a fresh market in Khon Kaen, Thailand.

2.2 Apparatus

Capsaicinoidd and phenolic compound contents in hot pepper extracts and their antioxidant activities were determined using Agilent 8453 diode array UV-Vis spectrophotometer (USA). The Hitachi EBA 20 centrifuge (Germany), Model B-490 rotary evaporator (Buchi, Switzerland) and Iowa 52001 magnetic stirrer (Germany) were used in the sample preparation step.

2.3 Analysis of capsaicinoids in hot pepper extracts

Extraction: Extraction of capsaicinoids in hot pepper samples were done followed by Juagsamut, 2012 [3]. Briefly, all pepper fruits were dried at 60°C for 4 days and ground to a fine powder using a blender

(Philips, Netherlands). The powder was sifted through a 500 μm mesh laboratory sieve (Endecotts Limited, England). Two grams of ground hot pepper samples were weight to a 15 mL centrifuge tube, and 20 mL of 90% methanol was added. The extraction was done by magnetic stirring method at heating temperature of 60°C for 2 hours. The extracts were centrifuged at 5000 rpm for 10 min and then filtered through a Whatman No.42 filter pater. The solvent in the extracts was evaporated to dryness using a rotary evaporator and the residue was dissolved with methanol to make a volume of 5 mL.

Capsaicinoids measurements: Stock standard dihydrocapsaicin solution (1000 mg/L) was prepared by dissoloving dihydrocapsaicin with methanol. Working solutions were prepared by dilution of the stock solution with Tris-HCl buffer pH 7.2. Standard calibration curve was generated in the range of 10 - 60 mg/L. The absorbance of the solutions was measured at 279 nm [3,4] and capsaicinoids content was determined by extrapolated the obtained values with the calibration curve.

2.4 Analysis of phenolic compounds in hot pepper extracts

Extraction: The phenolic compounds extracts were prepared using the same manner as above [10] but the extraction was carried out at room temperature by using methanol: 0.05%HCl (90:10) as an extraction solvent. The extracts were centrifuged, filtered, evaporated and the residue was dissolved with the extraction solvent to make a volume of 20 mL.

Total phenolics measurements: The Folin-ciocalteau method as previous described using gallic acid as a standard compound was used to estimate total phenolic content [12]. Stock standard solution (1000 mg/L) of gallic acid was prepared by accurately dissolving with methanol and kept into a dark vial and stored at 4°C prior to use. Working standard solutions were prepared dilution of stock solution. The calibration curve in the range of 1- 4.5 mg/L was generated by mixing gallic acid solution with deionized water, Na_2CO_3 and the Folin-Ciocalteau reagent. After incubated at room temperature for 90 min, the absorbance of the blue color reaction mixture was measured at 745 nm. The total phenolic compound in hot pepper extracts was determined by a comparison of the obtained absorbance with the calibration curve of gallic acid.

2.5 Autooxidation of oxymyoglobin

Myoglobin, an oxygen-binding protein, was used as an autooxidation reaction model system for studying the antioxidant properties of hot peppers extracts. The aim of this study was to investigate the effect of dihydrocapsaicin, gallic acid and hot pepper extracts (capsaicinoids and phenolic compounds) on deceleration of autooxidation reaction of horse heart oxymyoglobin.

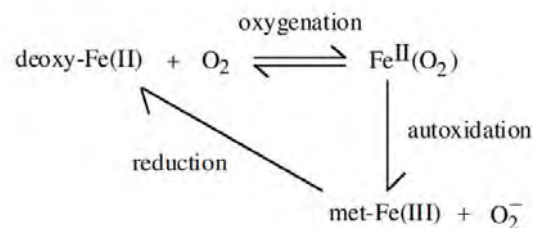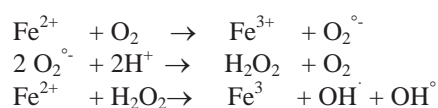*Autooxidation rate measurement:* Myoglobin in ferrous form can bind oxygen molecule reversibly as showed in figure 1.

Figure 1. Function cycle of myoglobin [13]

The mechanism for autooxidation of oxymyoglobin (oxy-Fe^{2+}) to metmyoglobin (met-Fe^{3+}) can be explained by the Fenton reaction as follow [14, 15]:

$$Fe^{2+} + O_2 \rightarrow Fe^{3+} + O_2^{°-}$$
$$2 O_2^{°-} + 2H^+ \rightarrow H_2O_2 + O_2$$
$$Fe^{2+} + H_2O_2 \rightarrow Fe^3 + OH^{.} + OH^{°}$$

Because temperature is one of factor affecting autooxidation of myoglobin, this reaction rate becomes faster as temperature increased. To obtain the optimum temperature for studying the effect of antioxidant on retardation of autooxidation of myoglobin, the various incubation temperatures were determined by monitoring the changes of oxidation state of Fe from (oxy-Fe^{2+}) to (met-Fe^{3+}). . The stock solutions of horse heart myoglobin (6,210 mg/L) were prepared by dissolving the protein with Tris-HCl buffer pH 7.2. An aliquot of the protein solution was converted to oxy-form by addition 10 μL of fresh sodium dithionite solution (100 mg/L) and makes a volume to 4 mL to obtain the final concentration of oxymyoglobin of 300 ppm. The solution was gently agitated with urging of oxygen gas for 2-3 min until the bright red coloured appeared.

The oxymyoglobin solution was quickly transferred to a quartz cell and place in thermostat connecting with UV-Vis spectrophotometer. The changes in the absorbance in the region of 450-650 nm were recorded at interval of 5 min for 2 hours by varying the incubation temperature for 25, 30, 33, 35, 37, 40 and 50°C. The solution was subjected to the absorbance measurement at 581 nm. The absorbance data were analyzed by plotting in terms of $[MbO_2]_t$/ $[MbO_2]_0$ versus time where the ratio of MbO_2 concentration after time t to that that at initial time t =0). From the slope of each straight line, the observed first-order rate constant, k_{obs} in hr^{-1}, was determined.

Effect of antioxidants on autooxidation reaction : According to the autooxidation of myoglobin, the superoxide radical ($O_2^{°-}$) and hydroxyl radical ($OH^{°}$) which produced by the reaction of ferrous iron in heme and hydrogen peroxide (H_2O_2). The present work studied the effect of antioxidant including capsaicinoids and phenolic compounds on the autooxidation of myoglobin because these compound

can retard oxidation by scavenging free radical intermediate ($O_2^{\circ -}$, OH°) by donationg hydrogen atom as follow:

$$ROO^{\circ} \; + \; AH \; \rightarrow \; ROOH \; + A^{\circ}$$
$$RO^{\circ} \; + \; AH \; \rightarrow \; ROH \; + A^{\circ}$$
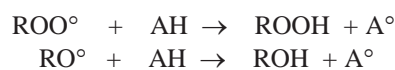
(ROO° RO° AH represents $O_2^{\circ -}$, OH° and antioxidant)

The oxymyoglobin was prepared as described above followed by the addition of various amount of dihydrocapsaicin or gallic acid. The final concentrations of dihydrocapsaicin and gallic acid were generated at 5, 10, 20, 30, 40, and 50 ppm. The oxymyoglobin and antioxidant solutions were then mixed and measured k_{obs} values at 37°C at every 5 min to 2 hours.

Effect of hot pepper extracts on autooxidation reaction: The hot pepper extracts were added to oxymyoglobin solution to set the final concentration of the extracts of 10 ppm. The autooxidation rate, k_{obs} was determined using the same conditions as described above.

3. Results and Discussion

Capsaicinoids contents in hot pepper samples: The contents of capsaicinoid in the eight of hot pepper samples were expressed based on dry basis as showed in table 1. The capsaicinoids content found in these samples as using UV-Vis measurement and calibration curve were ranged of 63.76 – 106.62 mg/g dry weight (mg/g DW). The highest capsaicinoids contents in the hot peppers was found in the sample A, while the lowest was found in the sample F. According to the extraction solvent for capsaicinoids and phenolic compounds, these compounds could extracted using methanol as solvent. We assumed that some of phenolic compounds may be released into methanol extracts. Therefore, the total phenolics contents in methonol extracts were determined by using Folin-Ciocalteau method. It was found that the phenolic compounds appeared in the extracts obtained from the extraction of capsaicinoids in the range of 16.56 – 21.91 mg/g DW (Table1).

Phenolics contents in hot pepper samples: Total phenolics contents in the eight samples of hot pepper were found to be 27.99 – 39.03 mg/g DW (Table1). The highest total phenolics content was found in the sample F and the lowest content was found in sample G. Based on our hypothesis, we had determined the capsaicinoids contents in acidified methanol extracts. The results showed that the capsaicinoids also presented in acidified methanol extracts in the range of 59,.02 – 113.81 mg/g DW. Surprisingly, the capsaicinoids contents in acidified methanol extracts was higher than those of methanol extracts itself. It may be suggested that an acidified methanol has been used to extract capsaicinoid compounds from the hot peppers. So. methanol: 0.05%HCl (90:10) was an optional solvent to use for extraction of capsaicinoids.

Therefore, we could be concluded that the each of hot pepper extracts obtained from two extraction methods are composed of both capsaicinoid and phenolic compounds.

Table 1 Capsaicinoids and total phenolics contents in the hot pepper samples based on dried basis (mg/g DW; n=3)

Sample code	Capsaicinoid extracts		Phenolics extracts	
	Capsaicinoid content	Phenolic content	Phenolic content	Capsaicinoid content
A	106.62	20.22	32.06	113.81
B	83.45	17.98	34.27	90.16
C	64.35	20.13	32.62	60.77
D	74.99	21.40	35.33	80.97
E	75.89	20.28	30.88	92.23
F	63.76	21.91	39.03	83.99
G	64.68	17.98	27.99	59.02
H	72.76	16.56	28.47	64.33

Effect of incubation temperature on autooxidation of myoglobin: The horse heart myoglobin solution was oxygenated to be oxymyoglobin and observed the Soret peak at 410 nm and visible band at 543 nm and 581 nm (Figure 1). When autooxidation reaction of the protein occurred, the Soret peak tend to slightly-blue shifted and the charge transfer band (543 nm peak and 581 nm peak) disappeared. Because of the oxidation of oxymyoglobin is favored by higher temperature. The observed first-order constant (k_{obs}) for the autooxidation reaction at various temperatures were determined.
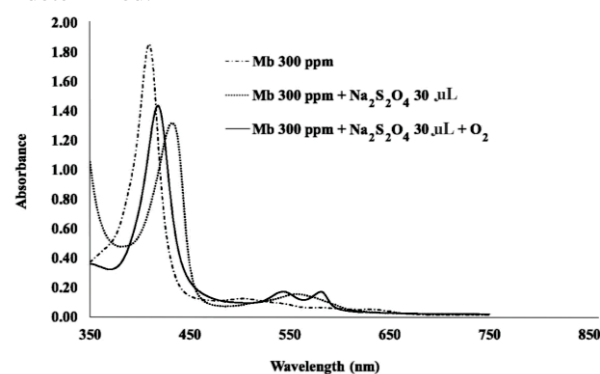
Figure 2. Absorption spectrum of metmyoglobin, reduced myoglobin and oxymyoglobin (300 ppm).

The first-order plots for autooxidation of oxymyoglobin at various temperatures showed in Figure 2. The results showed that incubation temperature increased, the slope of straight line (k_{obs}) also increased. The k_{obs} values obtained from the first plots are 0.179, 0.329, 0.443, 0.626, 0.779, 1.214 and 1.640 obtained from the incubation temperature of 25, 30, 33, 35, 37, 40 and 50°C, respectively. The incubation temperature of 37°C was selected to use as a system for studying the effect of antioxidant and hot pepper extracts on retardation of autooxidation of myoglobin because the k_{obs} could be obviously observed.

Figure 3. First-order plots for autoxidation of myoglobin at various incubation temperatures.
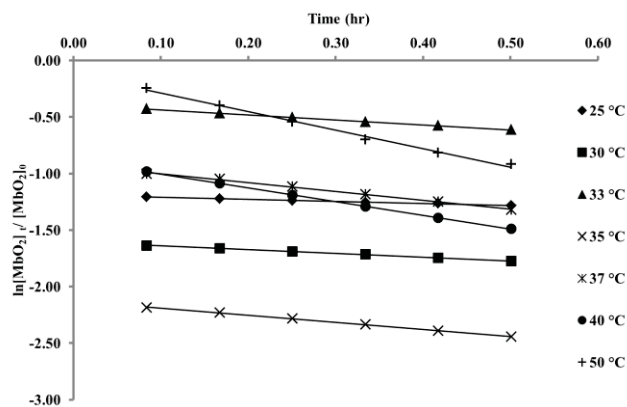
By contrast, the autoxidation rate at higher incubation time is difficult to observe because oxymyoglobin was rapidly oxidized.

Effect of dihydrocapsaicin and gallic acid concentration on autooxidation of myoglobin: Dihydrocapsaicin and gallic acid solution was chosen to be representatives of capsaicinoid compounds and phonolic compounds, respectively. The effect of various concentrations of dihydrocapsaicin and gallic acid on myoglobin were studied, found that an increasing of concentrations of both compounds could be decrease the k_{obs} values compared with oxymyoglobin solution without antioxidants. It is suggested that the dihydrocapsaicin and gallic acid could be stabilize the autooxidation reaction of myoglobin (Table 2).

Table 2 The k_{obs} values of autoxidation of myoglobin with adding myoglobin solution with dihydrocapsaicin and gallic acid at various concentration

Dihydrocapsaicin Concentration (ppm)	k_{obs} (hr^{-1})	Gallic acid Concentration (ppm)	k_{obs} (hr^{-1})
Control	-	Control	-
5	0.067	5	0.667
10	0.067	0	0.552
20	0.057	20	0.468
30	0.049	30	0.370
40	0.043	40	0.257
50	0.038	50	0.222

According to capsaicinoid extracts, the k_{obs} of sample H showed the lowest value. While, the phenolic extracts of sample H showed the lowest value (Table 3).

The results suggested that different hot peppers have different levels of deceleration activity. The crude extracts of hot pepper obtained from both extractions with 90% methanol (methanol extracts) and methanol: 0.05%HCl (90:10) (acidified methanol extracts) is composed of both capsaicinoid and phenolic compounds. Therefore, the antioxidant properties of the hot pepper extracts on deceleration of autoxidation of myoglobin have derived from both compounds.
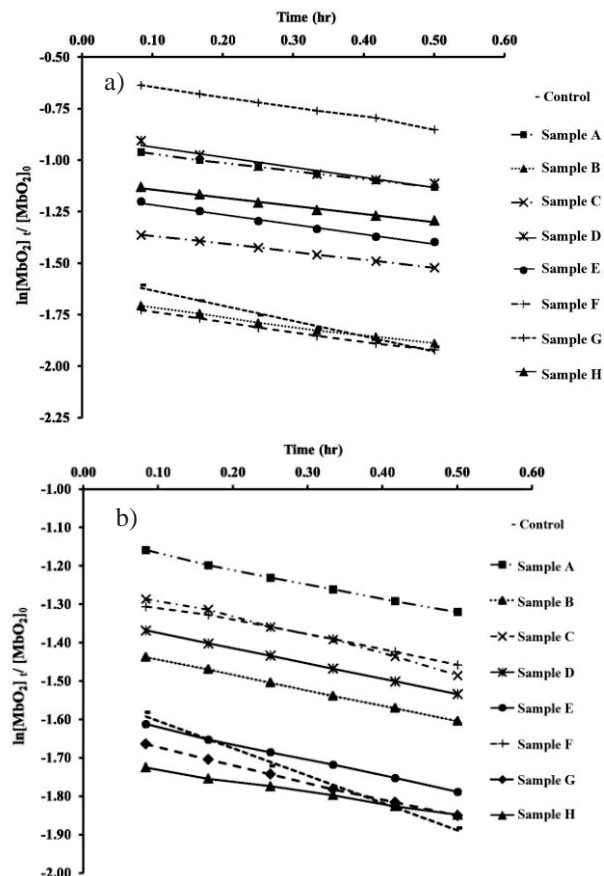

Figure 4. The effect of the crude extracts of hot pepper on deceleration of autoxidation of myoglobin. a) capsaicinoid extract and b) phenolic extracts.

Table 3: The k_{obs} values of autoxidation of myoglobin with adding myoglobin solution with capsaicinoid extract and phenolic extract.

Sample code	Capsaicinoid extract k_{obs} (hr^{-1})	Phenolic extract k_{obs} (hr^{-1})
Control	-	-
A	0.545	0.546
B	0.579	0.565
C	0.522	0.673
D	0.668	0.554
E	0.646	0.583
F	0.644	0.521
G	0.679	0.628
H	0.539	0.411

4. Conclusions

Capsaicinoids and phenolic compounds are successfully extracted using methanol and acidified methanol, respectively. The content of capsaicinoids and phenolic compounds in various hot pepper sample are different. Interestingly, hot pepper extracts with different extraction solvent are comprised of capsaicinoids and phenolic compounds and showed the antioxidant activity on deceleration of autoxidation reaction of myoglobin.

References

[1]   L.R Howard, S.T. Talcott, C.H., Brenes, and B. Villalon, *J. Agri. Food. Chem*. **48** (2000) 1713–1720.

[2]   P.G. Hoffman, M.C. Lego and W.G. Galleto *J. Agri. Food. Chem*. **31** (1983) 1326–1330.

[3]   J. Juangsamut, C. Ruangviriyachai, S. Techawongstien and S. Chanthai, *Int. Food. Res. J.* **19** (2012) 1217-1226.

[4]   C.B. Davis, C.E. Markey, M.A. Busch and K.W. Busch. *J.Agri. Food. Chem.* **25**(2007) 5925-5933.

[5]   D.E. Henderson and A.M. Slickman, *J. Agri. Food. Chem*. **48** (1999) 2563–2573.

[6]   A. Rosa, M. Deiana, V. Casu, S. Paccagnini, G. Appendino, M. Ballero and M.A. Dessi, *J. Agri. Food. Chem*. **50** (2002) 2563–2573.

[7]   T.H. Tsai, P.J. Tsai and S.C. Ho, *J. Food. Sci*. **70** (2005) 93-97

[8]   W. Si, Y. Liang, K.Y. Ma and Z-Y Chen, *J. Agri. Food. Chem*. **60** (2012) 6230-6234.

[9]   J.M. Navarro, P. Flores, C. Garrido and V. Martinez, *Food. Chem.* **96**(2006) 66-73

[10] G.F. Antonious, T.S. Kochhar, R.L. Jarret and J.C. Synder, *J. Environ. Sci. Healt. B* **41**(2006) 1237-1243.

[11] S. Chatteree, Z. Niaz, S. Guatan, S. Adhikari, S.V. Pasad and A. Sharma, *Food. Chem*. **102** (2007) 515-523

[12] P. Arnnok, C. Ruangviriyachai, R. Mahachai, S. Techawongstien and S. Chanthai, *Int. Food. Res. J.* **16** (2012) 235-243.

[13] K. Shikama. *Prog. Biophy. Mol. Bio*. **91**(2006) 83-162.

[14] H.O. Hultin. *In Advance in Seafood Biochemistry*. G.J. Frick and R.E. Martin, eds. (1992) p99-122.

[15] M.Chaijan. Songklanakarin J. Sci. Technol. **30**(2008) 47-53.

[16] V.L. Singleton and J.A. Rossi, *Amer. J. Enol. Vitticult*. **16** (1965) 144-58.